Extreme 13Ccarb enrichment in ca. 2.0 Ga magnesite--stromatolite--dolomite--red beds' association in a global context: a case for the world-wide signal enhanced by a ldots

Article *in* Earth-Science Reviews · October 1999

DOI: 10.1016/S0012-8252(99)00044-6

CITATIONS
192

READS
185

3 authors, including:

A.E. Fallick
University of Glasgow
723 PUBLICATIONS **19,586** CITATIONS

SEE PROFILE

Pavel Vladimirovich Medvedev
Karelian Research Centre of the Russian Academy of Sciences
32 PUBLICATIONS **561** CITATIONS

SEE PROFILE

ELSEVIER

Earth-Science Reviews 48 (1999) 71–120

EARTH-SCIENCE REVIEWS

www.elsevier.com/locate/earscirev

Extreme $^{13}C_{carb}$ enrichment in ca. 2.0 Ga magnesite–stromatolite–dolomite–'red beds' association in a global context: a case for the world-wide signal enhanced by a local environment

Victor A. Melezhik [a,*], Anthony E. Fallick [b], Pavel V. Medvedev [c], Vladimir V. Makarikhin [c]

[a] *Geological Survey of Norway, Leiv Eirikssons vei 39, 7004 Trondheim, Norway*
[b] *Scottish Universities Research and Reactor Centre, East Kilbride, Glasgow G75 0QF, Scotland, UK*
[c] *Institute of Geology of Karelian Scientific Centre, Russian Academy of Sciences, Pushkinskaya, 11, 185610 Petrozavodsk, Russian Karelia, Russian Federation*

Received 2 November 1998; accepted 25 June 1999

Abstract

The Palaeoproterozoic positive excursion of $\delta^{13}C_{carb}$ is now considered as three positive shifts of $\delta^{13}C_{carb}$ separated by returns to 0‰, which all occurred between 2.40 and 2.06 Ma. This isotopic event is unique in terms of both duration (> 300 Ma) and ^{13}C enrichment (up to +18‰). The mechanism responsible for one of the most significant carbon isotopic shifts in Earth history remains highly debatable. To date, $\delta^{13}C$ of +10‰ to +15‰ cannot be balanced by organic carbon burial (f_{org}) as there is no geological evidence for an enhanced C_{org} accumulation prior to or synchronous with the excursion. Instead, termination of these excursions is followed by formation of a vast reservoir of ^{13}C-depleted organic material (−45‰ at Shunga) and by one of the earliest known oil-generation episodes at 2.0 Ga. None of the three positive excursions of $\delta^{13}C_{carb}$ is followed by a negative isotopic shift significantly below 0‰, as has always been observed in younger isotopic events, reflecting an overturn of a major marine carbon reservoirs. This may indicate that f_{org} was constant: implying that the mechanism involved in the production of C_{org} was different. Onset of intensive methane cycling resulting in Δ_c change is another possibility. The majority of sampled $^{13}C_{carb}$-rich localities represents shallow-water stromatolitic dolostones, 'red beds' and evaporites formed in restricted intracratonic basins, and may not reflect global $\delta^{13}C_{carb}$ values. Closely spaced drill core samples ($n = 73$) of stromatolitic dolostones from the $> 1980 \pm 27$ Ma Tulomozerskaya Formation in the Onega palaeobasin, Russian Karelia, have been analysed for $\delta^{13}C_{carb}$ and $\delta^{18}O_{carb}$ in order to demonstrate that different processes were involved in the formation of $^{13}C_{carb}$-rich carbonates. The 800 m-thick magnesite–stromatolite–dolomite–'red beds' succession formed in a complex combination of environments on the Karelian craton: peritidal shallow marine, low-energy protected bights, barred basins, evaporative ephemeral ponds, coastal sabkhas and playa lakes. The carbonate rocks exhibit extreme ^{13}C enrichment with $\delta^{13}C$ values ranging from +5.7 to +17.2‰ vs. V-PDB (mean + 9.9 ± 2.3‰) and $\delta^{18}O$ from

* Corresponding author. Tel.: +47-73-90-40-11; fax: +47-73-92-16-20; E-mail: victor.melezhik@ngu.no

0012-8252/99/$ - see front matter
PII: S0012-8252(99)00044-6

18.6 to 26.0‰ vs. V-SMOW (mean 22.0 ± 1.6‰). The Tulomozerskaya isotopic excursion is characteristic of the global 2.4–2.06 Ga positive shifts of carbonate $^{13}C/^{12}C$, although it reveals the greatest enrichment in ^{13}C known from this interval. An external basin(s) is considered to have provided an enhanced C_{org} burial and global seawater enrichment in ^{13}C: the global background value for the isotopic shift at Tulomozero time (ca. 2.0 Ga) is roughly estimated at around +5‰. An explosion of stromatolite-forming microbial communities in shallow-water basins, evaporative and partly restricted environments, high bioproductivity, enhanced uptake of ^{12}C, and pene-contemporaneous recycling of organic material in cyanobacterial mats with the production and consequent loss of CO_2 (and CH_4?) are believed to be additional local factors which may have enhanced $\delta^{13}C$ from +5‰ up to +17‰. Such factors should be taken into account when interpreting carbon isotopic data and attempting to discriminate between the local enrichment in ^{13}C and globally enhanced $\delta^{13}C$ values. We propose that many previously reported $\delta^{13}C$ values from other localities, where environmental interpretations are not available or have not been taken into account may not represent the global $\delta^{13}C$ values.

Keywords: Palaeoproterozoic; carbonate platform; shallow water environment; stromatolite; dolomite; magnesite; red beds; evaporates; strontium; carbon; oxygen; isotopes

1. Introduction

Studies of Cenozoic carbonates have revealed strong $\delta^{13}C_{carb}$ secular variations through time which were assigned to fluctuations in the ratio of oxidised inorganic/reduced organic carbon fluxes (e.g., Scholle and Arthur, 1976, 1980; Berger, 1977; Shackleton, 1977; Kroopnick et al., 1977; Zachos and Arthur, 1986). Veizer et al. (1980) first identified the global character of long-term positive shifts in $\delta^{13}C_{carb}$ at the Precambrian–Cambrian boundary, through the Phanerozoic, especially in the Permian (Fig. 1). Later, Qing and Veizer (1994) and Brenchley et al. (1994; 1997) recorded a prominent positive shift in $\delta^{13}C_{carb}$ (up to +7‰) in the Late Ordovician. Intensive studies on the Permian carbon positive excursion have revealed a sharp rise in $\delta^{13}C_{carb}$ by approximately 5–8‰ in Upper Permian carbonates (Fig. 1). More recently, many detailed investigations have focused on isotopic variations across the Precambrian–Cambrian boundary and through the Neoproterozoic interval (Tucker, 1986; Magaritz et al., 1986; Aharon et al., 1987; Fairchild et al., 1990; Pokrovsky and Vinogradov, 1991; Derry et al., 1992; Kaufman et al., 1993, 1996; Pokrovsky and Gertsev, 1993; Brasier et al., 1994; Iyer et al., 1995; Knoll et al., 1995a,b; Kaufman and Knoll, 1995). These studies revealed a series of positive and negative excursion of $\delta^{13}C_{carb}$ (Fig. 1).

Although the positive excursions in $\delta^{13}C_{carb}$ outlined above occurred at different times throughout Earth history similar models have been proposed for their explanation: large scale perturbations in organic matter burial rate. It has been suggested that the required high C_{org} burial was driven by high sedimentation rates and high productivity which were, in turn, ascribed to anoxia in seawater, orogenic events, sea-level fluctuations or combinations of these factors (e.g., Jenkyns, 1980; Magaritz et al., 1983; Derry et al., 1992). However, Magaritz et al. (1983) recognised an obvious mass-balance problem in the carbon cycle in the Late Permian as the excess net

Fig. 1. Major $\delta^{13}C_{carb}$ anomalies in Earth history based on published material. Cretaceous–Tertiary boundary: Lloyd and Hsü (1971), Osaki (1973), Saito and Van Donk (1974), Veizer and Hoefs (1976), Scholle and Arthur (1976; 1980), Zachos and Arthur (1986). Upper Permian: Compston (1960), Keith and Weber (1964), Degens and Epstein (1964), Dorman (1968), Murata et al. (1972), Osaki (1973), Davies and Krouse (1975), Davies (1976), Veizer and Hoefs (1976), Clark (1980), Magaritz and Schultze (1980), Veizer et al. (1980), Botz and Müller (1981), Magaritz et al. (1981; 1983), Magaritz and Turner (1982), Rao and Green (1982), Beauchamp et al. (1987). Late Ordovician: Qing and Veizer (1994), Brenchley et al. (1997). Neoproterozoic to Cambrian: Veizer et al. (1980), Tucker (1986), Magaritz et al. (1986), Aharon et al. (1987), Magaritz (1989), Fairchild et al. (1990), Pokrovsky and Vinogradov (1991), Asmerom et al. (1991), Kaufman et al. (1991), Derry et al. (1992), Kaufman et al. (1992), Pokrovsky and Gertsev (1993), Kaufman et al. (1993), Corsetti and Kaufman (1994), Brasier et al. (1994), Narbonne et al. (1994), Smith et al. (1994), Iyer et al. (1995), Knoll et al. (1995a,b), Kaufman et al. (1996). Palaeoproterozoic: Schidlowski et al. (1976), McNaughton and Wilson (1983), Feng (1986), Baker and Fallick (1989a; b), Gauthier-Lafaye and Weber (1989), Zagnitko and Lugovaya (1989), Yudovich et al. (1991), Karhu (1993), Tikhomirova and Makarikhin (1993), Akhmedov et al. (1993), Bekker and Karhu (1996), Karhu and Holland (1996), Melezhik and Fallick (1996a,c), Sreenivas et al. (1996), Melezhik et al. (1997a).

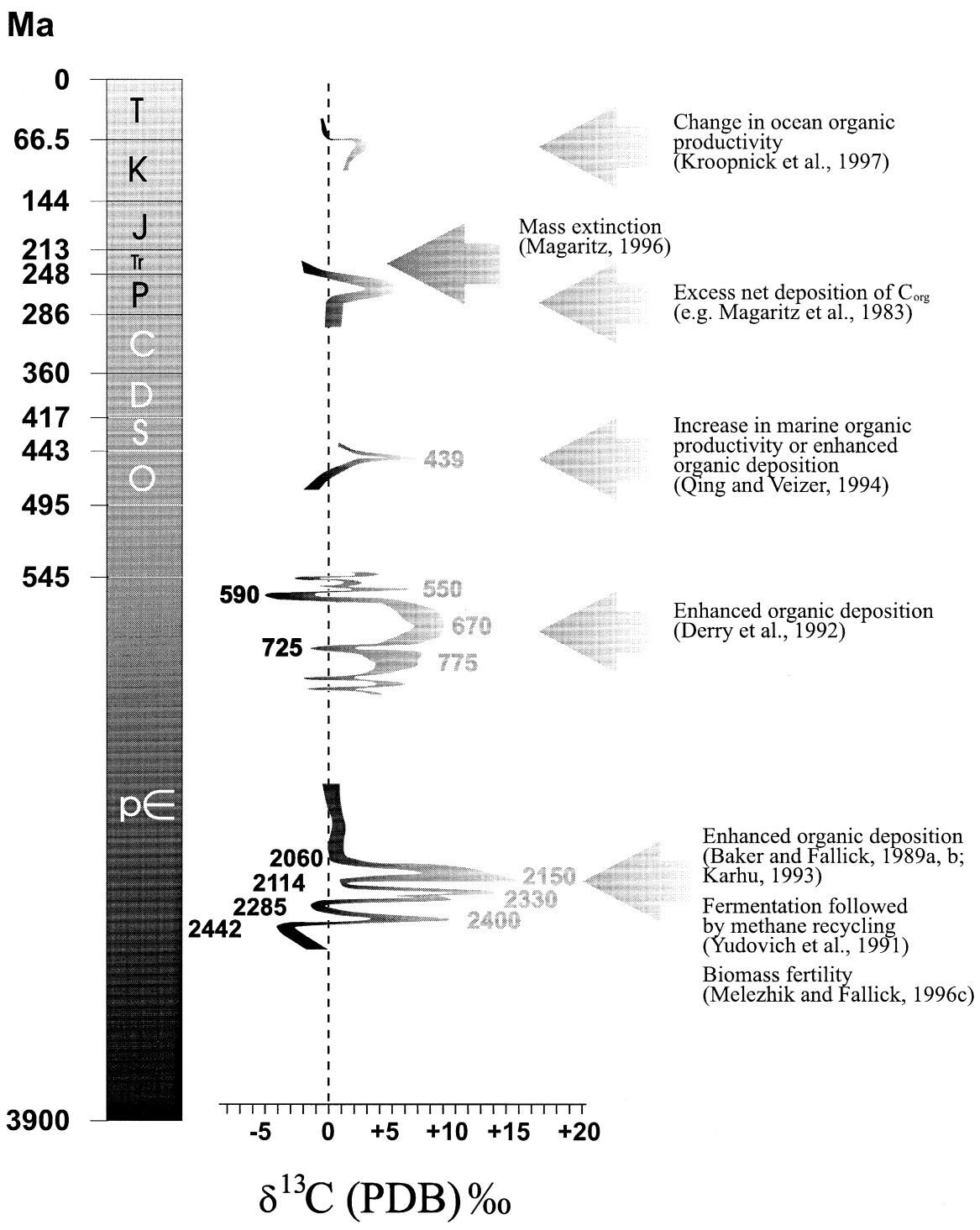
Ma
0
66.5
144
213
248
286
360
417
443
495
545
3900
T
K
J
Tr
P
C
D
S
O
pЄ
439
590
550
670
725
775
2060
2114
2285
2442
2150
2330
2400
-5
0
+5
+10
+15
+20
δ13C (PDB)‰
Change in ocean organic productivity (Kroopnick et al., 1997)
Mass extinction (Magaritz, 1996)
Excess net deposition of Corg (e.g. Magaritz et al., 1983)
Increase in marine organic productivity or enhanced organic deposition (Qing and Veizer, 1994)
Enhanced organic deposition (Derry et al., 1992)
Enhanced organic deposition (Baker and Fallick, 1989a, b; Karhu, 1993)
Fermentation followed by methane recycling (Yudovich et al., 1991)
Biomass fertility (Melezhik and Fallick, 1996c)

deposition of C_{org} necessary to generate the $> +5‰$ rise in $\delta^{13}C_{carb}$ has not been documented. Similarly, it is difficult to reconcile the highly ^{13}C-enriched (up to $+16‰$) carbonates in the Neoproterozoic sediments of the Bambuí Group in Brazil (Iyer et al., 1995) with appropriate organic-rich sediments.

It is also relevant that most Phanerozoic and Neoproterozoic positive excursions in $\delta^{13}C_{carb}$ have

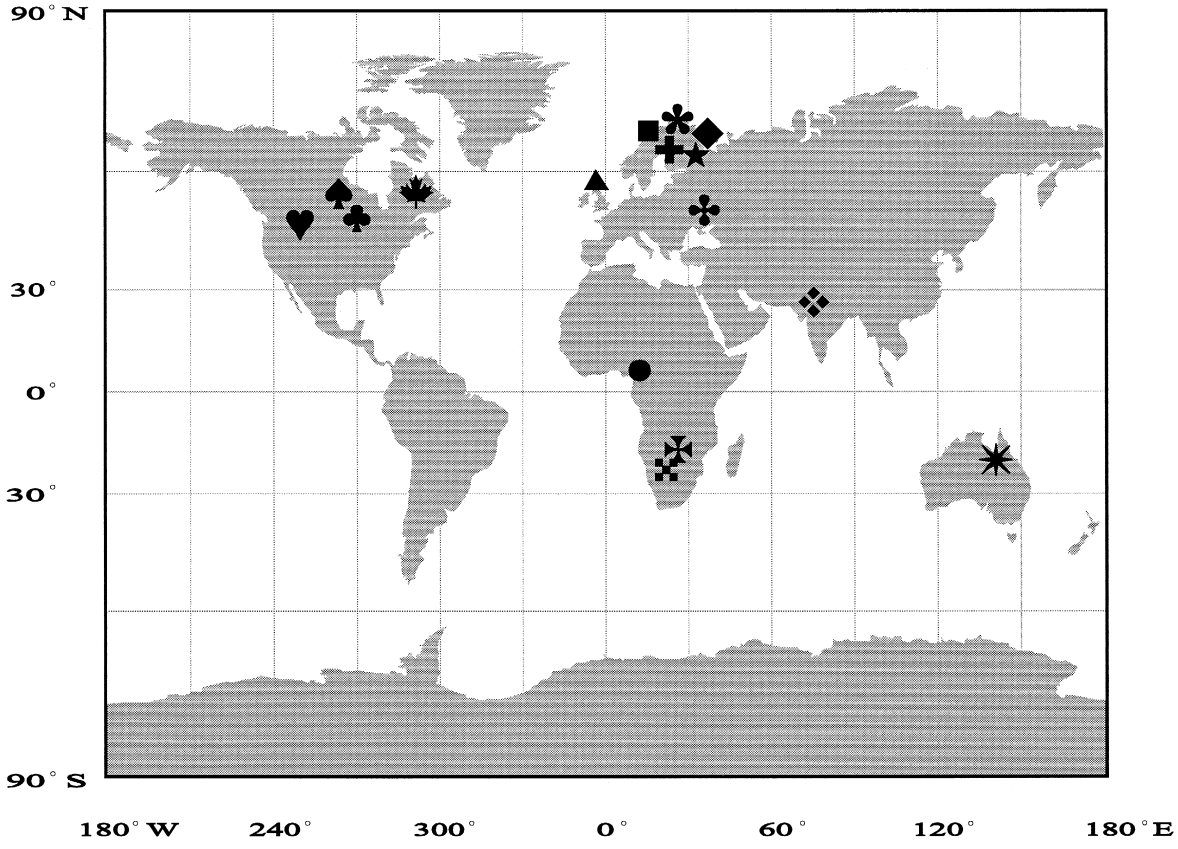

Fig. 2. World-wide distribution of the Palaeoproterozoic (2.40–2.06 Ga) ^{13}C-rich carbonate rocks (modified from Melezhik et al., 1997a).

one persistent feature in common: being followed by a sharp negative shift in $\delta^{13}C_{carb}$ (Fig. 1, e.g., Magaritz, 1989). This was the case for the Neoproterozoic to Early Cambrian positive excursions in $\delta^{13}C_{carb}$, many of which are accompanied by negative shifts in $\delta^{13}C_{carb}$. The latter have been correlated with glacial periods (e.g., Knoll et al., 1986; Derry et al., 1992; Kaufman et al., 1997; Hoffman et al., 1998). Magaritz (1989) has assigned the fall in $\delta^{13}C_{carb}$ at the end of the Precambrian–Cambrian, Permian–Triassic and Cretaceous/Tertiary positive excursions to extinction events.

More recently, attention has been drawn to the study of $\delta^{13}C_{carb}$ variations within individual Palaeoproterozoic (1.8–2.5 Ga) successions. Since the pioneering work of Schidlowski et al. (1976), the existence of unusually ^{13}C-enriched carbonates in Africa deposited at around 2.07 Ga (the Lomagundi event) has puzzled geologists. While this so-called Lomagundi event was ascribed to locally enhanced burial of organic matter in a restricted basin (Schidlowski et al., 1976), two new discoveries of ca. 2.0 Ga-old carbonates with extremely positive $\delta^{13}C_{carb}$ values led to a reassessment of this event as global in nature (Baker and Fallick, 1989a,b). Baker and Fallick (1989b) suggested that it was caused by accelerated burial of reduced carbon with subsequent release of oxygen and perturbation in the terrestrial carbon cycle. Similarly high $\delta^{13}C_{carb}$ values have recently been reported from a number of localities in the Fennoscandian Shield, N. America, and in India essentially covering the whole globe (Fig. 2). The radiometric age constraints for Finnish records of $\delta^{13}C_{carb}$ (Karhu, 1993) show a single, broad Palaeoproterozoic $\delta^{13}C_{carb}$ excursion in carbonates (up to +8 to +10‰) deposited from 2.3 to 2.06 Ga. However, three discrete isotopic anomalies which occurred between 2.43 and 1.93 Ma have recently reported from the Palaeoproterozoic in the Kaapvaal craton, South Africa (Buick et al., 1998).

2. Major evolutionary events related to the Palaeoproterozoic positive carbon isotope excursion

2.1. Palaeoenvironmental and biological changes

Fig. 3 lists some of the major Palaeoproterozoic events. A world-wide continental rift expansion (Lowe, 1992) and interrelated development of large shallow-water intercontinental seas (Timopheev et al., 1986) have been assigned to 2.5–2.3 Ga. Most

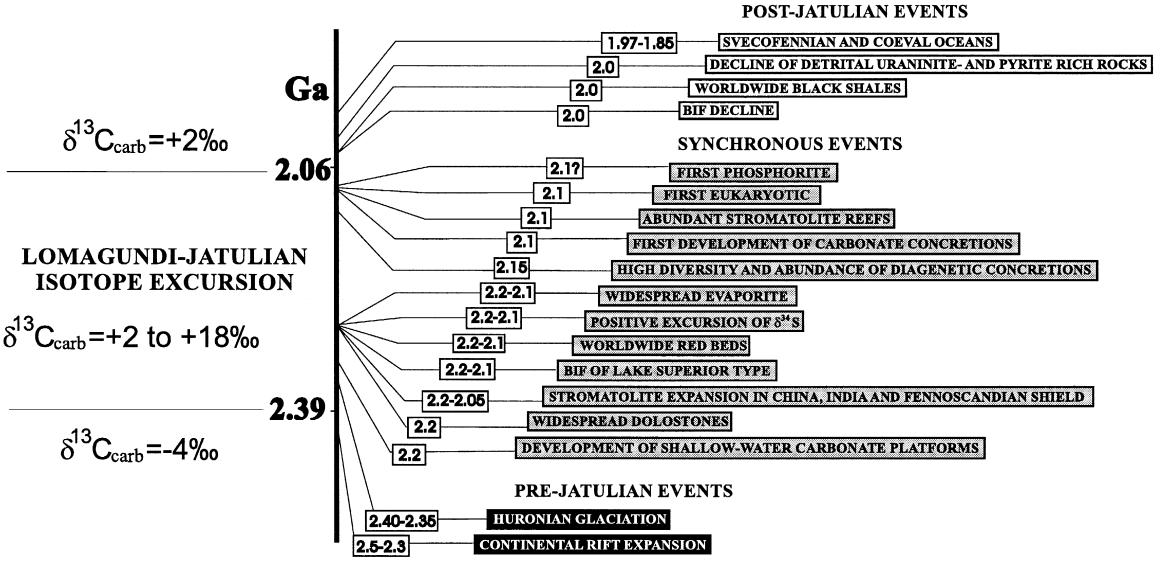

Fig. 3. Major phenomena interrelated to the Palaeoproterozoic (Lomagundi–Jatulian) isotopic event (modified from Melezhik et al., 1997c).

continents yield evidence for a 2.40–2.35 Ga Huronian glacial epoch (e.g., Ojakangas, 1985), which preceded the Palaeoproterozoic isotope excursion (Fig. 3).

Onset of the isotope excursion coincides with the development of shallow-water carbonate platforms (Grotzinger, 1989), widespread deposition of dolostones (Melezhik and Predovsky, 1989) and evapor-

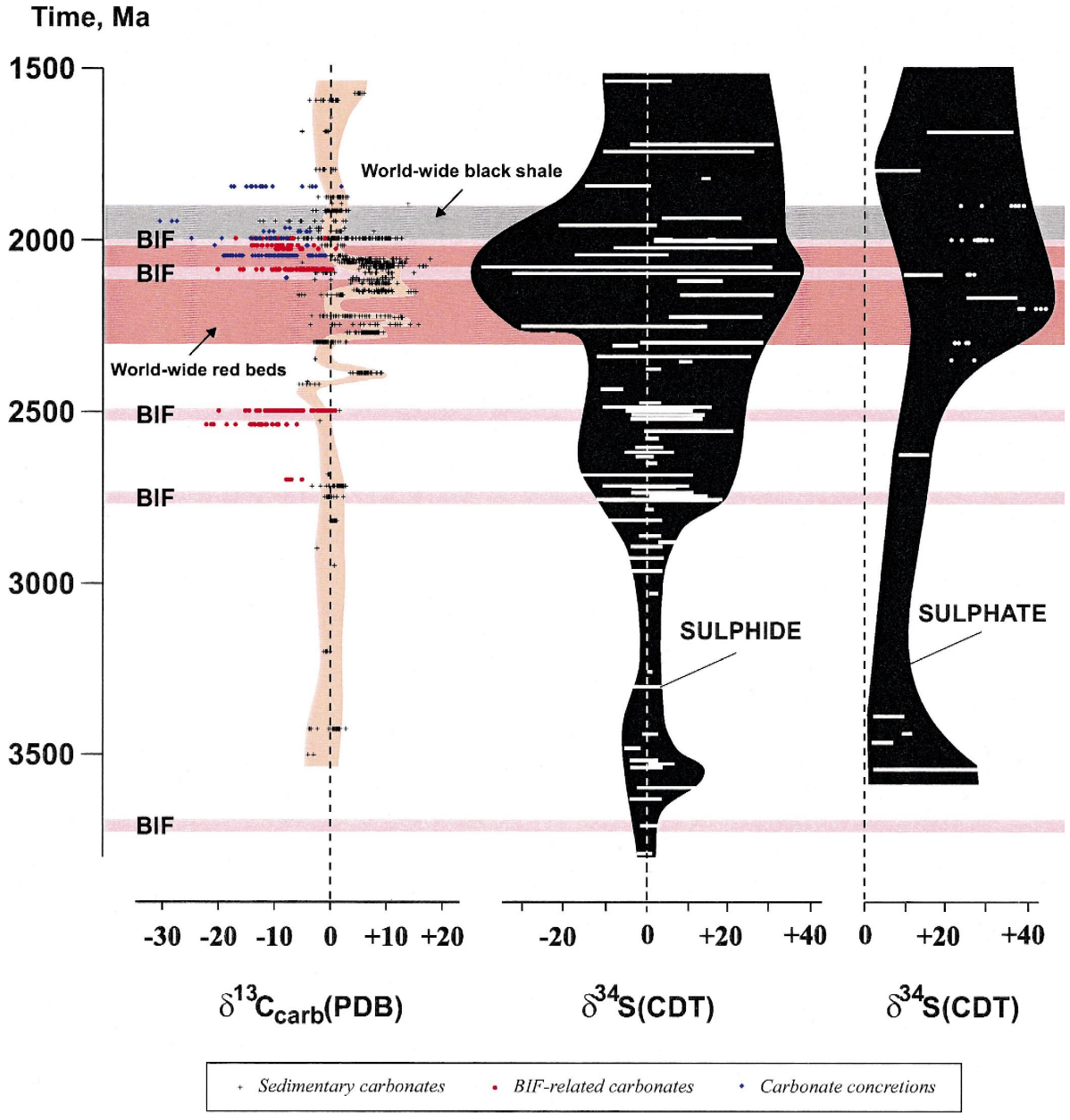

Fig. 4. $\delta^{13}C_{carb}$, $\delta^{34}S_{sulphide}$ and $\delta^{34}S_{sulphate}$ variations in relation with the appearance of banded iron formation (BIF), world-wide 'red beds' and black shales. $\delta^{13}C_{carb}$, $\delta^{34}S_{sulphide}$ and $\delta^{34}S_{sulphate}$ data are largely from Strauss and Moore (1992), Melezhik et al. (1998), and sources listed in Fig. 5.

ites (Salop, 1982). China, India and the Fennoscandian Shield provide evidence of 2.2–2.0 Ga stromatolite explosion (Semikhatov and Raaben, 1994; Melezhik et al., 1997b). This overlaps with worldwide development of 'red beds' (e.g., Sochava, 1979).

Several lines of evidence indicate that the level of oxygen in the atmosphere rose between 2.2 and 2.0 Ga by factor of 15 (Holland, 1994). This coincides with the onset of diagenetic alterations rather similar to present diagenetic processes, in that they are manifested by formation of abundant concretions with highly oxidised iron and manganese, phosphate concretions and carbonate concretions, as a result of organic carbon recycling (Melezhik, 1992; Melezhik and Fallick, 1996b).

One of the earliest (2.1 Ca) appearances of organelle-bearing eukaryotic cells, apparently provoked by the development of oxygenated atmosphere (Han and Runnegar, 1992), may be assigned to the second half of the isotope excursion. This major biological event corresponds to the formation of sedimentary and diagenetic phosphorites (Bekasova and Dudkin, 1981; Melezhik, 1992).

Termination of the Palaeoproterozoic isotopic shift at 2.06 Ga (Karhu, 1993) is concurrent with decline of banded iron formation and detrital uraninite and pyrite (Fig. 3). This final episode occurred pene-contemporaneously with the breakup of the Kenorland (Bekker, 1998) and the Fennoscandian Shield, and formation of the Svecofennian and other coeval oceans (Barbey et al., 1984; Kontinen, 1987; Dahl-Jensen et al., 1990) which, through middle oceanic ridge systems, may have allowed introduction of a substantial amount of isotopically light mantle CO_2.

2.2. Isotopic evolution of diagenetic carbonates, sulphides and sulphates

World-wide data compiled on Fig. 4 demonstrate that prior to 2.1 Ga isotopically light carbonates are strictly associated with banded iron formations. These carbonates were attributed to either specific diagenetic-metamorphic reactions (Perry and Tan, 1973; Melezhik and Fallick, 1996b) or specific sedimentary environments (Becker and Clayton, 1972). The end of the Palaeoproterozoic isotope excursion is marked by the first appearance, and then by the world-wide development, of diagenetic carbonate concretions marked by negative $\delta^{13}C_{carb}$ values. This may be the first reliable evidence that organic material was recycled during diagenesis under oxic conditions.

Although sizeable fractionation of sulphur isotopes has been occasionally documented since Archaean time, some of these ancient cases are associated with banded iron formation sulphides (2750 and 2500 Ma, Fig. 4). This has recently been reemphasised by Kakegawa et al. (1992). However, a sharp increase in dispersal of $\delta^{34}S$ clearly coincides with the first appearance of isotopically heavy carbonates, suggesting that sulphides were formed via bacterial sulphate reduction (Fig. 4). Although both highly negative and positive values have been documented, ^{34}S-rich sulphides dominate. The latter suggests that (1) sulphate was widely available in seawater and (2) sulphides abundantly formed in restricted environments with a limited SO_4^{2-} supply.

3. One or several Palaeoproterozoic positive excursions of $\delta^{13}C_{carb}$?

The compilation by Karhu and Holland (1996) demonstrated a single positive excursion lasting over 200 Ma. This long-lasting shift is very unusual. Given the fact that Palaeoproterozoic ^{13}C-rich carbonate sequences are poorly dated, it has not been clear whether they represent a single positive excursion in $\delta^{13}C_{carb}$ or a series of excursions (Baker and Fallick, 1989a,b). Although three discrete isotopic anomalies have recently reported from the Palaeoproterozoic in South Africa «it is not clear how many of these excursions reflect global rather than local processes» (Buick et al., 1998, p. 875).

Based on data from South Africa (Buick et al., 1998), the Pechenga (Melezhik and Fallick, 1996a) and Imandra/Varzuga (Karhu and Melezhik, 1992; Pokrovsky and Melezhik, 1995) Belts, and the Labrador Trough (Melezhik et al., 1997a) the suggested Palaeoproterozoic $\delta^{13}C_{carb}$ curve (Karhu and Holland, 1996) can be revised (Fig. 5). The long-lasting, single, isotopic event may perhaps be better considered as three or four positive shifts of $\delta^{13}C_{carb}$ separated by returns to 0‰ (Fig. 5).

The positive excursion is preceded by a 2.3‰ negative isotopic shift represented by 2.442 Ga Sei-

dorechka Formation carbonates (7, Fig. 5, $\delta^{13}C_{carb} = -3.7‰$). A sharp increase in $\delta^{13}C_{carb}$ values from $-3.7‰$ to $+6.5‰$ appears between 2.44 and 2.39 Ga (10, Fig. 5, Duitschland Formation, Buick et al., 1998). The depositional age of the Duitschland Formation has not been dated directly but was constrained between 2.43 and 2.35 Ga (Buick et al., 1998).

The Duitschland positive isotope excursion is followed by a 7‰ negative shift in $\delta^{13}C_{carb}$ reported from the Bruce limestones (11, Fig. 5, Veizer et al., 1992a) and the Timeball Hill Formation (12, Fig. 5, Buick et al., 1998). Bruce limestones of the Espanola Formation are characterised by $\delta^{13}C_{carb}$ of $-1.3 \pm 0.7‰$ with the time constraints of 2.35 ± 0.10 Ga (Veizer et al., 1992a) whereas Timeball Hill Forma-

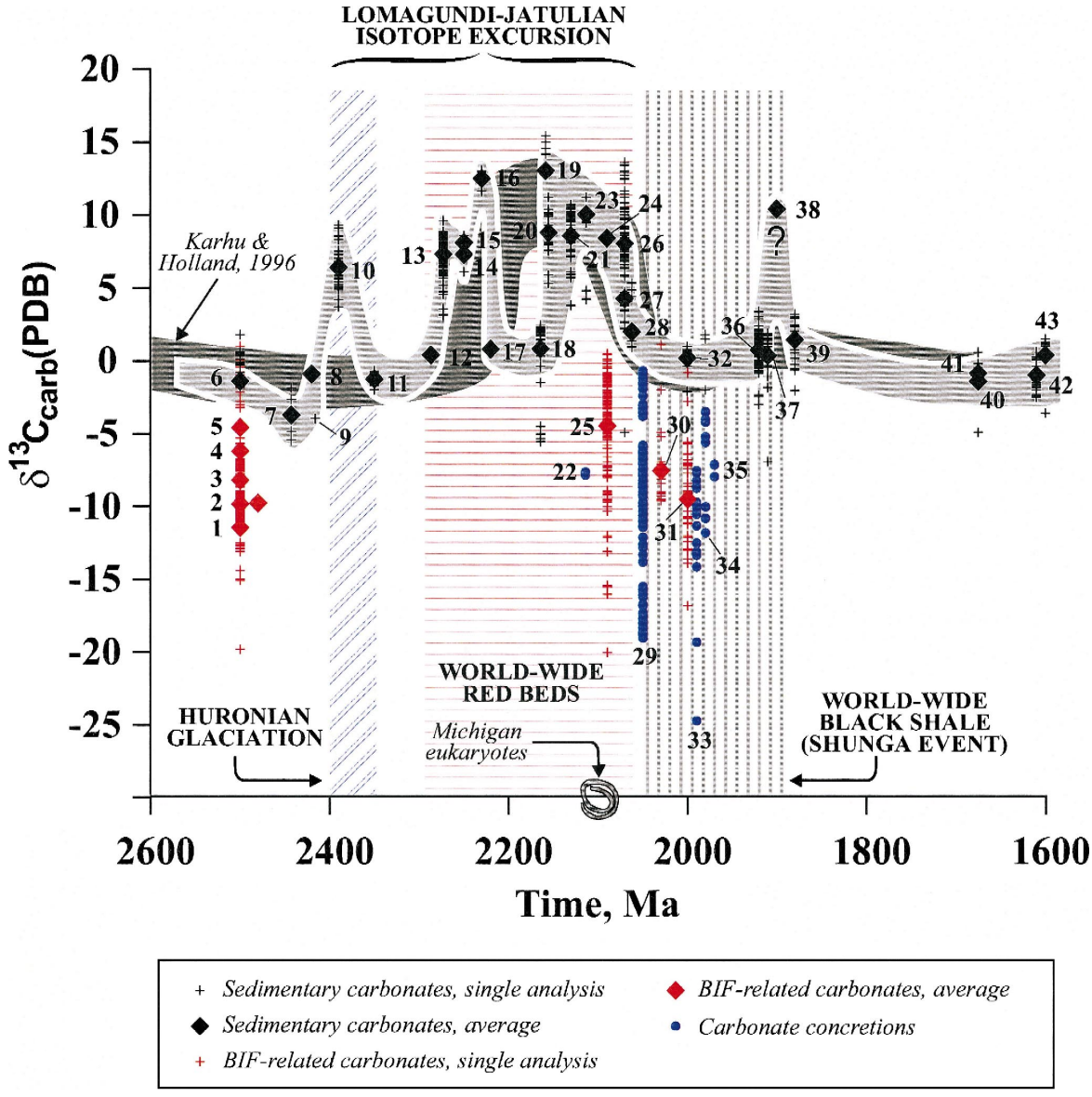

tion carbonates marked by the $\delta^{13}C_{carb}$ of +0.4‰, which occurred between 2.35 and 2.22 Ga (Buick et al., 1998).

At about 2.3 Ga, there appears to be a new sharp increase in the $\delta^{13}C_{carb}$ values reported from South Africa and from a series of localities on the Fennoscandian Shield (13–16, Fig. 5). This is either a single positive excursion or two positive oscillations (13 and 16, Fig. 5) separated by a limited downward shift (15–14, Fig. 5).

Based on the data from the Pechenga Belt we speculate that a second prominent negative excursion may occur between 2.21 and 2.11 Ga represented by Kolasjoki carbonates (17, Fig. 5, $\delta^{13}C_{carb}$ of +0.4 ± ‰). The Kolasjoki Formation is younger that 2.214 ± 54 and older than 2.114 ± 52 Ga. Although both age estimates are based on the Rb–Sr technique (Balashov, 1995), these two dates together with other Rb–Sr ages obtained from the Pechenga Belt sequence are in a good agreement with U–Pb, Pb–Pb and Sm–Nd techniques, which have been applied to both younger and older formations of the Pechenga Belt (Balashov, 1995). Moreover, taking into the consideration that 2.1–2.2 Ga isotopically light or 'normal' carbonates have been documented (for the references see Strauss and Moore, 1992) from the Kasegalik Formation (−0.6‰), Manitounuk Group (−1.6 to −2.2‰) the Gandarella Formation (−0.8‰), and the Pretoria Group (+0.8‰), the Kolasjoki $\delta^{13}C_{carb}$ negative shift may well be of a global significance.

The next, 2.15–2.07 Ga positive excursion seems to have been most widely developed as it was recorded from the Canadian (19, 20, Fig. 5) and Fennoscandian (21, 23, 24, Fig. 5) Shields, and in South Africa (26, 27, Fig. 5). Carbonates representing this excursion exhibit an unusually high enrichment in ^{13}C, up to +18‰ (Yudovich et al., 1991). The positive excursion ends with a sharp drop of 10‰ in the $\delta^{13}C_{carb}$ values at 2.062 (28, Fig. 5, Karhu, 1993).

The significance of the youngest $\delta^{13}C_{carb}$ positive anomaly represented by the red bed dominated 2.0–1.9 Ga Lucknow Formation (38, Fig. 5, Master, 1998 cited in Buick et al., 1998) remains unclear. This requires further geochemical, geochronological and correlation work (Buick et al., 1998).

Regardless of whether the youngest positive (38, Fig. 5) $\delta^{13}C_{carb}$ excursion was shown to be not well constrained, the current data suggest that (1) the positive isotopic event starts as early as 2.4 Ga ago; (2) the Palaeoproterozoic positive $\delta^{13}C_{carb}$ excursion is better considered as a series of isotopic shifts separated by two (Espanola–Timeball and Pretoria–

Fig. 5. $\delta^{13}C$ variation of sedimentary and diagenetic carbonates through the Palaeoproterozoic, and some interrelated phenomena. Source of isotopic and age data: (1) Dales Gorge Member, banded iron formation (Becker and Clayton, 1972); (2) Marra Mamba Iron Formation (Strauss and Moore, 1992); (3) Dales Gorge Member, banded iron formation (Kaufman et al., 1990); (4) Dales Gorge Member 1, banded iron formation (Becker and Clayton, 1972); (5) Yellowknife Supergroup (Veizer et al., 1989); (6) Wittenoom Dolomite (Strauss and Moore, 1992), (7) Seidorechka Formation (Pokrovsky and Melezhik, 1995; Amelin et al., 1995); (8) Itabira Group (Karhu and Holland, 1996); (9) Neverskrukk Formation (Melezhik and Fallick, 1996a; Sturt et al., 1994); (10) Duitschland Formation (Buick et al., 1998); (11) Bruce Limestone (Veizer et al., 1992a); (12) Timeball Hill Formation (Buick et al., 1998); (13) Kuetsjärvi Sedimentary Formation (Melezhik and Fallick, 1996a; Melezhik et al., 1997b); (14) Sompujärvi Formation (Karhu, 1993; Karhu and Holland, 1996); (15) Sericite Schist Formation (Karhu, 1993); (16) Misi Dolomite (Karhu, 1993); (17) Pretoria Group (Karhu and Holland, 1996); (18) Kolasjoki Sedimentary Formation (Pokrovsky and Melezhik, 1995; Melezhik and Fallick, unpublished; Melezhik et al., 1997b); (19) Dunphy, and Portage Formations (Melezhik et al., 1997a); (20) Alder and Uvé Formations (Melezhik et al., 1997a); (21) Silverton Formation (Buick et al., 1998); (22) Kolasjoki Volcanic Formation (Melezhik and Fallick, 1996a; Melezhik et al., 1997b); (23) Lower Vistola Formation (Karhu, 1993); (24) Jouttiaapa Formation (Karhu, 1993); (25) Gunflint Formation (Carrigan and Cameron, 1991); (26) Lomagundi Group (Schidlowski et al., 1976; Treloar, 1988); (27) Francevillian Series (Gauthier-Lafaye and Weber, 1989; Bros et al., 1992); (28) Upper Petonen Formation (Karhu, 1993); (29) (Winter and Knauth, 1992); (30) Belozero Banded Iron Formation (Zagnitko and Lugovaya, 1989); (31) Krivoi Rog Banded Iron Formation (Zagnitko and Lugovaya, 1989); (32) Duck Creek Dolomite (Strauss and Moore, 1992); (33) Pilgujärvi Sedimentary Formation (Melezhik and Fallick, 1996a); (34) Saonezhskaya Formation (Akhmedov et al., 1993; Puchtel et al., 1998; Melezhik et al., 1999); (35) Pilgujärvi Volcanic Formation (Melezhik and Fallick, 1996a; Hanski et al., 1990); (36) Svecofennian carbonates (Karhu, 1993); (37) Coronation Supergroup (Veizer et al., 1992b); (38) Lucknow Formation (Buick et al., 1998); (39) Abner, Fleming and Denault Formations (Melezhik et al., 1997a); (40) McArthur Group (Strauss and Moore, 1992); (41) McArthur Group (Veizer et al., 1992b); (42) Lynott Formation, Hot Spring Member (Veizer et al., 1992b); (43) Kaladgi Group (Strauss and Moore, 1992).

Table 1
Major localities of Palaeoproterozoic ^{13}C-rich carbonate rocks

Geographic and geological location	Carbonate lithology	Associated sediments and biosedimentary structure	Palaeoclimatic indicator	$\delta^{13}C_{carb}$ variation {‰}	Palaeo-environment	References
Fennoscandian Shield						
Pechenga Belt, Kuetsjärvi Sedimentary Fm.	Dolostones	Red beds, travertines, stromatolites	Mudcracks, tepees, pseudomorphs after gypsum, sulphates	+3 to +10	Fluvial, continental rift lake	Melezhik, 1992; Melezhik and Fallick, 1996a
Imandra/Varzuga Belt, Umba Sedimentary. Fm.	Dolostone	Red beds, chert	Barite	−2 to +7	Continental rift lake	Melezhik, 1992; Melezhik and Fallick, 1996a
Ust'-Ponoy Belt, carbonate beds	Dolostones	Red beds, manganite	–	+0.7 to +6	?	Melezhik, 1992; Melezhik and Fallick, 1996a
Onega Basin, Tulomozerskaya Fm.	Dolostones	Red beds, stromatolites	Mudcracks, tepees, pseudomorphs after gypsum and halite	+5 to +18	Fluvial, sabkha, playa, restricted lagoon, shallow-water marine	Yudovich et al., 1991; Akhmedov et al., 1993; Karhu, 1993; Melezhik et al.,1996
Kiihtelysvaara, Vistola and Petäikkö Fms.	Dolostones	Red beds		+6 to +11	?	Karhu, 1993
Kuusamo Schist Belt, Dolomite, Siltstone and Sericite–Schist Fms.	Dolostones	Red beds, stromatolites	Mudcracks	+8 to +11	Tidal, shallow-water, marine, subaerial	Silvennoinen, 1972; Pekkala, 1985; Karhu, 1993

Peräpohja Schist Belt, Rantamaa, Kvartsimaa, Kivalo, Sompujärvi Fms.	Dolostones	Red beds, stromatolites	Mudcracks, red beds	+3 to +11	Fluvial, shallow-water tidal	Krylov and Perttunen, 1978; Perttunen, 1991; Karhu, 1993
North America						
Labrador Trough, Dunphy, Portage, Alder and Uve Fms.	Dolostones	Red beds, stromatolites	Evaporites	+5 to +14	Fluvial, shallow-water marine	Dimroth, 1978; Chevé et al., 1985; Melezhik et al., 1997a
Marquette Trough, Kona Dolomite	Dolostones	Red beds, stromatolites	Sulphates, pseudomorphs after halite	+2 to +8	Shallow-water marine, sabkha	Larue, 1981; Feng, 1986; Bekker and Karhu, 1996
Africa						
Lomagundi Belt	Dolostones	Stromatolites	Gypsum, anhydrite in the underlying rocks	+3 to +14	?	Schidlowski et al., 1976; Master, 1998
Francevillian Series	Dolostones	Black shales, stromatolites	Gypsum, anhydrite and barite	+3 to +6	Shallow-water marine	Gauthier-Lafaye and Weber, 1989; Amard and Bertrand-Sarfati, 1997
Transvaal Supergroup, Duitschland Fm.	Dolostones	Chert, quartzite	–	+4 to +9	Restricted shallow-water, lacustrine	Eriksson and Reczko, 1995; Buick et al., 1998

'question mark': Palaeoenvironment is unknown.
'dashes': no indicators available.

Kolasjoki) returns to 0‰, and (3) that the total duration of the Palaeoproterozoic isotopic events may exceed 300 Ma.

4. Current problems

The Palaeoproterozoic $\delta^{13}C_{carb}$ excursions together with a series of major global palaeoenvironmental changes superficially resemble the Precambrian/Cambrian transition events (Melezhik and Fallick, 1996a; Buick et al., 1998). Although there is very little doubt that the 2.40–2.06 Ga positive excursions of $\delta^{13}C$ have a widespread character, the isotopic event is unique in terms of both duration (> 300 Ma) and ^{13}C enrichment (up to +18‰).

However, the mechanism responsible for one of the most significant carbon isotopic shifts in Earth history remains highly debatable (Yudovich et al., 1991; Schidlowski and Aharon, 1992; Dix et al., 1995; Melezhik and Fallick, 1996a, 1997; Shields, 1997). To date, $\delta^{13}C$ of +5‰ to +18‰ cannot be balanced by organic carbon burial (f_{org} in equation) as there is no geological evidence for an enhanced C_{org} accumulation prior to or synchronous with the excursion:

$$\delta_{carb} = \delta_{in} + f_{org}\,\Delta_c, \qquad (1)$$

where δ_{in} is the isotopic composition of carbon entering the global surface environment, δ_{carb} represent the isotopic composition of carbonate carbon, f_{org} is the fraction of carbon buried in organic form, and Δ_c is the isotopic difference between organic and inorganic carbon. For the interval 2.4–2.06 Ga there is a paucity of published $\delta^{13}C_{org}$ data at the time when the positive carbonate excursion developed. Consequently, neither Δ_c nor f_{org} can be established with meaningful precision. Somewhat surprisingly, the Palaeoproterozoic isotopic event is followed by formation of a vast reservoir of ^{13}C-depleted organic material (−45‰ at Shunga, Melezhik et al., 1999) and by one of the earliest known oil-generation episodes at 2.0 Ga.

None of the three positive excursions of $\delta^{13}C_{carb}$ is followed by a negative isotopic shift significantly below 0‰ (Figs. 4 and 5), as has usually been observed in younger isotopic events (Fig. 1) reflecting an overturn of a major marine carbon reservoirs. Could the absence of such shifts in the Palaeoproterozoic indicate that perhaps there were no such reservoirs (i.e., f_{org} was constant)? If so, it is necessary to investigate other options to explain the Palaeoproterozoic positive excursion of $\delta^{13}C_{carb}$. Perhaps the traditional approach via f_{org} (Eq. (1)) change is not applicable to 2.40–2.06 Ga. As this period of time was marked by transition from generally oxygen-free to gradually oxygenated atmosphere, this might have influenced the mechanism involved in the production of organic carbon. Onset of intensive methane cycling (e.g., Hayes, 1994) resulting in Δ_c change (Eq. (1)) is another possibility.

A significant change in δ_{in} seems implausible. The common assumption that organic carbon accumulated in open marine environments and subsequently underwent complete recycling during subduction processes should have two consequences. First, the subducted ^{13}C-depleted, C_{org}-rich sediments should be recycled within 200 Ma. This would cause a negative isotopic shift at around 1.9–1.8 Ga. However, there are no records of such (Strauss and Moore, 1992; Des Marais et al., 1992b; Des Marais, 1997). Secondly, the subduction of ^{13}C-depleted, C_{org}-rich sediments implies that coeval carbonates from open marine environments would also be recycled. Consequently, the majority of sampled $^{13}C_{carb}$-rich localities should represent shallow-water, partly or completely restricted environments and may not reflect the global $\delta^{13}C_{carb}$ values. In fact, known $^{13}C_{org}$-rich carbonate formations are mostly associated with shallow water stromatolites, 'red beds' and evaporites formed in non-marine or in marine restricted intracratonic basins (Table 1). Therefore, the extreme enrichment in ^{13}C (above +5‰?) might well have been caused by local factors such as an intensive development of cyanobacteria, coupled with evaporation in restricted basins which were apparently not in full equilibrium with atmospheric CO_2. Furthermore, the Gunflint Formation carbonates deposited at ca. 2.09 Ga (Strauss and Moore, 1992) are considered to have formed in open marine environments: ''Heaviest $\delta^{13}C_{carb}$ values of siderite, and of dolomite in the Upper Limestone Member, are consistently near 0‰ (Fig. 5) throughout the stratigraphic section, indicating that marine bicarbonate was the source of carbon'' (Carrigan and Cameron,

1991, p. 347). If the proposed depositional age of the Gunflint Formation is constrained accurately then it should be coeval with the 2.09 Ga Jouttiaapa carbonates which have $\delta^{13}C_{carb}$ of +8.4‰ on average (Karhu, 1993; Karhu and Holland, 1996). Based on this, it is a debatable question as which of these two $\delta^{13}C_{carb}$ values, either the Gunflint 0‰ or the Jouttiaapa +8.4‰, reflects the global signal.

It is notable that the first red beds indicating free atmospheric oxygen seem to have appeared almost 200 Ma later than the first positive carbon isotope excursion (Fig. 5). Therefore, there need not be a direct link between the earliest positive carbon isotope shift, the world-wide development of red beds, and formation of oxygenated atmosphere, as has been suggested by Karhu and Holland (1996). We have to accept that a 'cause-and-effect' relationship between the excursion and a series of related phenomena is still not fully understood, and global $\delta^{13}C_{carb}$ values are not constrained.

5. Significance of the Tulomozerskay Formation carbonates in a global context

In order to cover some gaps in our knowledge related to the Palaeoproterozoic $\delta^{13}C$ excursion, an international project was launched entitled 'Worldwide 2 billion-year-old isotopically heavy carbonate carbon: the evolutionary significance and driving forces'. The two year-long project is supported by INTAS-RFBR (Brussels–Moscow) and aims to contribute new data on one of the most challenging problems in Palaeoproterozoic Earth history. This article presents some results obtained by the international research group working in the framework of this project.

To date, most reported high $\delta^{13}C$ values for Palaeoproterozoic successions are based on scattered samples that have limited information on depositional and post-depositional environments (e.g., Schidlowski et al., 1976; Karhu, 1993; Baker and Fallick, 1989a,b; Melezhik and Fallick, 1996a), and no detailed sampling was undertaken for deciphering mid- to small-scale fluctuations.

The following sections focus on the ca. 2 billion-year-old carbonate formation of the Onega Lake area, Russian Karelia (Fig. 6). The Onega Lake area is an example of a Palaeoproterozoic shallow water carbonate platform. The 2300-m thick carbonate–shungite rock [1] succession has been intensively drilled. Consequently, drill core material has become available enabling detailed litho- and chemostratigraphic subdivision as well as palaeontological study. The Onega Lake area occupies an exceptional position in the Palaeoproterozoic high $\delta^{13}C$ records, as reported in the literature, because ^{13}C-rich carbonates have a relatively low metamorphic grade and are both extensively and thickly developed.

This paper addresses the questions: (1) Are there any mid- to small-scale variations in $\delta^{13}C$ and $\delta^{18}O$, and is so in what range?; (2) Are any such variations environmentally dependent?; (3) To what mechanism might measured fluctuations of $\delta^{13}C$ and $\delta^{18}O$ values be ascribed?

6. Analytical methods

Whole-rock oxygen and carbon isotope analyses were carried out at Scottish Universities Research and Reactor Centre using the phosphoric acid method of McCrea (1950) as modified by Rosenbaum and Sheppard (1986) for operation at 100°C. Carbon and oxygen isotope ratios were measured on a VG SIRA 10 mass spectrometer. Calibration to international reference material was through NBS 19 and precision (1σ) for both isotope ratios is better than ± 0.2‰. Oxygen isotope data were corrected using the fractionation factor 1.00913 recommended by Rosenbaum and Sheppard (1986) for dolomites. The $\delta^{13}C$ data are reported in per mil (‰) relative to PDB and the $\delta^{18}O$ data in ‰ relative to SMOW.

The major and trace elements were analysed by X-ray fluorescence spectrometry at NGU using a Philips PW 1480 X-ray spectrometer. The accuracy (1σ) is typically better than 2% of the oxide present (SiO_2, Al_2O_3, MgO, CaO). The analytical uncertainties (1σ) for Sr, MnO Fe_2O_3 are better than ± 5.5 ppm, ± 0.01% and ± 0.01%, respectively. The ana-

[1] Shungite is a mineral comprising partly crystallised, non-graphitized, reduced, free carbon. The mineral was discovered a 100 years ago in Karelia, near the tiny village of Shunga from which its name originates. Later, all rocks (chert, dolostone, limestone, siltstone, tuff) containing the mineral shungite have been termed by Russians as 'shungite rocks'.

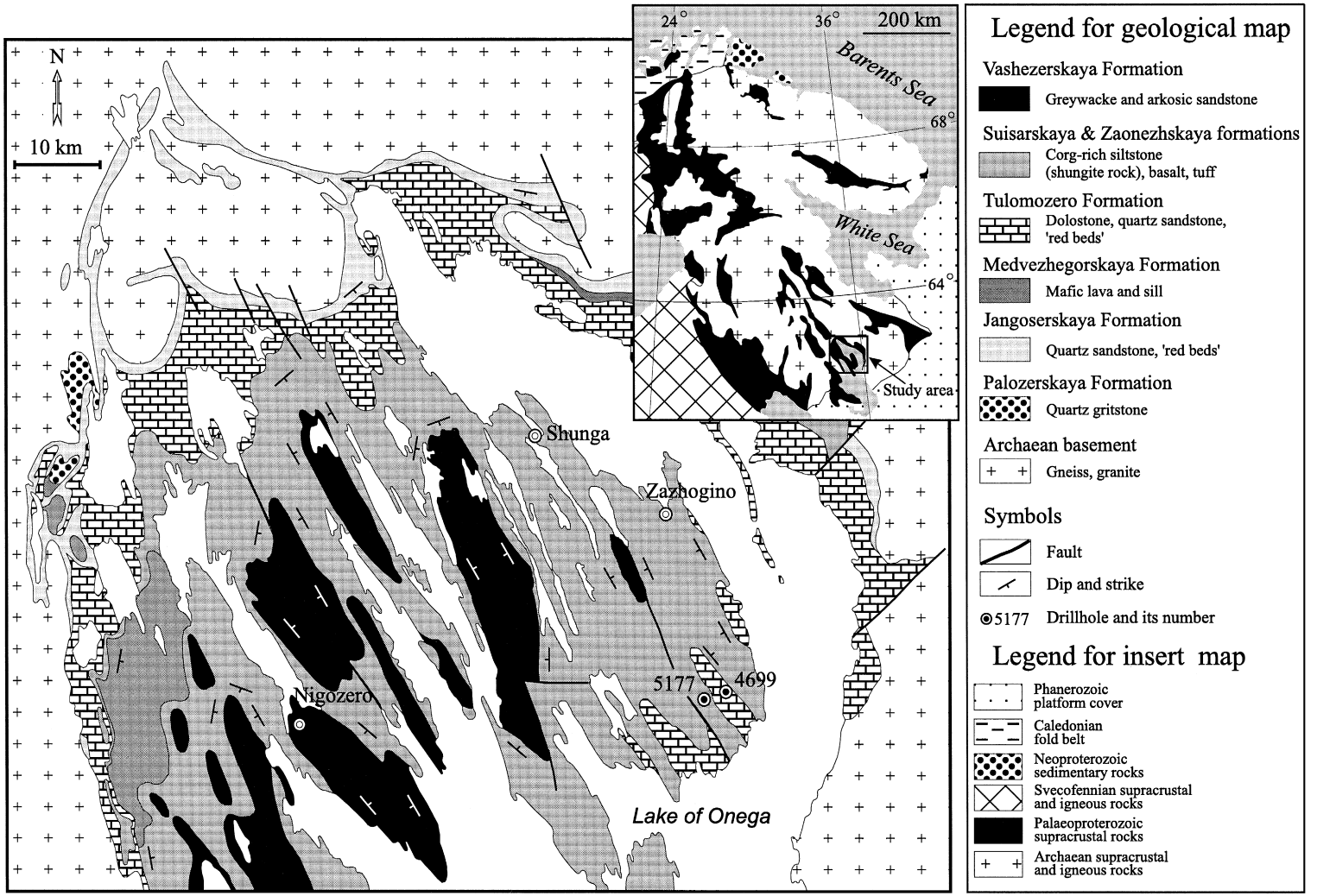

Fig. 6. Geographical and geological location of the study area (inset map), and geological map of the northern Onega Lake area (simplified from Akhmedov et al., 1993).

Table 2
Instrumental accuracy and precision of Philips PW 1480 X-ray spectrometer shown by six runs on synthetic standard ZGI-KH

	SiO_2 (%)	Al_2O_3 (%)	Fe_2O_3 (%)	TiO_2 (%)	MgO (%)	CaO (%)	Na_2O (%)	K_2O (%)	MnO (%)	P_2O_5 (%)	Sr (ppm)
Accepted	8.6	2.39	0.92	0.13	0.74	47.8	0.13	0.41	0.088	0.121	545
Run 1	8.5	2.69	0.96	0.15	1.35	46.4	0.28	0.43	0.100	0.116	592
Run 2	8.6	2.69	0.97	0.15	1.34	46.4	0.28	0.42	0.099	0.117	594
Run 3	8.6	2.68	0.96	0.15	1.35	46.4	0.28	0.43	0.100	0.119	590
Ran 4	8.5	2.68	0.96	0.15	1.33	46.4	0.28	0.42	0.098	0.122	588
Ran 5	8.6	2.68	0.96	0.15	1.34	46.4	0.29	0.43	0.100	0.125	594
Average	8.6 ± 0.04	2.69 ± 0.004	0.96 ± 0.004	0.15 ± 0	1.34 ± 0.007	46.4 ± 0	0.280 ± 0.004	0.420 ± 0.005	0.0990 ± 0.0001	0.1200 ± 0.004	592 ± 3

lytical accuracy and precision may be also evaluated from multiple analyses of the synthetic carbonate standard presented in Table 2.

From several samples, acid-soluble Sr concentration was additionally measured using standard isotope dilution and solid-source mass spectrometry (Finnigan MAT 261) at the Institute of Precambrian Geology and Geochronology in St. Petersburg, Russia. Duplicate analyses have been made in order to assess the accuracy of Sr measurements using a Philips PW 1480 X-ray spectrometer. Duplicate analyses are reported in Table 3. As the discrepancy in most cases is below 10% we have used the results obtained by a X-ray spectrometer.

Back-scattered electron images, electron-probe microanalyses and cathodoluminescence of carbonate minerals were carried out at IKU Petroleum Research in Trondheim. A SEM Microprobe Jeol733, NORAN Instruments with a silicon/lithium detector and NORWAR window-type has been used. The operating conditions were as follows: take-off angle = 40°, acceleration voltage = 15 kV, beam current = 15 nA, beam diameter = 1 μm, and working distance = 11 mm.

Table 3
Discrepancy of Sr (ppm) measurements by using a Philips PW 1480 X-ray spectrometer and solid-source mass spectrometry on a Finnigan MAT 261

Depth (m)	Sr*	Sr**	Discrepancy (%)
Drill hole 5177			
349.5	47	44.1	6.2
351.7	39	35.9	7.9
356.0	70	64.2	8.3
366.0	77	71.6	7.0
380.4	44	42.8	2.7
391.5	49	46.4	5.3
392.7	24	26.4	−10.0
449.8	203	191	5.9
542.0	219	194	11.4
542.5	185	177	4.3
554.5	169	154	8.9
556.0	166	157	5.4
563.0	83	80.9	2.5
569.5	193	185	4.1
Drill hole 4699			
512.0	130	117	10.0
527.5	491	531	−8.1
530.0	449	438	2.4
535.5	396	484	−22.2
560.0	70	90.0	−28.6
761.5	215	276	−28.4

Sr*: Total Sr values determined by using a Philips PW 1480 X-ray spectrometer.
Sr**: Acid soluble Sr values determined by using standard isotope dilution and solid-source mass spectrometry on a Finnigan MAT 261.
Discrepancy = $100 \times (Sr^{*} - Sr^{**})/Sr^{*}$.

7. Geological background

The Tulomozerskaya siliciclastic–carbonate succession is one of the Palaeoproterozoic formations which are preserved in a synform exposed on the northern side of the Lake Onega, as well as on its islands and peninsulas (Fig. 6). The entirely Palaeoproterozoic sequence of the N. Onega Lake area includes seven formations (Fig. 7, Sokolov, 1987). The lowermost Palozerskaya basal polymict conglomerates unconformably overlie the Archaean substratum. The following 50–120-m-thick Jangozersakaya Formation rests either conformably on the Palozerskaya conglomerates or unconformably on weathered Archaean gneisses and granites. The Jangozersakaya strata are composed of predominantly oxidised, red terrigenous sediments and subordinate calcareous siltstones. All rocks are cross-bedded and marked by desiccation cracks. This unit is conformably overlain by the 70-m-thick Medvezhegorskaya Formation consisting of mafic lava with subordinate cross-bedded quartz sandstones, gritstones and ‘red beds’. The Tulomozerskaya Formation conformably overlies the Medvezhegorskaya succession. The formation is described in detail in following sections. The Tulomozerskaya carbonates are unconformably overlain by C_{org}-rich rocks (shungite) with subordinate dolostones of the 1500-m-thick Zaonezhskaya Formation. This is followed by the Suisarskaya Formation, a 400-m-thick unit of basalts intercalated with numerous gabbro sills. A gabbro intrusion from the upper part of the Suisarskaya Formation has given a Sm–Nd mineral isochron age of 1980 ± 27 Ma (Pukhtel et al., 1992). The succession ends with the 190-m-thick Vashezerskaya Formation comprising greywacke and arkosic sandstones.

The Palaeoproterozoic rocks were deformed and underwent greenschist facies metamorphism during

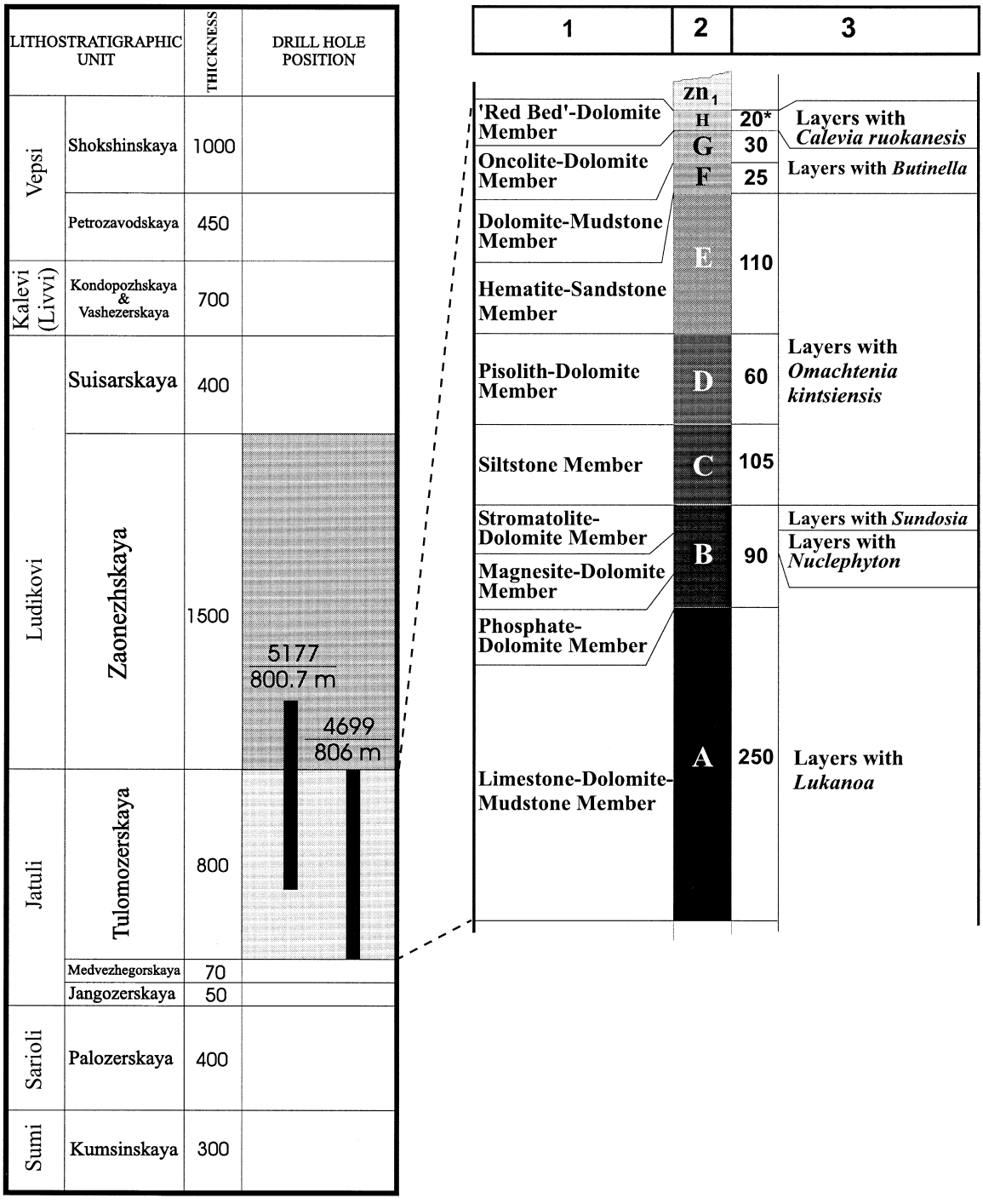

Fig. 7. Stratigraphic position of the studied drill holes and lithostratigraphical subdivisions of the northern Onega Lake area as suggested by: (1) Akhmedov et al. (1993), (2) present authors, (3) Makarikhin and Medvedev (cited in Akhmedov et al., 1993). The thickness is shown in metres as measured in drill hole 4699 (Member A) and 5177 (Members B, C, D, E, F, G and H). zn_1 is the Zaonezhskaya Formation.

the 1.8 Ga Svecofennian orogeny. The paragenesis chlorite–actinolite–epidote reflects a temperature of 300–350°C.

8. Lithostratigraphical subdivision of the Tulomozerskaya Formation

Drill core samples of carbonates analysed in this study were obtained from the drill holes 5177 (35°25′00″E, 62°14′29″N) and 4699 (35°28′00″E, 62°14′30″N), which intersected an 800-m-thick Tulomozerskaya succession (Fig. 7) located in the southeastern part of the Onega palaeobasin (Fig. 6).

Based on the lithology and mineralogical composition, the Tulomozerskaya Formation has been divided into a number of 'piles' (Akhmedov et al., 1993) renamed here as 'members' (Fig. 7), in accordance with the International Stratigraphic Code (ISSC, 1976). For practical reasons and for consistency we have substituted letters for Russian names,

Table 4
Lithostratigraphic characteristics of the Tulomozerskaya Formation (based on Melezhik et al., 1999a; submitted)

Member	Thickness (m)	Lithofacies	Rock assemblage	Colour	Stromatolite morphology
H	20	VII, X	Finely laminated dolostone and dolomitic marl	Red	Spaced, low-relief, bioherms, flat-laminated stomatolites.
G	30	X	Dolostone	Pink, brown	Very close-spaced bioherms, oncolites.
F	25	III, V	Siltstone, sandstone, dolostone, amygdaloidal basalt		Flat-laminated stromatolites, oncolites.
E	110	III, V, X	Quartz sandstone, siltstone with a carbonate matrix; two-three intervals of dolostone	Pink	Flat-laminated stromatolites.
D	60	IV, V, VIII IX, X	Dolostone with magnesite layers, dolostone collapse breccia, siltstone	Grey, pink	Oncolites; spaced, single, large, columns; laterally continuous biostromes.
C	105	IV, V, VIII X	Finely laminated siltsone and sandstone intercalated with dolostone	Red	Laterally continuous biostromes; flat-laminated stromatolites; oncolites.
B	90	I, VI, IX, X	Dolostone with 1 to 2 m thick magnesite band quartz sandstone	Pale grey	Laterally continuous biostromes; spaced bioherms; spaced, single, large columns; oncolites; flat-laminated stromatolites.
A	250	I, II, IV, V, VIII, IX, X	Dolostone alternating with quartz sandstone and finely laminated siltsone	Pink	Flat-laminated stromatolites; markedly divergent, small, columnar, stromatolites.

Table 5
Lithofacies and their palaeoenvironmental interpretation (based on Melezhik et al., 1999a; submitted)

Litho-facies	Rock assemblage	Rock colour	Bedding and lamination	Cement	Specific structural feature	Suggested palaeoenvironmental interpretation
X	Micritic and sparry stromatolitic dolostones	Red, beige, white	Laminated	Not preserved	Tepee, tepee-related breccias, desiccation cracks	See Table 4
IX	Micritic, crystalline, stromatolitic magnesite	White, pale yellow	Massive, laminated	Not preserved	–	Playa, sabkha environment
VIII	Dolomite collapse breccias	Brown, red	–	Sericite, chlorite, hematite	–	Subsurface dissolution of halite/sulphate in playa, sabkha environment
VII	Micritic allochemical dolostones	Red	Thinly-laminated	Not preserved	Allochems are exclusively dolomitic oolites	Lower energy tidal zone
VI	Sparry and micritic allochemical dolostones	Red	Structureless, crudely stratified	Syntaxial dolomite spar	Gypsum pseudomorphed by cauliflower-like quartz aggregates	Low energy protected bights
V	Crystalline dolostones	Beige, pink	Structureless, indistinct parallel-laminated	Not preserved	Desiccation cracks, dolomite pseudomorphed gypsum, tepee	Upper tidal zones of protected bights and lagoons
IV	Dolomite-rich sandstones and siltstone	Beige, pale pink	Herringbone cross-bedded, flaser-bedded, tidal-bedded	Not present	–	Low energy tidal and supratidal sandflat
III	Hematite siltstones and sandstones	Brown, red	Platty, cross-stratified	Dolomite	Mud cracks, low-relief hummocks, small-wave ripples, halite cube casts	Playa or ponded tidal flat under evaporitic condition
II	Sandstones and siltstones	Grey	Thin-bedded or lenticular-bedded	Dolomite, quartz	–	Occasionally flooded supratidal zone on a tidal flat
I	Quartz sandstones	Grey, red	Ripple-marked, cross-stratified or structureless	Quartz, sericite	Channels, tabular sets of cross-stratification, asymmetric ripples	Meandering fluvial system on a carbonate coastal plain

starting with 'A' for the lowermost Limestone–Dolomite–Mudstone Member (Fig. 7). The whole succession, consisting of the eight lithostratigraphic members (A–H), can also be divided into six biostratigraphic units each with distinctive stromatolites, oncolites and microfossils (Fig. 7). Lithostratigraphic Members A to H are characterised in Table 4.

9. Lithofacies and palaeoenvironments of the Tulomozerskaya Formation

Lithofacies analysis has been discussed in detail in Melezhik et al. (1999a, submitted). Drill core logging has revealed a series of lithofacies and their frequent variation in the stratigraphic column. The Tulomozerskaya lithofacies assemblage includes several groups, namely siliciclastic-dominated, mixed siliciclastic clastic–carbonate lithofacies and carbonate-dominated. The latter is subdivided into magnesite, non-stromatolitic dolostone lithofacies, and stromatolitic 'biofacies'. All lithofacies are marked by numbers from I to X starting from the lower part of the sequence. The lithofacies are summarised in Tables 5 and 6, and Figs. 8 and 9. The carbonate lithofacies are illustrated and briefly described in Fig. 10.

The overall palaeoenvironmental interpretation of the Tulomozerskaya sequence based on the lithofacies analysis along with stromatolite morphologies (in detail see Melezhik et al., 1999a, submitted) is that it represents a complex combination of shallow marine deposits and non-marine 'red beds' with evaporitic affinities. Although part of the carbonate rocks formed in peritidal shallow marine settings, the dolostones of Members A and C may be assigned to a restricted evaporative environment developed either in ephemeral ponds in upper tidal zones of a carbonate flat or in coastal sabkhas and playa lakes. The latter are especially typical for Member C carbonates. The main part of the Tulomozerskaya carbonates, which are interpreted to have formed in shallow marine conditions, display features of lower energy deposits, accumulated in protected environments. These could be either bights, lagoons or barred basins. Only a small proportion of carbonates developed in the middle part of Member B, in the

Table 6
Stromatolite morphologies and their palaeoenvironmental interpretation (based on Melezhik et al., 1999a; submitted)

Stromatolite morphology	Stratigraphic position	Suggested palaeoenvironmental interpretation
Lower relief, flat-laminated stromatolites.	Members A and E, lower part of Member B, middle part of Members C and F	Members A, B, C and F: drained depressions and ephemeral ponds in an upper tidal zone of carbonate flat. Member E: evaporative, playa lake environment.
Laterally continuous biostromes of columnar stromatolites.	Members A, C and H	Intertidal settings in protected bights.
Very close-spaced bioherms separated by laminated dolostones and red, structureless, dolorudites.	Member G	Sub-tidal settings.
Spaced bioherms with synoptic relief up to 20 cm.	Member B	Sub-tidal or intertidal settings, close to shorelines, fully exposed to wave action.
Spaced, single large columns, 0.2 m wide, up to 1.5 m high.	Very limited development in the lower part of Member D	Intertidal settings, close to shorelines, fully exposed to wave action.

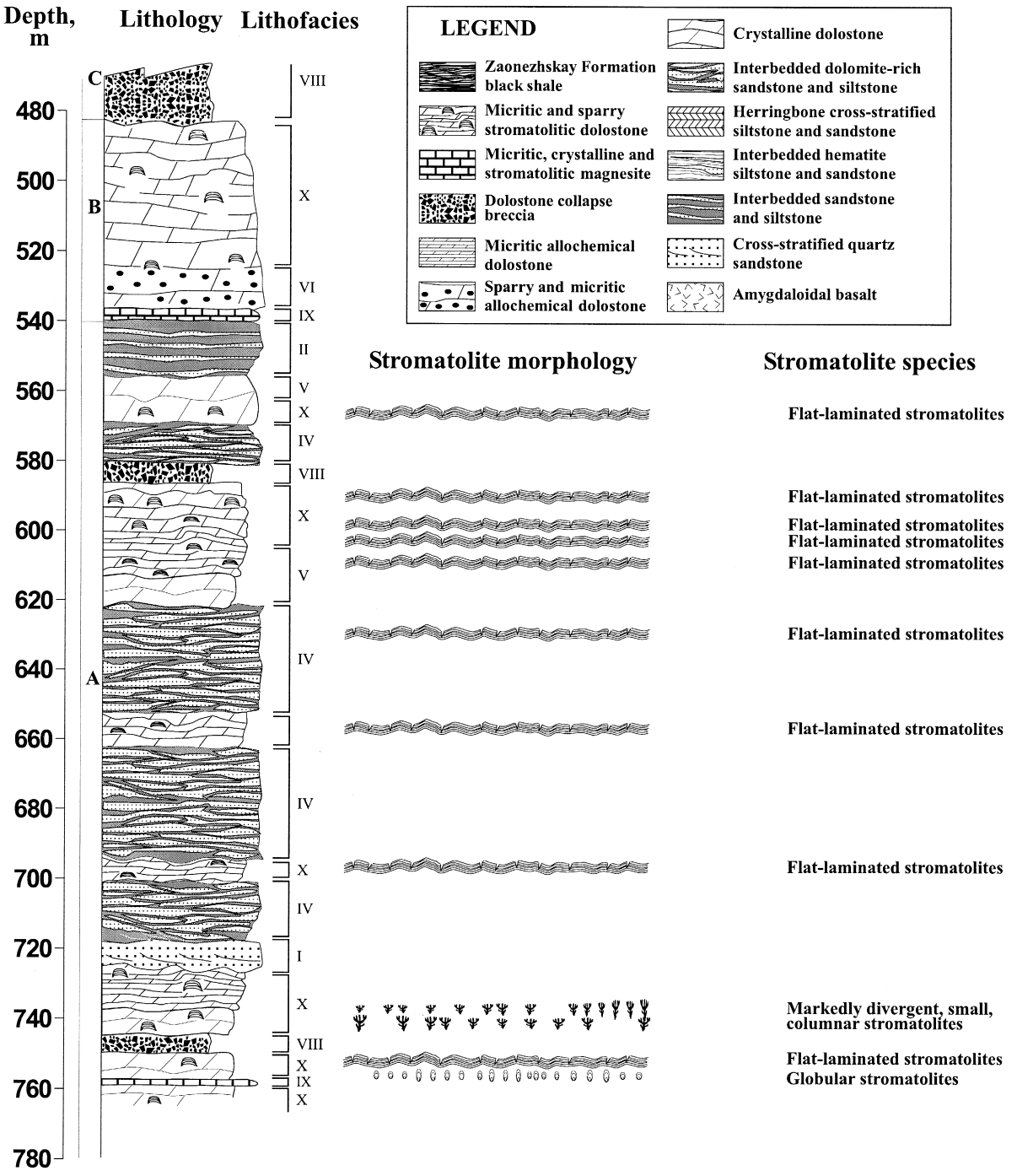

Fig. 8. Lithofacies and the main stromatolite morphologies vs. stratigraphy, drill hole 4699. Simplified after Melezhik et al. (1999a) (submitted).

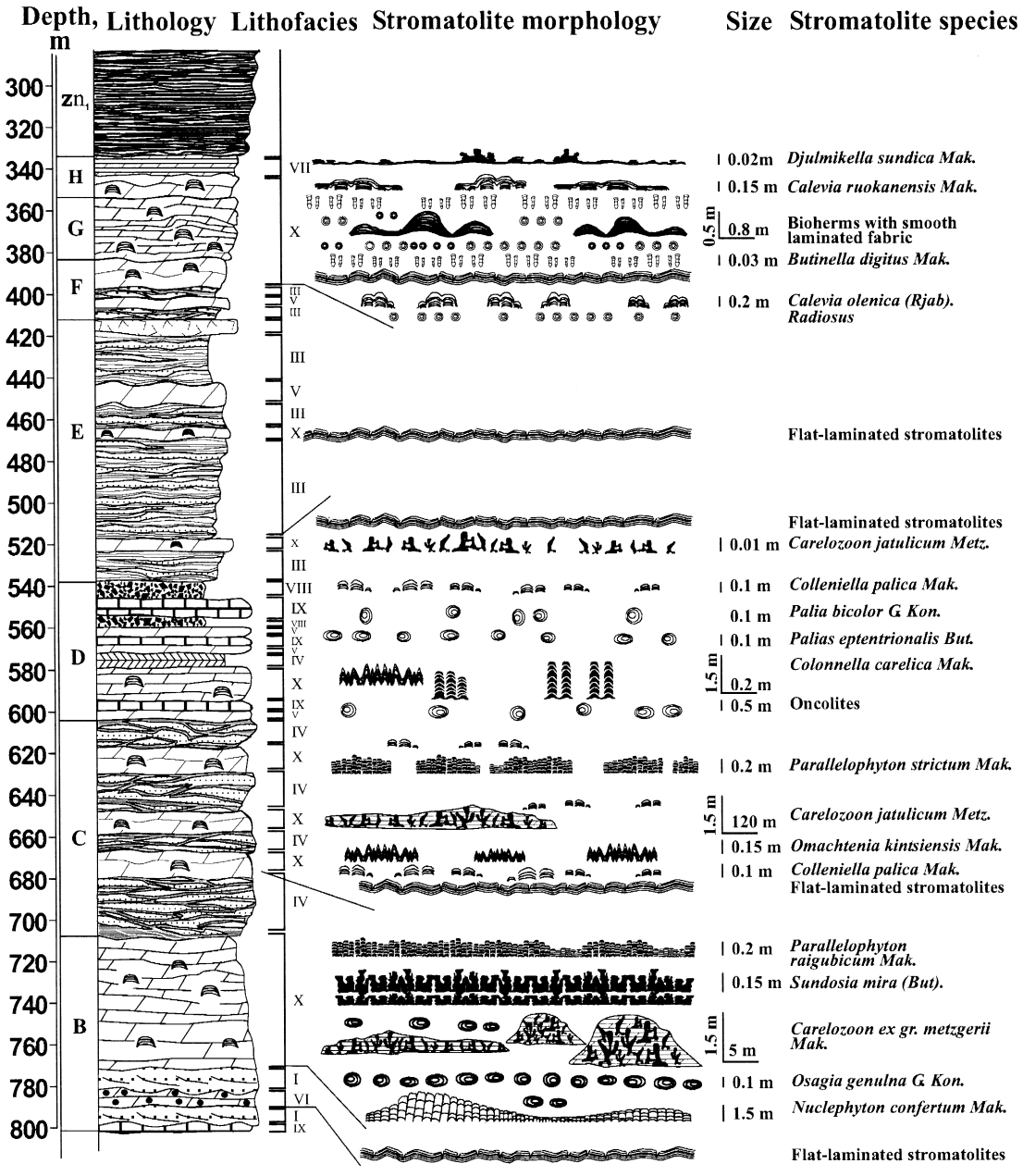

Fig. 9. Lithofacies and the main stromatolite morphologies vs. stratigraphy, drill hole 5177. For the legend see Fig. 8. Simplified after Melezhik et al. (1999a, submitted).

base of Member D, and particular in the upper part of Member G, may represent deposits which accumulated in relatively 'open' environments. They show some analogy to basins exposed to strong wave actions.

The magnesites are associated with dolomite collapse breccia and precipitated from seawater derived brine, diluted by meteoric fluids. Magnesitisation was accomplished under evaporitic conditions in sabkha to playa lake environment which was pro-

posed to be similar to the Coorong or Lake Walyungup coastal playa magnesite (Melezhik et al., 1999b, submitted).

10. Petrographic characteristics of carbonate rocks

Petrographic characteristics of the carbonates have been dealt with details in Melezhik et al. (1999a, submitted). All the carbonates underwent moderate recrystallisation though they contain some remnants of primary petrographic features. Cathodoluminescence did not show detectable differences between various carbonate phases and is therefore not discussed further.

Those dolostones in which only sparse primary petrographic features are preserved are referred to here as crystalline dolostones. This type is most common throughout the sequence.

Sparry allochemical dolostones, both dolarenites and dolorudites, are most abundant in Member A and the lower portion of Member B. Allochems are represented by intraclasts of micritic, oolitic and sparry dolomite, rounded quartz grains and sporadic hematite and siliceous oolites. Cement, when preserved, is represented by earlier (prior to burial), inclusion-rich, syntaxial dolomite spar overgrowths (Melezhik et al., 1999a, submitted). Burial, clear syntaxial dolomite overgrowths have rarely been documented. The matrix of sparry allochemical dolostones may be classified as crystalline dolomite and mosaic dolomite spar, both are rich in gas inclusions indicating diagenetic alteration at low water/rock ratios (e.g., Carpenter and Lohman, 1997).

Micritic allochemical dolorudites and dolarenites have a limited development. Allochems are represented exclusively by dolomitic oolites.

Stromatolitic dolostones have undergone recrystallisation. When fine lamination is preserved, the thin, dark laminae are predominantly dolomicrite and thicker, light laminae are dolospar.

The major developments of magnesite beds are composed of cryptocrystalline and crystalline both stromatolitic and non-stromatolitic magnesite. The crystalline magnesite consists of 0.1–0.5 mm idiomorphic or subidiomorphic magnesite crystals replacing either micritic aggregate of 15–10 μm magnesite crystals and subordinate dolomite rhombs or silty dolomitic micrite (Melezhik et al., 1999b, submitted). Cryptocrystalline magnesite is composed of micritic magnesite (5–10 μm) with remnants of dolomite. Micritic magnesite replaced dolomite in a texture-preserving manner. This produced very fine grained magnesite that apparently mimics the pre-magnesitisation texture of sediments. The magnesite originated during early diagenesis, if dolomite is considered to be a primary precipitate. Alternatively, magnesites formed somewhat later if dolomite is an early diagenetic replacement of a calcite precursor. The magnesite crystals replaced dolomite before the major portion of the burial carbonates formed (Melezhik et al., 1999a, submitted).

11. Geochemical results

Oxygen and carbon isotopes as well as major and trace elements have been measured from 54 whole-rock samples. Including the 19 values communicated in previous paper (Melezhik et al., 1999b, submitted), Table 7 list 73 values. Results of electron-probe microanalysis carried out on the selected samples are presented in Table 8.

The overall bulk rock chemical composition of Tulomozerskaya carbonates approximates to a sandy dolostone with rare magnesite. Limestones have not been observed among the collected samples. If magnesite-bearing layers are excluded the overall range of Mg/Ca ratio is 0.56–0.66 with an average value of 0.61 ± 0.07 which is very close to stoichiometric dolomite (0.62). Mg/Ca ratios of dolomite based on electron-probe microanalyses range 0.46–0.63 (Table 8). Syntaxial, inclusion-rich, burial dolomite cement is enriched in Mn as compared to the cemented intraclasts (Table 8, 4699–506.0) though their Mg/Ca ratios are similar.

Five thin layers of magnesite or magnesite-bearing dolostones detected in the whole succession are characterised by Mg/Ca ratios ranging from 2.5 to 26 (Fig. 11). Mg/Ca ratios of the mineral magnesite exhibit strong variations correlating with the petrographic characteristics. Large, neomorphic/metamorphic crystals of magnesite have high ratios in the range 230–663. Mg/Ca ratios of micritic magnesite drop to 108–172, which corresponds to 0.78–0.53 $CaCO_3$ wt.% (Melezhik et al., 1999b, submitted).

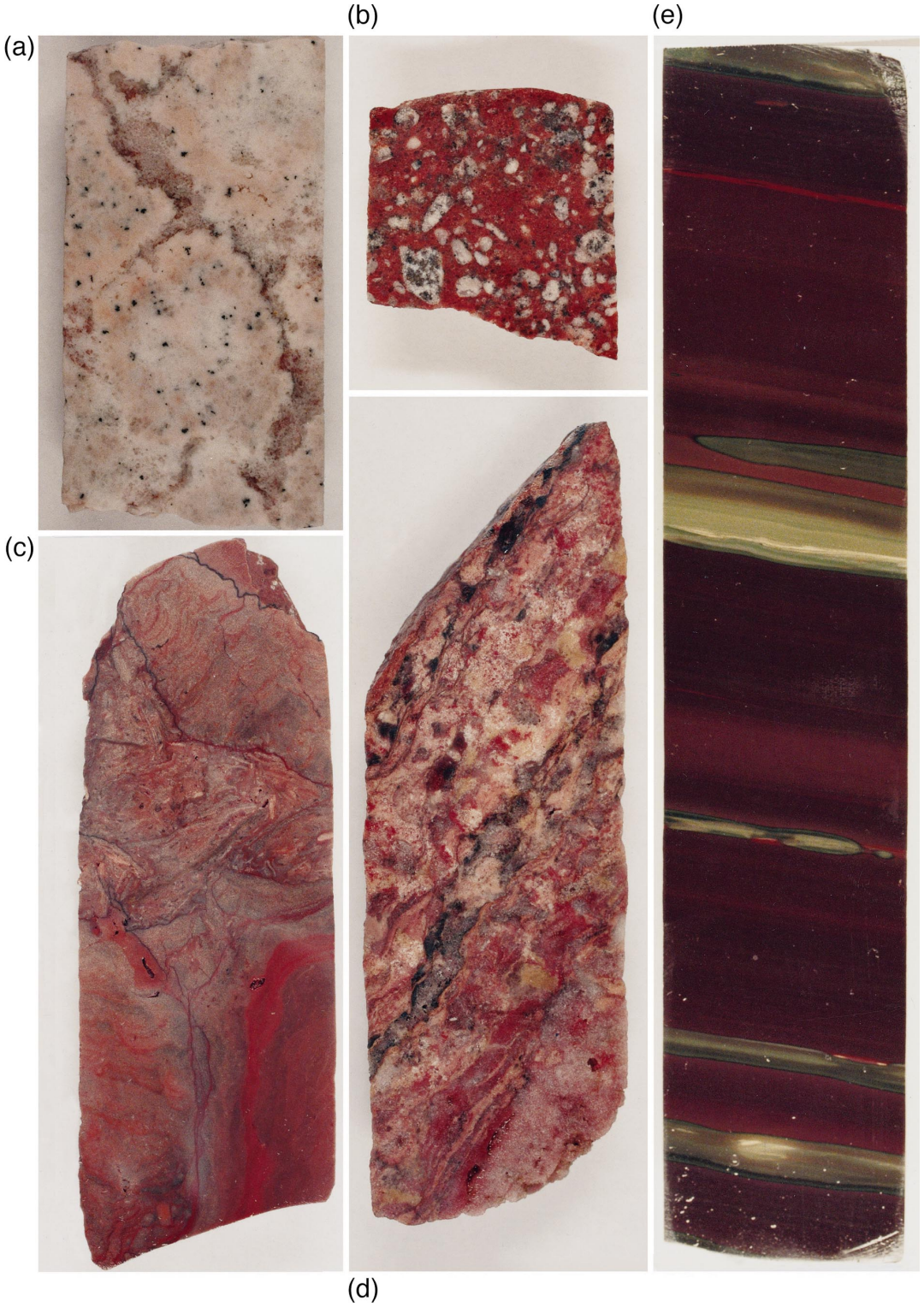
(a)
(b)
(c)
(d)
(e)

The whole-rock analyses show that the Sr content displays considerable variation with a range from < 5 to 491 ppm (Fig. 12). The average Sr values for the Members A–E carbonates (199, 138, 77, 130 and 129 ppm, respectively) are essentially higher than the average figures for the carbonates of the three uppermost Members, F, G, and H (26, 54 and 64 ppm, respectively). Sr does not exhibit any covariation with manganese content ($r \sim 0$). Scatter of Sr content in dolostones is also independent of the Mg/Ca ratio ($r = 0.18$), though the magnesite-bearing dolostones show depletion in Sr as the Mg/Ca ratio increases (Table 7).

The available O/C isotope measurements are summarised in Figs. 11 and 13. The spread of oxygen and carbon isotope values in the available data set is 17.5–26.0‰ (mean 22.3 ± 1.6‰), and from ± 5.6 to $+17.2$‰ (mean $+9.9 \pm 2.3$‰), respectively. The histogram of the carbon isotope data reveals two modes: a strong one at 9.4 ± 1.4‰ and a weaker one at $+16.5 \pm 0.8$‰ (Fig. 13). The first mode represents 93% of the samples studied. Four of the samples from the second population are dolostones highly enriched in ^{13}C which are located in the lowermost part of the succession (Member A), and one sample is derived from Member B (Fig. 11). The carbon isotope values demonstrate an erratic decrease upwards in the sequence from $+17.2$‰ in the lowermost part of the Member A to $+8.0$‰ in Member C (Fig. 11). Higher up in the succession overall, the observed values $\delta^{13}C$ values of Members D–H are less variable and fall within the range from $+7.3$ to $+10.1$‰. The only exception to this pattern is the four samples from the lower portion of Member H carbonates with $\delta^{13}C$ of ± 5.6 to $+6.6$‰. Oxygen isotope composition is less variable and exhibits no apparent systematic variation related to the stratigraphy (Fig. 11).

Cross-plots reveal no statistically significant covariation between $\delta^{13}C$ and $\delta^{18}O$ ($r = 0.14$, Fig. 14a). No covariations are observed between the Mg/Ca ratio and C/O isotopes, nor between Mn, Mn/Sr and C/O isotopic values (Fig. 14b, d, e, f, h, i). Sr and $\delta^{13}C$ show positive covariation ($r = 0.50$, Fig. 14c), although, perhaps surprisingly, Sr and $\delta^{18}O$ exhibit no covariation ($r \sim 0$, Fig. 14g).

12. Evaluation of diagenesis

The studied carbonate samples are composed entirely of dolostones apart from five magnesite-bearing samples. Dolomite is generally considered as essentially a diagenetic mineral. Nonetheless, there is growing evidence that precipitation of dolomite in the Precambrian was either coeval with calcite, or that dolomitisation was an early diagenetic phenomenon caused by waters isotopically comparable to that of seawater (e.g., Veizer and Hoefs, 1976; Veizer et al., 1990, 1992a,b).

12.1. Oxygen isotopes

Several geochemical screening methods for evidence of diagenetic alteration are possible. Hudson (1977) found that oxygen isotopes may be a sensitive indicator of diagenetic alteration. Diagenesis commonly decreases $\delta^{18}O$ and the effect of diagenesis can be revealed by $\delta^{13}C$ and $\delta^{18}O$ cross-plot. Oxygen isotopes are commonly much more easily af-

Fig. 10. Photographs of drill core illustrating sedimentological features of rocks of the Tulomozerskaya Formation. (a) Bedding surface between two pale pink dolostone layers extended from left upper to lower right corner. The bedding surface is marked by desiccation cracks filled with sandy material (light grey). Drill hole 5177, depth 604.0 m. The lowermost part of Member D, Lithofacies V, upper tidal zone of protected lagoon. (b) Red, structureless dolorudite. Intraclasts are oolitic dolostones (white and grey) and red, hematite rich, sparry and micritic dolostones (red). Drill hole 4699, depth 535.5 m. The lower part of Member B, Lithofacies VI, low energy protected bight. (c) Red breccia of stromatolitic dolostones related to a tepee structure. Note marginal reddening of some of the fragments (lower right corner) which suggests that breccia was exposed to air and subjected to oxidation. Drill hole 5177, depth 670.0 m. Member C, Lithofacies X, upper tidal zone of carbonate flat. (d) Red, flat-laminated, weakly domed stromatolites with fenestrae (blister stromatolite). Stromatolite laminae are cracked and syngenetically brecciated which resulted in the development of clotted fabric. Drill hole 5177, depth 660.0 m. Member C, Lithofacies X, drained depressions and ephemeral ponds in an upper tidal carbonate flat. (e) Red, finely laminated siltstone. Note light coloured bleaching zones and 'rolls structure' developed along more permeable sandstone layers. Bleaching is due to the introduction of reducing solutions to red siltstone. Solutions were likely derived from overlying C_{org}-rich sediments of the Zaonezhskaya Formation during late diagenesis-catagenesis. Beds are transitional from the Tulomozerskaya to the Zaonezhskaya Formation, lacustrine environment. Core diameter in all cases is 42 mm.

Table 7
Chemical composition of Tulomozerskaya Formation carbonate rocks from the Onega area, Russian Karelia

Depth (m)	SiO_2 (%)	Al_2O_3 (%)	Fe_2O_3 (%)	MgO (%)	CaO(%)	Na_2O(%)	MnO(%)	F (%)	Sr (ppm)	$\delta^{13}C$ (‰)	$\delta^{18}O$ (‰)	Mg/Ca	Ca/Sr	Mn/Sr
Drill hole 5177														
335.0	n.d.	n.d.	n.d.	n.d.	n.d.	n.d.	n.d.	n.d.	n.d.	8.3	20.0	n.d.	n.d.	n.d.
337.5	n.d.	n.d.	n.d.	n.d.	n.d.	n.d.	n.d.	n.d.	n.d.	9.2	25.0	n.d.	n.d.	n.d.
344.0	15.80	0.67	0.17	18.26	23.51	0.12	0.01	0.54	101	9.1	21.0	0.66	1653	0.76
344.6	2.71	0.21	0.14	22.25	30.63	0.13	0.02	0.48	115	5.7	20.0	0.61	1891	1.34
347.0	0.76	0.23	0.15	23.71	31.51	0.13	0.01	0.51	134	8.5	21.1	0.64	1670	0.57
349.5	1.41	–	0.11	21.75	31.64	0.15	0.03	0.46	47	6.2	22.6	0.58	4780	4.91
351.2	33.33	–	0.05	14.68	21.14	0.12	0.02	0.27	24	6.6	22.2	0.59	6254	6.42
351.7	0.78	–	0.08	22.27	32.04	0.15	0.03	0.47	39	5.6	22.4	0.59	5833	5.92
356.0	6.69	–	0.04	20.24	28.89	0.16	0.02	0.46	70	8.9	23.7	0.59	2930	2.20
359.6	6.49	–	0.06	19.79	28.99	0.16	0.01	0.40	51	8.9	24.7	0.58	4036	1.51
360.0	8.62	–	0.07	19.07	28.12	0.14	0.04	0.37	29	9.2	23.5	0.57	6885	10.62
366.0	–	–	0.03	23.23	32.55	0.13	0.04	0.48	77	9.2	22.1	0.60	3001	4.00
380.4	1.13	–	0.03	21.95	31.92	0.14	0.03	0.43	44	8.9	23.8	0.58	5151	5.25
391.5	1.7	–	–	21.75	31.61	0.14	0.04	0.44	49	8.4	25.1	0.58	4580	6.29
39.02	13.03	–	0.01	17.57	25.81	0.14	0.02	0.33	20	7.9	26.0	0.58	9163	7.70
392.7	11.81	–	0.01	17.80	26.57	0.14	0.03	0.34	24	7.3	25.2	0.57	7860	9.63
395.2	9.04	–	0.01	19.42	27.67	0.14	0.04	0.35	15	8.5	21.7	0.59	13097	20.53
403.2	12.74	–	0.07	17.11	25.83	0.15	0.37	0.35	21	9.2	22.7	0.56	8733	135.67
448.0	9.19	–	0.03	18.85	27.68	0.14	0.15	0.34	87	8.4	22.3	0.58	2259	13.28
449.8	0.44	–	0.04	22.48	32.07	0.13	0.17	0.45	203	8.8	21.7	0.59	1122	6.45
520.0	16.41	0.37	0.17	16.54	23.85	0.13	0.02	0.38	97	10.1	20.8	0.59	1746	1.59
542.0[a]	1.28	–	0.02	21.94	31.78	0.14	0.25	0.43	219	9.0	18.6	0.58	1030	8.79
542.5[a]	2.77	–	0.02	21.46	30.90	0.14	0.17	0.41	185	8.9	19.6	0.59	1186	7.08
553.5[a]	13.96	–	–	26.06	0.83	–	0.17	–	5	9.0	23.1	26.53	1179	261.80
554.5[a]	–	–	0.02	22.78	32.39	0.13	0.08	0.44	169	7.9	21.8	0.59	1361	3.64
555.5[a]	1.54	–	0.02	22.50	31.37	0.13	0.07	0.45	158	8.1	21.8	0.61	1410	3.41
556.0[a]	0.23	–	0.02	22.43	32.15	0.13	0.07	0.46	166	8.0	22.2	0.59	1375	3.25
560.5[a]	7.54	–	0.02	19.27	28.29	0.14	0.07	0.40	118	9.3	21.7	0.58	1702	4.57
563.0[a]	13.21	–	0.02	17.63	25.16	0.13	0.01	0.34	83	9.3	17.5	0.59	2152	0.93
568.5[a]	–	–	–	30.62	3.51	–	0.19	–	11	9.4	24.3	7.37	2266	133.00
569.5	0.12	–	0.02	22.73	32.12	0.13	0.06	0.46	193	n.d.	n.d.	0.60	1182	2.39
584.5[a]	34.13	0.25	0.14	14.06	20.53	0.13	0.09	0.25	82	7.9	21.1	0.58	1778	8.45
593.0[a]	7.58	–	0.03	19.63	28.26	0.14	0.05	0.38	181	8.2	21.7	0.59	1109	2.13
598.7[a]	8.19	1.60	0.35	26.78	9.07	–	0.05	–	62	9.6	21.4	2.50	1039	6.21
599.0[a]	3.86	0.45	0.24	21.96	29.50	0.13	0.06	0.43	193	8.3	22.5	0.63	1085	2.39
654.0	37.84	–	0.03	12.25	18 00	0.12	0.03	0.20	73	7.8	21.1	0.58	1751	3.16
678.5	35.92	0.75	0.19	14.26	18.31	0.11	0.02	0.27	81	8.3	22.1	0.66	1605	1.90

718.0	10.31	3.11	0.93	19.26	25.31	0.15	0.07	0.43	87	9.1	23.4	0.64	2066	6.20
720.0	7.31	2.11	0.66	20.22	27.45	0.38	0.09	0.42	83	8.9	23.6	0.62	2348	8.35
724.5	7.47	2.00	0.84	19.83	27.16	0.38	0.09	0.42	80	10.7	24.8	0.62	2410	8.66
727.0	37.02	7.98	3.49	15.83	13.97	1.45	0.09	0.50	50	9.3	22.1	0.96	1984	13.86
729.0	11.27	2.94	1.76	19.46	24.75	0.46	0.08	0.40	82	9.7	23.1	0.66	2143	7.51
732.5	2.51	0.57	0.24	22.46	30.61	0.17	0.10	0.43	107	9.8	24.3	0.62	2031	7.20
757.0	34.40	0.71	0.24	15.43	19.22	0.10	0.02	0.33	144	10.5	20.7	0.68	948	1.07
760.0	48.87	–	0.03	9.23	12.68	–	0.02	–	112	16.0	23.0	0.62	804	1.38
764.5	2.78	0.30	0.11	21.67	30.61	0.16	–	0.55	65	10.7	23.3	0.60	3344	0.59
766.5	6.73	0.14	0.09	20.31	28.51	0.15	–	0.52	69	10.6	22.9	0.60	2934	0.56
767.5	8.04	0.08	0.08	19.43	27.91	0.16	–	0.53	66	10.2	23.6	0.59	3002	0.58
788.0	n.d.	n.d.	n.d.	n.d.	n.d.	0.16	n.d.	0.57	67	10.6	22.8	n.d.	n.d.	n.d.
796.5	n.d.	n.d.	n.d.	n.d.	n.d.	0.13	n.d.	0.37	318	10.7	22.0	n.d.	n.d.	n.d.
799.0	n.d.	n.d.	n.d.	n.d.	n.d.	–	n.d.	–	71	11.3	20.9	n.d.	n.d.	n.d.
Drill hole 4699														
493.5	34.12	0.88	0.32	16.3	19.19	0.20	0.03	0.35	97	10.3	21.4	0.72	1405	2.38
497.5	39.83	0.28	0.15	12.11	16.38	–	0.02	0.27	71	10.1	20.6	0.62	1638	2.17
506.0	13.35	–	0.05	17.69	25.39	0.13	0.03	0.41	109	10.4	21.0	0.59	1654	2.12
512.0	0.22	–	0.04	22.56	32.08	0.14	0.02	0.52	130	10.2	21.9	0.59	1752	1.18
514.0	18.46	0.31	0.14	15.66	22.52	0.13	0.01	0.30	92	10.6	21.0	0.59	1738	0.84
516.5	37.27	0.15	0.08	12.54	18.26	0.11	–	0.22	67	10.6	21.3	0.58	1935	0.57
522.5[a]	15.30	0.10	0.08	17.05	24.75	0.14	0.04	0.32	55	9.6	21.6	0.58	3195	5.60
524.1[a]	7.79	–	0.02	19.41	28.32	0.15	0.06	0.43	75	9.3	20.9	0.58	2681	6.16
527.5[a]	4.51	–	0.06	21.43	29.65	0.13	0.04	0.55	491	10.8	23.0	0.61	429	0.63
530.0[a]	1.47	–	0.04	21.99	31.36	0.13	0.04	0.53	449	10.9	23.3	0.59	496	0.69
535.5[a]	14.70	–	0.02	17.47	24.56	0.12	0.04	0.34	396	11.1	22.0	0.60	440	0.78
537.5[a]	1.50	–	0.02	32.80	10.58	–	0.05	–	151	11.2	21.0	2.62	497	2.55
560.0	37.51	–	0.03	12.20	18.45	0.11	0.03	0.24	70	11.0	20.7	0.56	1871	3.30
566.5	36.15	0.83	0.16	18.58	15.92	–	0.03	0.43	120	13.1	25.2	0.99	942	1.93
589.0	8.31	0.04	0.08	19.85	27.76	0.14	0.12	0.41	173	11.2	23.2	0.60	1139	5.34
595.5	45.92	2.39	0.28	8.94	12.95	0.14	0.05	0.11	189	11.4	22.3	0.58	486	2.04
660.0	1.38	0.48	0.26	22.78	31.20	0.13	0.18	0.54	33	12.2	21.1	0.62	6713	42.00
732.0	2.25	0.03	0.02	22.04	30.89	0.15	0.05	0.43	406	16.6	24.1	0.60	540	0.95
750.0	15.13	5.47	1.50	17.79	21.17	0.13	0.07	0.35	381	16.8	23.2	0.71	395	1.41
756.0	16.55	1.46	0.43	17.45	22.86	0.12	0.04	0.33	97	n.d.	n.d.	0.65	1673	3.18
758.0	6.70	0.60	0.13	26.09	19.75	0.12	0.04	0.26	308	17.2	22.2	1.12	455	1.00
761.5	16.20	–	0.01	16.61	23.76	0.16	0.05	0.29	215	16.0	22.4	0.59	785	1.79

[a] Samples incorporated from Melezhik et al. (1999b).

n.d., not determined; dashes, below detection limit. Detection limit is < 0.1 for SiO_2, < 0.01 for Al_2O_3, Fe_2O_3, Na_2O, MnO, F and < 5 for Sr.

Table 8
Electron-probe microanalyses of carbonate minerals from the Tulomozerskaya Formation

Component	5177–796.5												4699-506.0					
	Recrystallised dolomitic, micritic, oolite										Cement, syntaxial dolomite	Matrix, dolomite spar	Dolomite allochem			Cement, syntaxial dolomite		
	Core			Mantle				Rim										
	1[c]	2[c]	Average	3[c]	4[c]	5[c]	Average	6[c]	7[c]	Average	8[c]	9[c]	10[c]	11[c]	Average	12[c]	13[c]	Average
MgO[a]	30.87	31.92	31.40	35.87	35.14	36.11	35.71	32.70	31.80	32.25	38.65	38.49	37.93	38.22	38.08	36.59	37.46	37.03
FeO[a]	0.04	0.15	0.10	0.37	0.00	0.00	0.12	0.00	0.00	0.00	0.00	0.22	0.34	0.00	0.17	0.19	0.00	0.10
CaO[a]	66.95	66.92	66.94	62.40	62.36	63.10	62.62	66.07	66.80	66.44	60.09	60.92	60.73	61.55	61.14	62.48	61.72	62.10
MnO[a]	0.25	0.12	0.19	0.51	1.36	0.49	0.79	0.00	0.61	0.31	0.46	0.00	0.00	0.00	0.00	0.32	0.31	0.32
Sum	98.11	99.11		99.15	98.86	99.70		98.77	99.21		99.20	99.63	99.00	99.77		99.58	99.49	
$MgCO_3$[b]	35.14	35.93	35.53	40.11	39.46	40.13	39.90	36.86	35.77	36.32	42.97	42.63	42.30	42.28	42.29	40.68	41.62	41.15
$FeCO_3$[b]	0.03	0.13	0.08	0.32	0.00	0.00	0.11	0.00	0.00	0.00	0.00	0.19	0.29	0.00	0.15	0.16	0.00	0.08
$CaCO_3$[b]	64.60	63.84	64.22	59.14	59.36	59.45	59.31	63.14	63.70	63.42	56.63	57.19	57.41	57.72	57.56	58.88	58.12	58.50
$MnCO_3$[b]	0.22	0.10	0.16	0.44	1.18	0.42	0.68	0.00	0.53	0.26	0.39	0.00	0.00	0.00	0.00	0.27	0.27	0.27
Sum	100.00	100.00		100.00	100.00	100.00		100.00	100.00		100.00	100.00	100.00	100.00		100.00	100.00	
Mg/Ca	0.46	0.48	0.47	0.58	0.57	0.58	0.58	0.50	0.48	0.49	0.64	0.64	0.63	0.63	0.63	0.59	0.61	0.60

[a] Measured values.
[b] Calculated values.
[c] Analysis points.

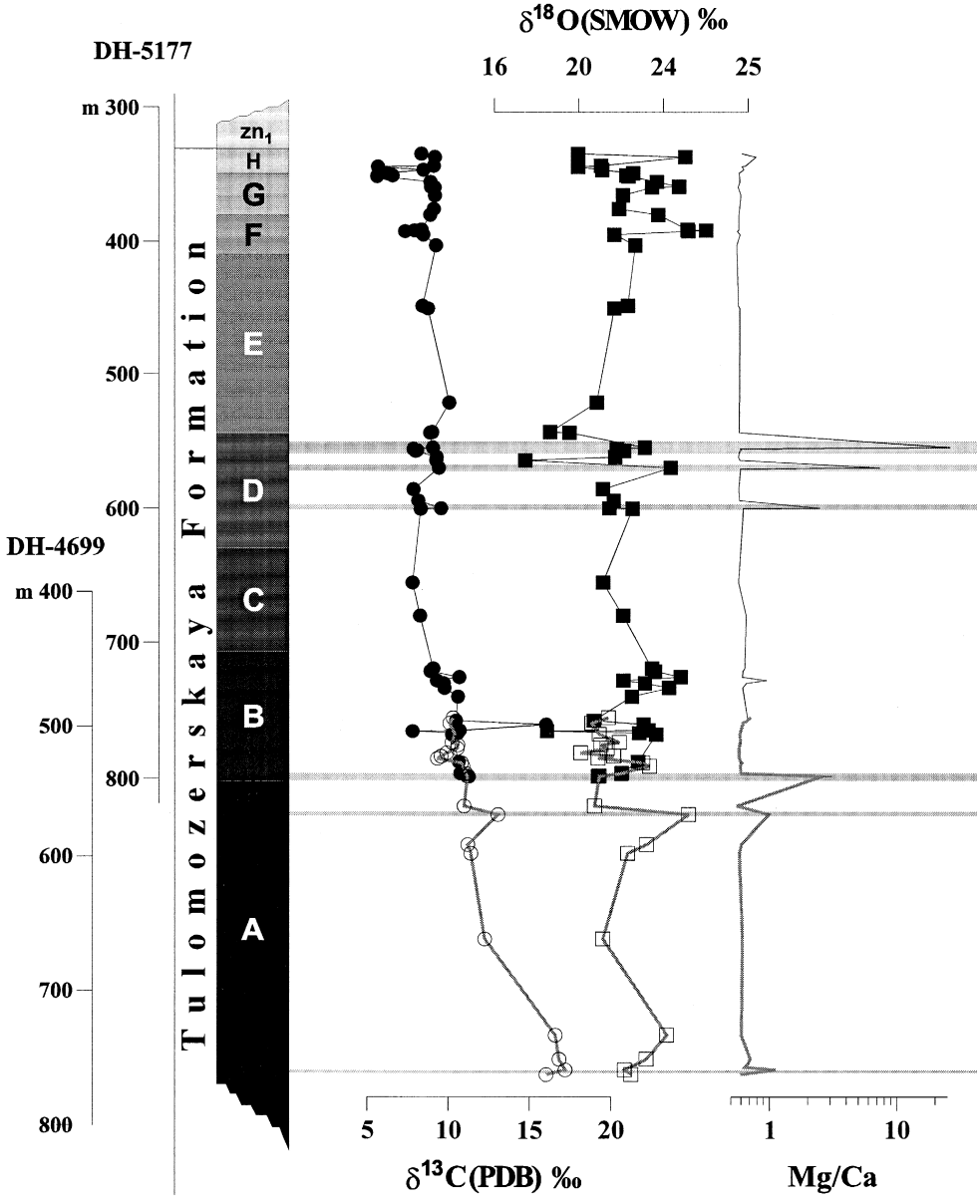

Fig. 11. The $\delta^{13}C$, $\delta^{18}O$ values and Mg/Ca ratio of carbonate rocks as a function of depth for the complete sequence of the Tulomozerskaya Formation in the northern Onega Lake area. Note magnesite-rich layers (shown by shaded bars) appear in Members A, B and D. The $\delta^{13}C$ values increase erratically with depth while $\delta^{18}O$ values show no apparent systematic variations.

fected by exchangeable oxygen derived from either meteoric water or interstitial fluids at elevated temperatures (e.g., Fairchild et al., 1990) whereas $\delta^{13}C$ may be buffered by pre-existing carbonate. In general, depletion in both oxygen and carbon isotope values may be considerable during late diagenesis as well as in the course of low-grade metamorphism accompanied by deformation (Guerrera et al., 1997).

Although a $\delta^{13}C$ and $\delta^{18}O$ cross-plot for the Tulomozerskaya carbonates (Fig. 14a) shows no sig-

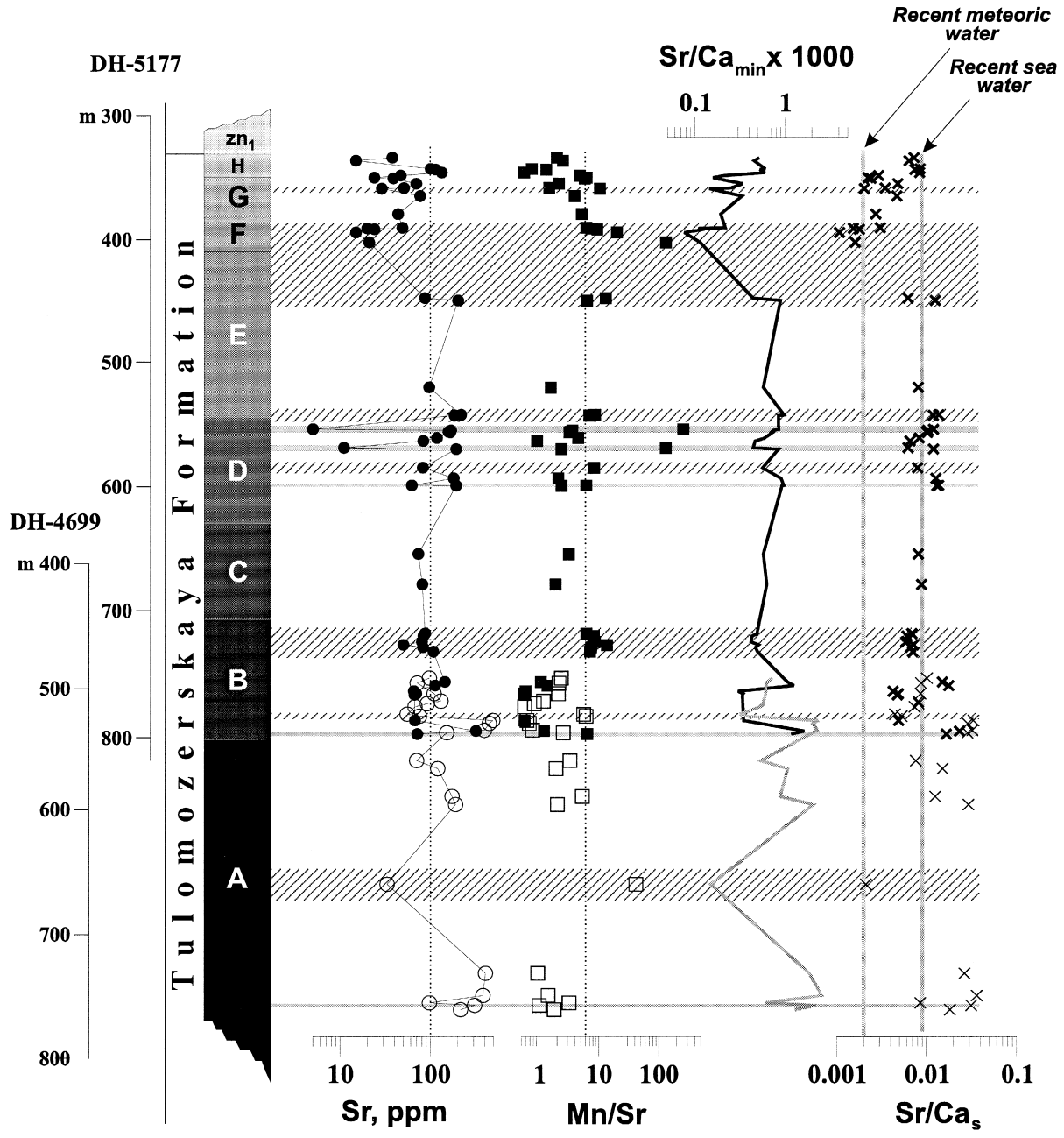

Fig. 12. Sr concentration, Mn/Sr, Sr/Ca$_{dol}$ (in rocks) and Sr/Ca$_s$ (in solution) ratios as a function of depth for the complete sequence of the Tulomozerskaya Formation in the northern Onega Lake area. Light-shaded horizontal bars are layers of magnesite. Striped horizontal bars are intervals of rocks affected by alteration (Mn/Sr > 6). Two vertical lines against Sr/Ca$_s$ are Sr/Ca$_s$ ratios of Recent meteoric water and seawater as based on Veizer (1983). A–H are Members of the Tulomozerskaya Formation, zn$_1$ — the Zaonezhskaya Formation.

nificant correlation between $\delta^{13}C$ and $\delta^{18}O$, the wide spread in oxygen and carbon isotope values is evident and may reflect resetting of carbon and oxygen isotopes during recrystallisation. Based on

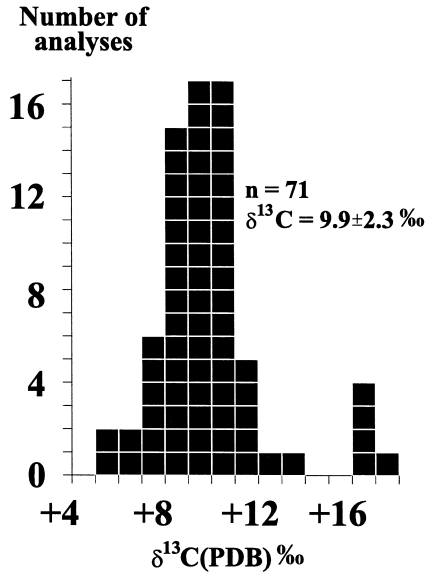

Fig. 13. Histogram of $\delta^{13}C$ values of Tulomozerskaya Formation carbonates. Note that dolostones extremely enriched in ^{13}C form a weak separate mode.

the observed spread, we suggest that oxygen isotopic compositions of the Tulomozerskaya dolostones were controlled by diagenetic alteration. If the highest $\delta^{18}O$ values of 25–26‰ are considered as the least altered, then all the lower values between 17.5 and 25.0‰ should have been affected by diagenetic/metamorphic resetting. The $\delta^{13}C$ values may still reflect isotopic parameters of coeval basinal water as they have been buffered by a pre-existing carbonate system. This is consistent with the work of Karhu (1993), and with the fact that the Tulomozerskaya Formation carbonates are highly recrystallised and both sparry and micritic dolomite are very rich in gas/fluid inclusions.

12.2. Strontium and manganese geochemistry

Brand and Veizer (1980) and Derry et al. (1992) reported that Mn and Sr can serve as a tool for calibration of the relative diagenetic rank of sequences. An increasing degree of post-depositional alteration leads to Sr depletion and Mn enrichment. For the samples studied, the Mn enrichment of dolomite, which formed during diagenetic cementation, is indicated by the microanalyses. Inclusion-rich, cloudy syntaxial dolomite overgrowths are enriched in Mn as compared to Mn-free intraclasts (Table 8, 4699–506.0). Following Kaufman and Knoll (1995) we assume that all the dolostones with Mn/Sr ratios exceeding 6.0 were affected by a post-sedimentary alteration. Such zones are indicated in the stratigraphic column in conjunction with Sr abundances (Fig. 12).

We assume that carbonates from each member, formed in various environments, might have had different initial (unaltered) Sr concentrations. Members A, B and D dolostones have the highest concentrations of Sr, namely 406, 491 and 181 ppm, respectively. The least altered samples of Members C, E, G and H yield 81, 94, 70 and 134 ppm, respectively. The lowest, least altered Sr value of 49 is assigned to Member F dolostones. The Member F dolostones have definitely experienced substantial loss of Sr as they have overall enhanced Mn/Sr ratios (Fig. 12).

If post-depositional resetting of Sr could be quantified, then the Sr content of carbonates may help constrain the nature of the dolomitising fluid. In general, Sr content in dolomite increases as a fluid salinity increases. It has been reported that for dolostones, high Sr concentrations are typical for facies with hypersaline tendencies (Veizer, 1978; Veizer et al., 1978; Lucia and Major, 1994; Budd, 1997). However, the Sr content in dolomite may be influenced by various factors. Under equilibrium conditions the amount of Sr in a mineral relative to that of the mineral's parent fluid is a function of the distribution coefficient for Sr (D^{Sr}). In the case of dolomite, Sr having a larger radius should substitute only for Ca (Kretz, 1982; Reeder, 1983). The relation between dolomite and parent fluid may be defined by (e.g., Budd, 1997):

$$(Sr/Ca)_{dol} = D^{Sr}_{dol} \times (Sr/Ca)_{fluid} \quad (2)$$

Given the Sr content of a dolomite, one may deduce the Sr chemistry of the parent fluid but we are limited by the great uncertainty in D^{Sr} values for dolomite, and unknown Sr/Ca for Palaeoproterozoic seawater. The published values of D^{Sr} range from 0.015 to 0.07 (e.g., Budd, 1997). This range yields estimated Sr contents of 50 to 600 ppm, respectively, for a stoichiometric dolomite formed from normal seawater, given its molar Sr/Ca to be about 0.0086. Budd (1997) has reported that recent developments

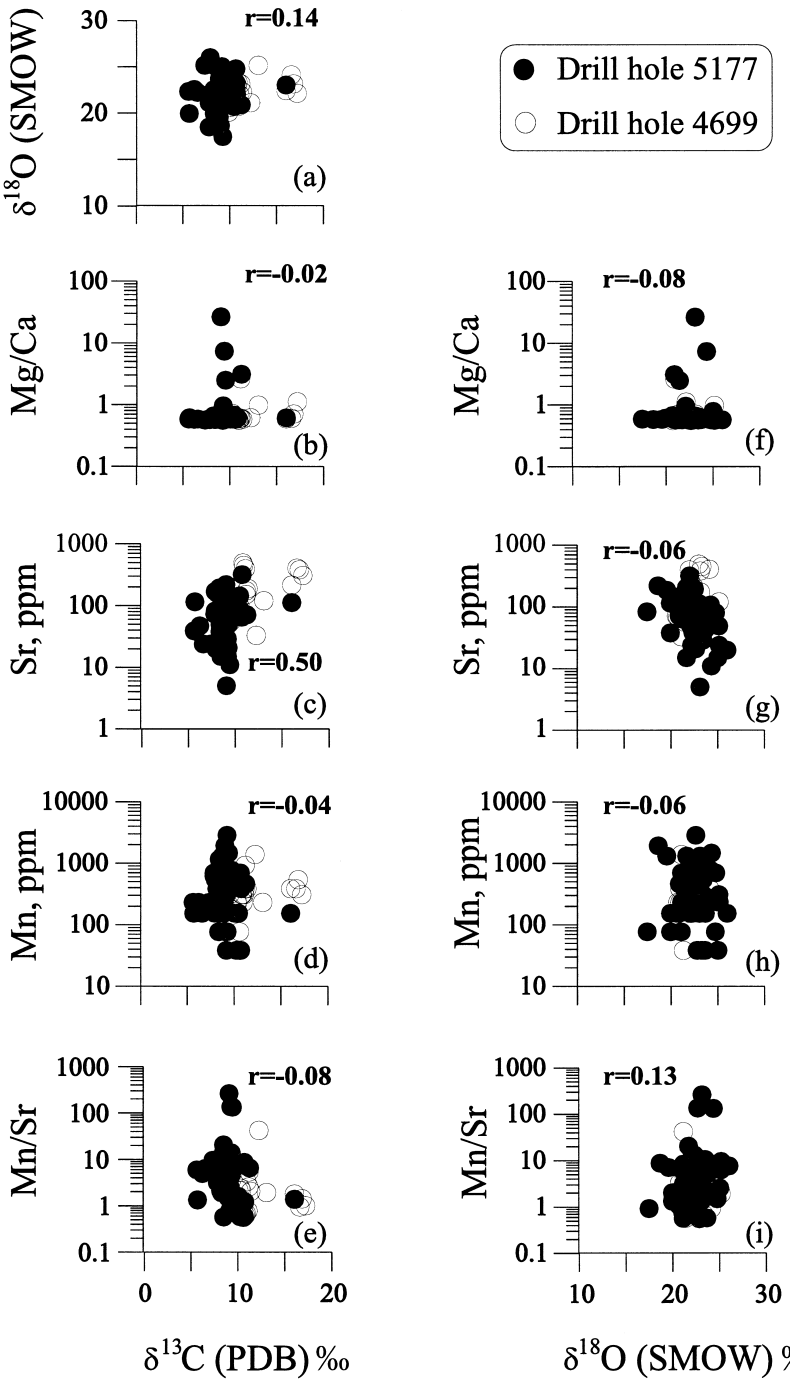

Fig. 14. Carbon and oxygen isotopes vs. Sr, Mn and Mg/Ca ratio for carbonate rocks of the Tulomozerskaya Formation. Note relatively little or no covariance between any components except Sr and carbon isotopes which show positive correlation.

in the understanding of D^{Sr} can indicate that values of 0.015–0.025 are most likely (Vahrenkamp and Swart, 1990; Banner, 1995). However, the observed range of Sr in early diagenetic dolomite best fits D^{Sr} with a value of 0.07 (Jacobson and Usdowski, 1976; Veizer, 1983).

The timing of dolomitisation is a most important factor in determining the dolomite Sr content (Tucker and Wright, 1990). Dolomite replacing aragonite in a relatively closed diagenetic system (low water/rock ratio) may inherit a marine-type Sr content (500–600 ppm) since the Sr/Ca ratio of aragonite is similar to seawater. Dolomite replacing marine high- and low-Mg calcite may contain several hundred ppm Sr. On the contrary, low-Sr diagenetic calcite will be replaced by very Sr-depleted dolomite. This has been exemplified by the chemistry of modern dolomite from the Arabian Gulf, the Bahamas and Florida Bays which contains around 600 ppm Sr (Behrens and Land, 1972; Land and Hoops, 1973). However, ancient dolomites may lose initial Sr content in the course of recrystallisation. For example, Lower Palaeozoic dolomite (early replacements of aragonite of a hypersaline environment) contains only 216 ppm Sr, relative to 66–72 ppm Sr in dolomite replacing open marine limestones (Veizer et al., 1978). Lower Cretaceous evaporitic dolomites have the highest average Sr concentration of 115 ppm, relative to burial (40 ppm) and lacustrine (100 ppm) dolomites (M'Rabet, 1981).

The highest Sr values of 406 and 491 ppm from the least altered Members A and B dolostones may reflect that they formed via diagenetic dolomitisation of a Sr-rich $CaCO_3$ precursor, such as aragonite (e.g., Mirota and Veizer, 1994). These Sr values correspond to Sr/Ca_{dol} ratios of 0.0018 and 0.0023, respectively. Using the Sr/Ca_{dol} ratios as well as an assumed value for D^{sr}_{dol} of 0.07 in Eq. (2), the dolomitising solution should have had a Sr/Ca_s ratio of 26×10^{-3} and 33×10^{-3}. However, if aragonite was not a $CaCO_3$ precursor one may alternatively suggest that the dolomite precipitated from a solution with enriched Sr/Ca_s ratios relative to modern seawater ($Sr/Ca_s = 8.6 \times 10^{-3}$, Veizer, 1983). Similar Sr/Ca_s ratios have been assigned elsewhere to dolomite formed from either evolved fluids or evaporated seawater (evaporated shortly after gypsum precipitation, Budd, 1997). In fact, overall Sr/Ca_s ratios obtained from the least altered Member A dolostones as well as from the lower part of Member B are compatible with their precipitation from evaporated seawater (Fig. 12). This is consistent with the sedimentological data and facies interpretations indicating upper subtidal to protected bight and lagoonal environments for Members A and B dolostones. The rest of the Member B dolostones are represented by two different populations. One has Sr/Ca_{dol} ratios ($0.4–0.6 \times 10^{-3}$) which are consistent with their precipitation from a fluid resembling modern seawater (Fig. 12). The second population with Sr/Ca_{dol} ranging $0.2–0.4 \times 10^{-3}$ apparently precipitated from a fluid with Sr/Ca_s ratio ($3–6 \times 10^{-3}$, Fig. 12) reflecting a strong dilution of seawater by meteoric water (2×10^{-3}).

Sr values in the least altered dolostones of Members C, D, E, G and H are much lower, namely 81, 181, 94, 70 and 134 ppm, respectively. The least altered dolostones of Members C, D, E and H have Sr/Ca_{dol} ratios ($0.4–0.6 \times 10^{-3}$) which may be ascribed to precipitation from a fluid resembling modern seawater (Fig. 12). Based on the lower Sr/Ca_{dol} ratios ($< 0.2 \times 10^{-3}$) the dolostones of Member F and those of the upper part of Member G should have formed from, or have been severely affected by, meteoric water with a resultant Sr/Ca_s ratio at around 2×10^{-3} (Fig. 12). The alteration of the dolostones of Member F, which exhibit the lowest Sr contents (46 ppm for the least altered sample) and high Mn/Sr ratios (Fig. 12), may be assigned to a mixing zone where the meteoric component was high in Ca but lower in Sr.

13. Comparison with other contemporaneous ^{13}C-rich carbonates

The mean $\delta^{13}C$ and $\delta^{18}O$ values of +9.9%% and 22.0‰, respectively, for the Tulomozerskaya carbonates are in agreement with those (+9.8‰ and 21.0‰) calculated from Tulomozerskaya data published previously (Fig. 15). The calculated average values of $\delta^{13}C$ and $\delta^{18}O$ for overall contemporaneous Palaeoproterozoic ^{13}C-rich carbonates reported from elsewhere are +6.9‰ and 17.9‰, respectively (Fig. 15). The younger (ca. 2.0 Ga) carbonate rocks

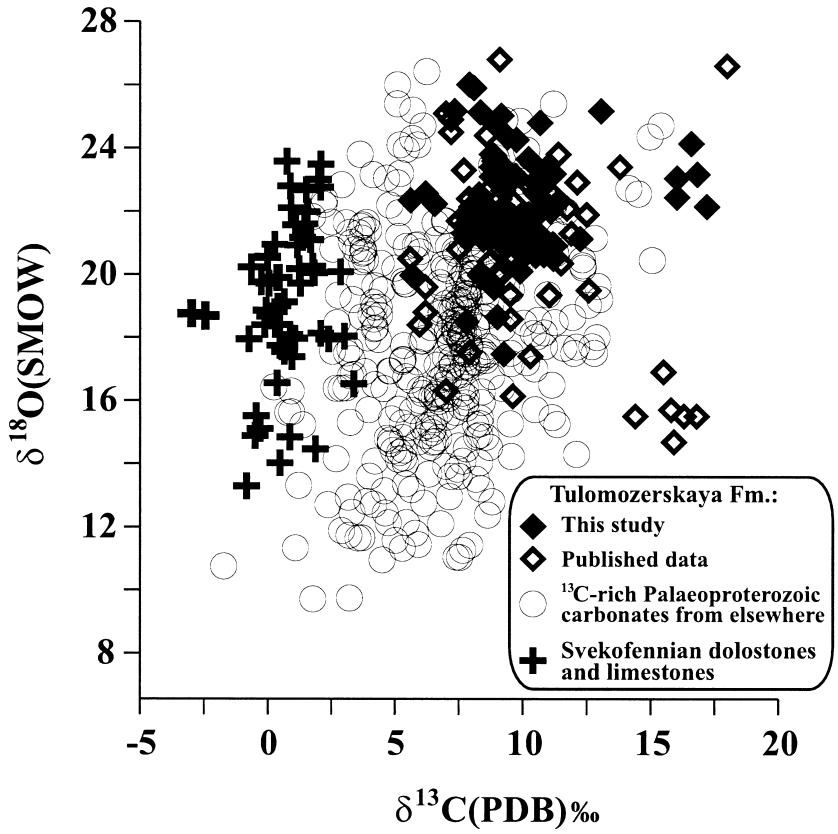

Fig. 15. $\delta^{13}C$–$\delta^{18}O$ cross-plots for Tulomozerskaya Formation carbonates in comparison with previously published data and also in comparison with ^{13}C-rich Palaeoproterozoic carbonate from elsewhere, and 2.0 Ga Svecofennian carbonates from the Fennoscandian Shield. Published data are from: Tulomozerskaya carbonates — Yudovich et al. (1991), Karhu (1993), Tikhomirova and Makarikhin (1993), Akhmedov et al. (1993). ^{13}C-rich Palaeoproterozoic carbonate from elsewhere — Schidlowski et al. (1976), McNaughton and Wilson (1983), Feng (1986), Baker and Fallick (1989a; b), Gauthier-Lafaye and Weber (1989), Zagnitko and Lugovaya (1989), Karhu and Melezhik (1992), Karhu (1993), Bekker and Karhu (1996), Melezhik and Fallick (1996a), Sreenivas et al. (1996), Melezhik et al. (1997a). Data for 2.0 Ga Svecofennian carbonates are from Karhu (1993), Melezhik and Fallick (1996a).

(with 'normal marine' $\delta^{13}C$, mean + 0.8‰) immediately overlying isotopically heavy carbonates on the Fennoscandian Shield show relatively depleted $\delta^{18}O$ value of 19.1‰ (Fig. 15).

The maximum $\delta^{13}C$ and $\delta^{18}O$ values of the Tulomozerskaya dolostones are +17.2‰ and 26‰, respectively. The Tulomozerskaya Formation carbonates have higher $\delta^{13}C$ than all other isotopically anomalous Palaeoproterozoic carbonates reported from elsewhere (Fig. 15). The maximum $\delta^{18}O$ value is also higher than those reported for isotopically anomalous carbonates by Baker and Fallick (1989a; b) from Norway (24.2‰) and Scotland (22‰), by Melezhik et al. (1997a) from the Labrador Trough (25.4‰), and by Sreenivas et al. (1996) from the Aravalli Group (22.8‰). The maximum $\delta^{18}O$ value measured from ^{13}C-rich dolostones and limestones in Finland (Karhu, 1993) is 23.8‰. Schidlowski et al. (1976) in reporting a mean $\delta^{18}O$ of 22.2 ± 1.6‰ at Lomagundi (maximum 26.9‰) commented that such a value was normal for Palaeoproterozoic sedimentary carbonates. Veizer et al. (e.g., Veizer et al., 1992a,b) have documented a $\delta^{18}O$ value of 26 ± 2‰ for Archaean to Palaeoproterozoic dolostones. Hence, the studied dolostones exhibit the highest (both mean and maximum) values of $\delta^{13}C$ ever reported from Palaeoproterozoic ^{13}C-rich carbonates. The $\delta^{18}O$ values are elevated to a lesser extent. Only the Loma-

gundi dolostones are comparable with the studied carbonates in terms of maximum $\delta^{18}O$ value.

14. Comparison with ^{13}C-rich carbonates of other ages

Neoproterozoic ^{13}C-rich dolostones show a mean $\delta^{18}O$ value of $23.0 \pm 3.1‰$ having much lower $\delta^{13}C$ on average than their Tulomozerskaya counterpart (Fig. 16a). However, a value of 23‰ does not seem to be a primary signal as Fairchild et al. (1989) reported Neoproterozoic carbonates with $\delta^{18}O$ as high as 42‰ and ascribed this to unusual resistance to recrystallisation.

Late Ordovician ^{13}C-rich (mean + 6.2‰) limestones exhibit $\delta^{18}O$ values averaging $29 \pm 1.9‰$ (Fig. 16b, Brenchley et al., 1997). Some values as high as 32‰ have been ascribed to a shortlived glaciation.

The mean $\delta^{18}O$ value for Permian ^{13}C-rich dolostones ($\delta^{13}C$ up to $+7.6‰$) of $28.5 \pm 2.9‰$ (Fig. 16c) is consistent with 28‰ which has been reported for Permian marine cement (Carpenter and Lohman, 1997). However, those Permian dolostones, which formed in evaporitic hypersaline environments, are characterised by $\delta^{18}O$ ranging between 28‰ and 37‰ (Guerrera et al., 1997). All these are much higher that those measured for the Tulomozerskaya dolostones.

Cretaceous carbonate rocks enriched in ^{13}C are exclusively limestones. Those, which have been compiled and shown on a $\delta^{18}O$–$\delta^{13}C$ cross-plot (Fig. 16d), have mean $\delta^{18}O$ of $28.1 \pm 2.5‰$.

The data compilation shows that the best estimates of $\delta^{18}O$ for different age dolostones enriched in ^{13}C are rather similar, namely around 28‰. This is the case for Neoproterozoic (28‰), Ordovician (29‰), Permian (28.5‰) and Cretaceous–Tertiary (28.1‰) carbonates. Similar $\delta^{18}O$ values have been reported from isotopically 'normal' ($\delta^{13}C = 0 \pm 2‰$) Palaeoproterozoic dolostones: the best estimate for the $\delta^{18}O$ from the 1.85-Ga-old Albanel formations is about 28.3‰ (Mirota and Veizer, 1994), and from the same age McArthur Group dolostones it is 27.9‰ (Veizer et al., 1992b). Thus, the Tulomozerskaya dolostones are characterised by the lowest, least altered $\delta^{18}O$ values of 26‰ compared to other $\delta^{13}C$-rich carbonates of other ages. We suggest this might have been a result of recrystallisation involving oxygen isotope exchange between the carbonates and meteoric fluids or a lower seawater $\delta^{18}O$ (Veizer, 1999).

15. Interpretation of ^{13}C enrichment

Sedimentary carbonates with $\delta^{13}C$ significantly higher than $0 \pm 2‰$ are usually formed in special environments. A restricted volume of isotopically heavy carbonates may form during fermentative diagenesis (Irwin et al., 1977). The deposition of relatively larger volumes of isotopically heavy carbonates may be formed in hot-spring (Friedman, 1970), hypersaline (Reitsema, 1980; McKenzie, 1981; Stiller et al., 1985) and stromatolite-dominated basin (Ferguson, Plumb and Walter, unpublished data cited in Knoll et al., 1986; Burne and Morre, 1987) environments as well as a closed-lake system with high bioproduction (e.g., Lake Kivi; Botz et al., 1988). Epochs of ^{13}C-rich carbonates of global significance are considered to be related to either Oceanic Anoxic Events (e.g., Schidlowski and Junge, 1981) or world-wide orogenic episodes (Derry et al., 1992; Des Marais, 1994), both leading to enhanced deposition of reduced carbon.

15.1. Diagenetic model

Fermentative diagenesis has been proposed for the explanation of ^{13}C-rich dolostones of the Tulomozerskaya Formation (Yudovich et al., 1991), for the isotopically heavy dolostones of the Palaeoproterozoic Dunphy Formation in the Labrador Trough (Schrijver et al., 1986; however, see Melezhik et al., 1997a) as well as for the majority of Palaeoproterozoic ^{13}C-rich carbonates (Dix et al., 1995).

In general, carbonate minerals formed in the course of fermentative diagenesis may show a wide range in $\delta^{13}C$, though the temperature dependent oxygen isotope ratios will show very little variation (e.g., Watson et al., 1995).

The Tulomozerskaya carbonates studied are characterised by an entirely different $\delta^{13}C$ stratigraphic pattern, which alone argues against a diagenetic model (Melezhik et al., 1996).

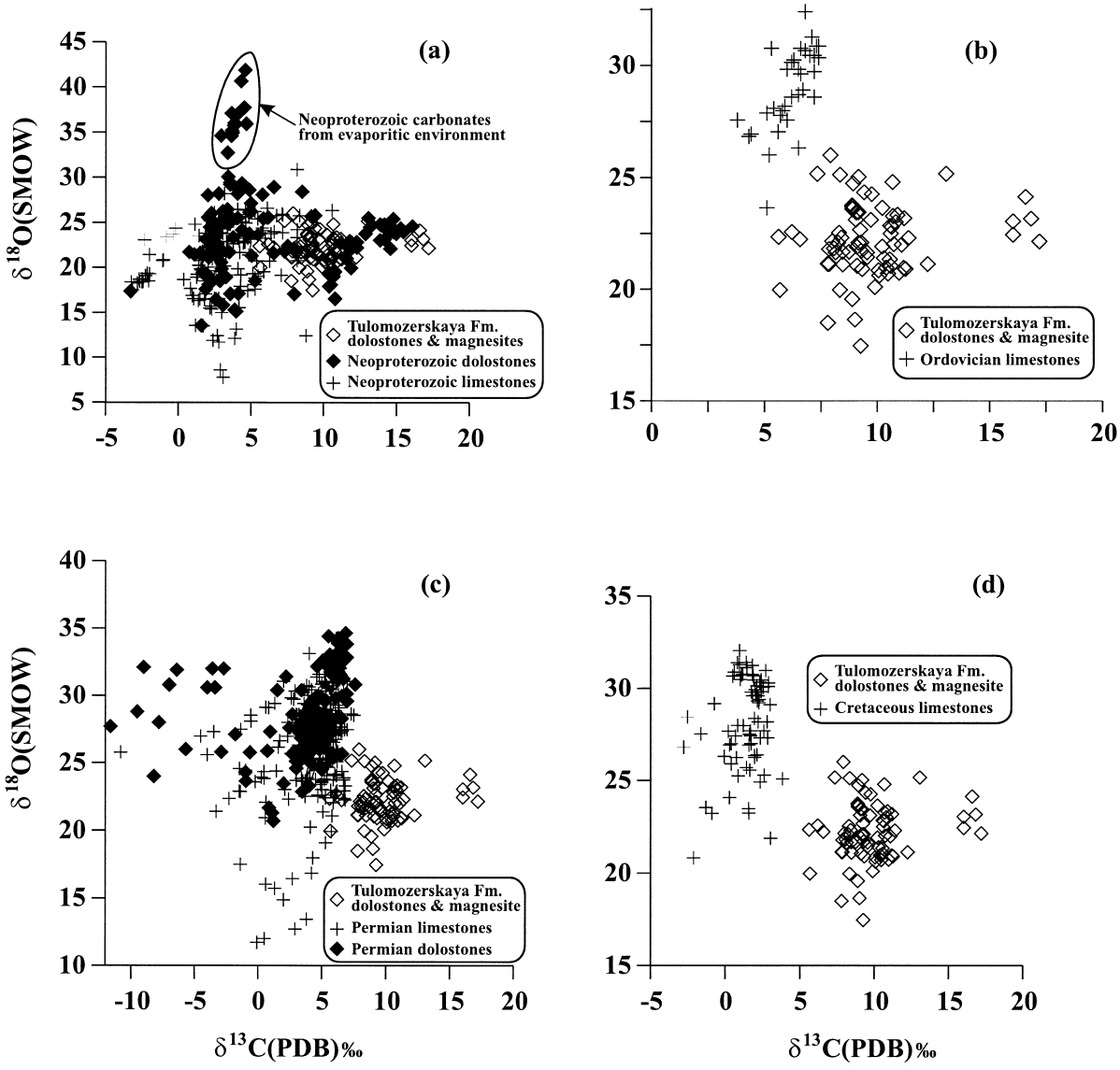

Fig. 16. $\delta^{13}C$ $\delta^{18}O$ cross-plots for Tulomozerskaya Formation carbonates in comparison with Neoproterozoic (a), Ordovician (b), Permian (c) and Cretaceous (d) ^{13}C-rich limestones and dolostones. Data are from: Neoproterozoic — Aharon et al. (1987), Fairchild et al. (1989; 1990), Kaufman et al. (1991; 1993; 1996), Asmerom et al. (1991), Derry et al. (1992), Corsetti and Kaufman (1994), Narbonne et al. (1994), Smith et al. (1994), Iyer et al. (1995), Knoll et al. (1995a; b). Ordovician — Brenchley et al. (1997). Permian — Compston (1960), Degens and Epstein (1964), Keith and Weber (1964), Dorman (1968), Murata et al. (1972), Osaki (1973), Davies and Krouse (1975), Davies (1976), Veizer and Hoefs (1976), Clark (1980), Rao and Green (1982), Beauchamp et al. (1987). Cretaceous — Lloyd and Hsü (1971), Osaki (1973), Veizer and Hoefs (1976).

15.2. Model of evaporitic basin

On a small scale, enrichment in ^{13}C can be caused by persistent evaporative conditions. Stiller et al. (1985) reported extreme ^{13}C enrichments in the dissolved inorganic carbon pool ($\delta_{\Sigma CO_2}$) in evaporitic brines of the Dead Sea. There, under natural conditions, in solar evaporitic ponds, an abiotic effect in evaporating brines resulted in ^{13}C enrichments of up to +16.5‰. Stiller et al. (1985) have also reported

^{13}C enrichment of up to +34.9‰ in laboratory experiments. The calculated fraction of remaining ΣCO_2, which corresponds to that $\delta^{13}C$ value, is 0.18 (the initial value is considered to be 1.0). However, it is not clear to what extent ^{13}C-rich carbonates may be formed from such evaporating pools. Katz et al. (1977) studying aragonite laminae in deposits from the highly evaporated and saline Lake Lisian, the Pleistocene precursor of the Dead Sea, found carbonates only moderately enriched in ^{13}C. Although the evaporation rate of Lake Lisian was higher than that of the Dead Sea, the evaporating system of the former was not persistent and resulted in $\delta^{13}C$ ranging from −7.7 to +3.5‰ coupled with extremely heavy oxygen, from +32.4 to +38.1‰. The latter is higher by 3‰ on average than $\delta^{18}O$ of the Dead Sea due to a higher rate of evaporation (Katz et al., 1977).

Calcium and magnesium carbonate sediments formed in highly evaporative coastal sabkhas of Abu Dhabi, the Arabian side of the Persian Gulf (McKenzie, 1981), have average $\delta^{13}C$ of +3‰. $\delta^{18}O$ values range between 30.4 and 34.5‰.

From the data reviewed above it can be inferred that even in highly evaporated system $\delta^{13}C$ values are generally negative to slightly positive (Bonatti et al., 1971; Pierre, 1982; Magaritz et al., 1983). However, known Recent evaporitic carbonates are characterised by highly elevated $\delta^{18}O$ averaging between 32 and 37‰.

A review of ancient evaporitic carbonates formed at times of known high seawater $\delta^{13}C$ values shows that the Late Permian carbonates exhibit both very pronounced enrichment in ^{13}C and clear evaporitic affinities. It has been emphasised by Beauchamp et al. (1987, p. 410) that all the Late Permian basins with markedly ^{13}C-rich carbonates, including the Delaware, Zechstein and Sverdrup, are remarkably similar: ''isolated or semi-isolated, intra- or pericratonic depressions, intermittently connected with the open ocean, and marked by several episodes of evaporation, desiccation and progradation of carbonate platforms''. Beauchamp et al. (1987) have also suggested that the primary ^{13}C enrichment of the Sverdrup Basin carbonates (up to +7‰) as compared to the coeval ocean (+1 to +3‰) may only be explained if a number of factors were involved. An intensive evaporation and ^{13}C enrichment of surficial brines through escape of CO_2 to the atmosphere during episodic closure of the basin was considered one of the factors which caused the formation of ^{13}C-rich carbonates. They have also stated that the Permian isotopic evolution should be re-evaluated in terms of a global areal heterogeneity (Beauchamp et al., 1987).

From sedimentological and palaeoenvironmental points of view the Tulomozerskaya sequence closely resembles those deposited in Late Permian time and exhibits a certain degree of heterogeneity in $\delta^{13}C$ values as revealed by the two distinct modes in the histogram (Fig. 13). The mode which is highly enriched in ^{13}C is represented by Member A dolostones. Two separate modes of ^{13}C-rich carbonates may indicate that processes involved in their formation were either different or an extra factor(s) should be considered for the extreme mode.

Based on the combined sedimentological and geochemical criteria Member A carbonates have been assigned to a restricted evaporative environment developed either in ephemeral ponds in the upper tidal zone of a carbonate flat or in coastal sabkhas and playa lakes (Melezhik et al., 1999a, submitted). Thus, it is very likely that enhanced evaporation is one of the factors leading to extreme enrichment of Member A carbonates in ^{13}C.

However, several arguments conflict with an entirely evaporitic origin of high $\delta^{13}C$ of Tulomozerskaya carbonate rocks (Melezhik et al., 1996). For instance, the evaporitic signatures appear irregularly through the sequence. This is not consistent with the assumption that Tulomozerskaya carbonates were formed in a sustainable evaporitic system which was able to maintain $\delta^{13}C$ between +6 and +10‰ for the duration of deposition of a 700-m-thick succession.

15.3. Model of restricted basin with high bioproduction [2]

The Onega palaeobasin was marked by a high level of bioproductivity, since stromatolites are very abundant. Carbonates of Members A, B, C, D and E

[2] We distinguish bioproduction from bioproductivity. Bioproductivity refers to the organic mass produced but not necessary deposited within sediments whereas bioproduction refers to the organic mass deposited.

are clearly associated with accumulation of evaporates indicating some periods of negative water balance, and are highly suggestive of closed/semi-closed-basin conditions (Melezhik et al., 1999a, submitted). As primary shifts in the isotopic composition of sedimentary carbon can also be caused by enhanced rates of burial of organic material leading to enrichment of ^{13}C in deposited carbonates (e.g., Scholle and Arthur, 1980) a model of a restricted basin with high bioproduction is considered here. The scale of this effect can be global or basinal and assessment of these alternatives is crucial for the interpretation of the carbon isotope excursion.

Talbot (1990) and Talbot and Kelts (1990) reported that C–O isotopic covariance is most typical of carbonates from hydrologically closed lakes whereas relatively invariant carbonate oxygen isotopic values suggest hydrologically open lakes.

A significant C–O covariance has only been observed in the Member A and lower part of Member B carbonates ($r = 0.51$, $n = 31$). These formed either in ephemeral ponds in upper tidal zones of a carbonate flat or in coastal sabkhas and playa lakes and are characterised by the highest $\delta^{13}C$ values of $+10‰$ to $+17‰$. On this basis, we assume that the Member A and lower part of Member B carbonates may be consistent with hydrologically closed lakes.

In a small restricted basin, biological fixation and removal (deposition) of reduced carbon may lead to isotopic disequilibrium between the basin and the open atmosphere–hydrosphere system. This will cause enrichment of ^{13}C in precipitated carbonates. Isotopically heavy carbonates ($\delta^{13}C = +5.0$ to $+13.6‰$) have formed by this mechanism in Lake Kivu, East Africa (Botz et al., 1988). The most ^{13}C-rich carbonates have formed during times of low water-level stands in those parts of the lake which were isolated from the main lake and their waters 'chemically' stratified. In all cases, ^{13}C-rich sediments contain 2–19% C_{org} (Botz et al., 1988). At a depth of 1.2–4.2 m, diagenetic carbonates with $\delta^{13}C$ of -1.2 to $-2.3‰$ have been detected. This indicates the contribution of CO_2 or bicarbonate derived from oxidation of organic matter (Botz et al., 1988).

The data obtained from the Tulomozerskaya Formation carbonates militate against the geochemical features of carbonates reported for the Lake Kivu environments. First, no negative $\delta^{13}C$ values have been measured in the Tulomozerskaya carbonates (all above $+5.5‰$). Secondly, C_{org} content in carbonate rocks is around 0.02% (e.g. Karhu, 1993). Thirdly, no other rocks containing detectable amounts of C_{org} have been found to be deposited prior to, or simultaneously with, ^{13}C-rich carbonates in the Onega palaeobasin (Golubev et al., 1984). On the contrary, all rocks are highly oxidised 'red beds'. An assumption that all initial C_{org} mass buried in a closed system might have been eventually oxidised in the course of the post-depositional alteration raises three crucial questions: when, why and how did it happen without isotopically depleting previously deposited carbonates, and/or without forming a new generation of carbonates depleted in ^{13}C? The last question may be clarified by using differential measurements on neoformed carbonate cement if this could be recognised. One may suggest that organic material was mobilised and migrated upward in the sequences and formed shungite rocks. This is in entire conflict with the geological observations, as no evidence of a such migration has been recognised in the area. Instead, migration of organic-rich fluids downwards from shungite sequences into the Tulomozerskaya Formation has been widely detected (Melezhik et al., 1999a, submitted).

Complete removal of all the organic material by secondary oxidation related to metamorphism is highly unlikely. A simple calculation shows that in order to balance $\delta^{13}C$ of $+10‰$ (which corresponds to $f_{org} = 0.55$, assuming $\Delta\delta^{13}C_{carb-org}$ was 27‰) the rocks of a closed basin should contain 16 wt.% C_{org}. This is not an amount which can be easily removed by a secondary oxidation related to greenschist facies metamorphism. Instead, we suggest that the C_{org} concentration in the Tulomozerskaya carbonates might have been at a lower level and an essential amount of organic material was buried in an external basin. The organic material which was produced by microbial communities in the Onega palaeobasin has been continuously oxidised and converted to CO_2 pene-contemporaneously with the formation of stromatolites. This was apparently due to an extremely shallow water environment leading to the exposure of microbial mats to the air (Fig. 17, see further discussion). As a result, a high bioproductivity has not resulted in a high bioproduction. Thus, although a restricted basin environment matches a

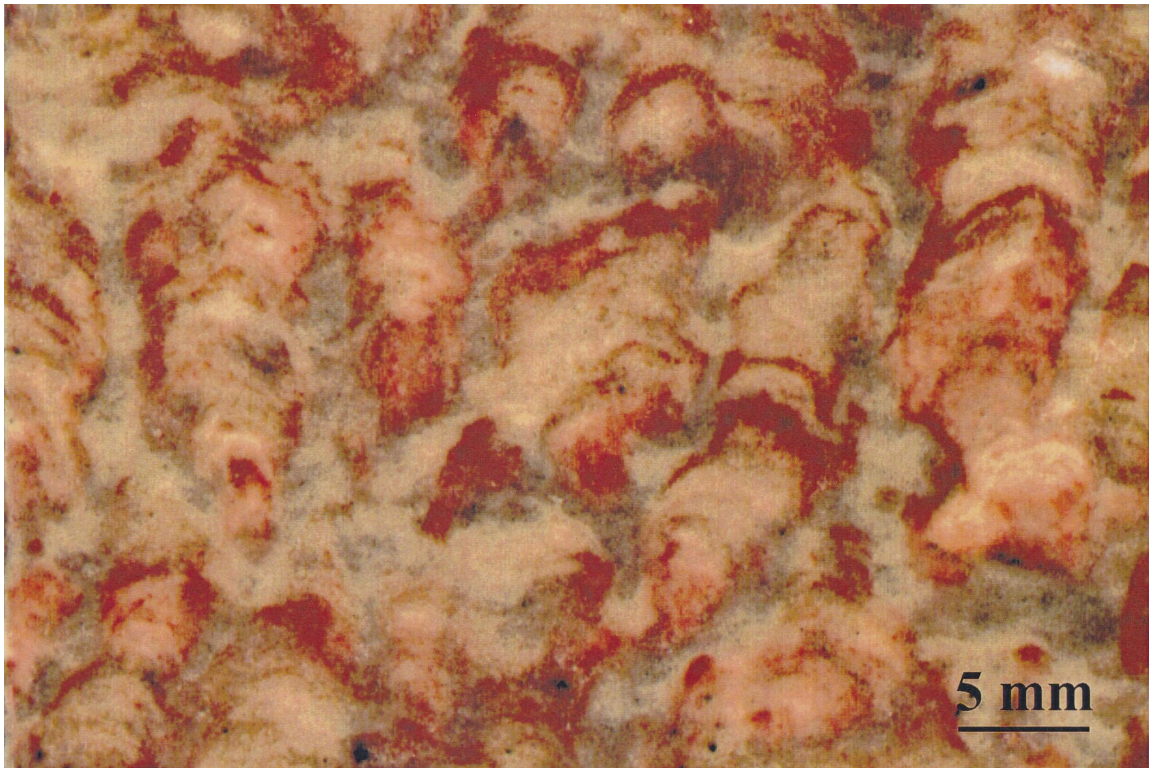

Fig. 17. Red, columnar stromatolites from Member C. Note intercolumnar space filled with light grey and white dolarenite whereas stromatolite laminae and margins of column are composed of pink dolomite. Pink colour is interpreted to have formed due to photosynthetically induced precipitation of iron oxide in an extremely shallow water environment.

part of the Tulomozerskaya sequence this is unlikely to have been coupled with a high local bioproduction. Consequently, the whole process might have led to only local enrichment of the Tulomozerskaya carbonates in ^{13}C though it should have contributed ^{12}C-rich CO_2 to the atmosphere as all the produced organic material was recycled. This, in turn, would decrease $\delta^{13}C_{carb}$ of coeval seawater. Therefore, an external basin is conjectured to complement the organic mass buried and to balance ^{13}C-rich carbonates world-wide. However, a high level of bioproductivity with low or zero bioproduction leads us to the next model.

15.4. Model of stromatolite basin

Primary shift in the isotopic composition of sedimentary carbon can also be due to preferential biological fixation of ^{12}C into organic material (e.g., Broecker, 1970; Hayes, 1983). On a basinal scale, enrichment in heavy isotopes may be caused by widespread stromatolite-forming bacteria in shallow-water, closed or semi-closed environments. Des Marais et al. (1992a) have reported that dissolved carbon net fluxes in a Guerrero stromatolitic pond include day input of HCO_3^- (water to mat) and night outflow (mat to water, in an amount of 80% from the initial HCO_3^- day input) with the carbon component having $\delta^{13}C$ of $-6‰$ and $+1‰$, respectively. Purely organic microbial mats, in which cyanobacteria constitute the dominant mat-building organism, are often characterised by very high organic productivity (Castenhols et al., 1992; Jørgensen et al., 1992). Consequently, the rate of biological uptake of ^{12}C is higher than the rate of carbon diffusion to mat (Des Marais et al., 1992a). As a result, the dissolved

inorganic carbon reservoir becomes enriched in ^{13}C. It is well known (e.g., Des Marais et al., 1992a) that both $\delta^{13}C_{org}$ and $\delta^{13}C_{carb}$ of recent stromatolitic mats are typically enriched in ^{13}C, ranging from -19.1 to $+3.0$‰ in organic matter, and from $+2.5$ to $+6.6$‰ in inorganic phases (Fig. 18a). This should also be valid for carbonate-precipitating cyanobacterial mats (close analogues of stromatolite-building benthic Proterozoic communities) as they show similar ^{13}C-enriched values of both organic and inorganic material. This is evident from many Australian lakes where carbonates precipitating on calcifying microbial mats have $\delta^{13}C$ of $+5$ to $+10$‰ (Fig. 18b, Burne and Morre, 1987). A high rate of biological uptake of ^{12}C in shallow water conditions combined with lower energy settings may lead to enrichment in ^{13}C of the whole water column. This assumption is consistent with ^{13}C-rich carbonates accumulated in stromatolitic carbonates and living shells at Shark Bay (Fig. 18a,c).

Another remarkable characteristic of cyanobacterial mats which is relevant for this discussion is a rapid decomposition and recycling of the microbial biomass with almost zero net production (Jørgensen et al., 1992). Anaerobic (e.g., sulphate reduction) and aerobic respiration, fermentation and methanogenesis are common processes leading to degradation of the microbial biomass produced. The end products can be easily lost (degassed, dissolved, etc.) in calcifying mats with the development of various fenestrea. Thus a high bioproductivity, almost zero net bioproduction combined with ^{13}C-rich carbonates precipitated on microbial mats is a characteristic feature of carbonate-precipitating cyanobacterial mats.

We believe that a stromatolitic basin model is a potential target which may elucidate some of the statements and the discussions presented above. It has already provided evidence of both direct precipitation of ^{13}C-rich stromatolitic carbonates (up to $+10$‰) and a ^{13}C-enriched carbon component escaping into the water column, which apparently causes the ^{13}C enrichment in shell carbonates. Theoretically this ^{13}C-rich water environment can be maintained over long periods of time, as long as a stromatolitic community functions, and therefore the system seems to be capable of producing a large amount of ^{13}C-rich carbonates.

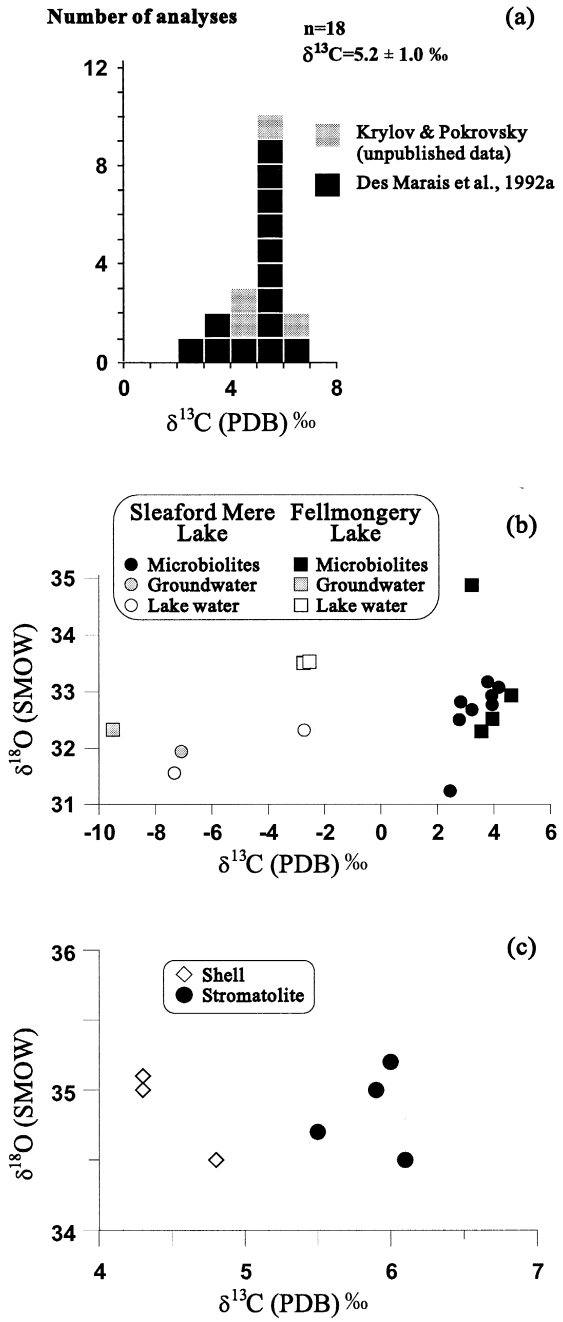

Fig. 18. Histogram of $\delta^{13}C$ values of carbonates from Shark Bay stromatolites (a), and $\delta^{13}C$–$\delta^{18}O$ cross-plot for Australian lake stromatolitic carbonates (b, Burne and Morre, 1987), and for Shark Bay stromatolitic carbonates and shell carbonates (c, Pokrovsky and Krylov, unpublished data).

One may argue that there are other examples of Neoproterozoic stromatolites which do not show an enrichment in ^{13}C in precipitated carbonates (e.g., Fairchild et al., 1990; Fairchild, 1991). We argue that the capability of carbonate-precipitating cyanobacterial mats to enrich the environment in ^{13}C will be strongly dependent on the media surrounding them. In well stirred, open basins this will be a very unlikely process.

The Onega palaeobasin possesses all the indispensable components of a stromatolite environment (Melezhik et al., 1999a, submitted). Therefore, there is apparently no restriction for employing a stromatolite basin model as a principal mechanism leading to the enhancement of $\delta^{13}C$ values. Based on the modern analogues, we assume that the Onega stromatolites might have contributed around +5‰ to $\delta^{13}C$ of the Tulomozerskaya carbonates. If this is subtracted from the average $\delta^{13}C$ of +9.9‰ then the background (global?) value will be around +5‰. This value is consistent with the assumption made earlier (Section 4) and based on independent data (Melezhik et al., 1997c).

However, an external basin is needed to complement the organic mass buried and is necessary to balance $\delta^{13}C_{carb}$ of +5‰ of if this is considered to be a global background value for the Palaeoproterozoic ocean. It is unlikely that stromatolitic basins could have enriched carbonates in ^{13}C on a global scale. On the contrary, it may decrease the ^{13}C content in the coeval ocean in the long run as synchronously accumulated, isotopically light organic carbon was recycled and returned to the global carbon cycle.

15.5. Model of oceanic anoxic event

An oceanic anoxic event should normally result in a stratified ocean with high preservation of organic

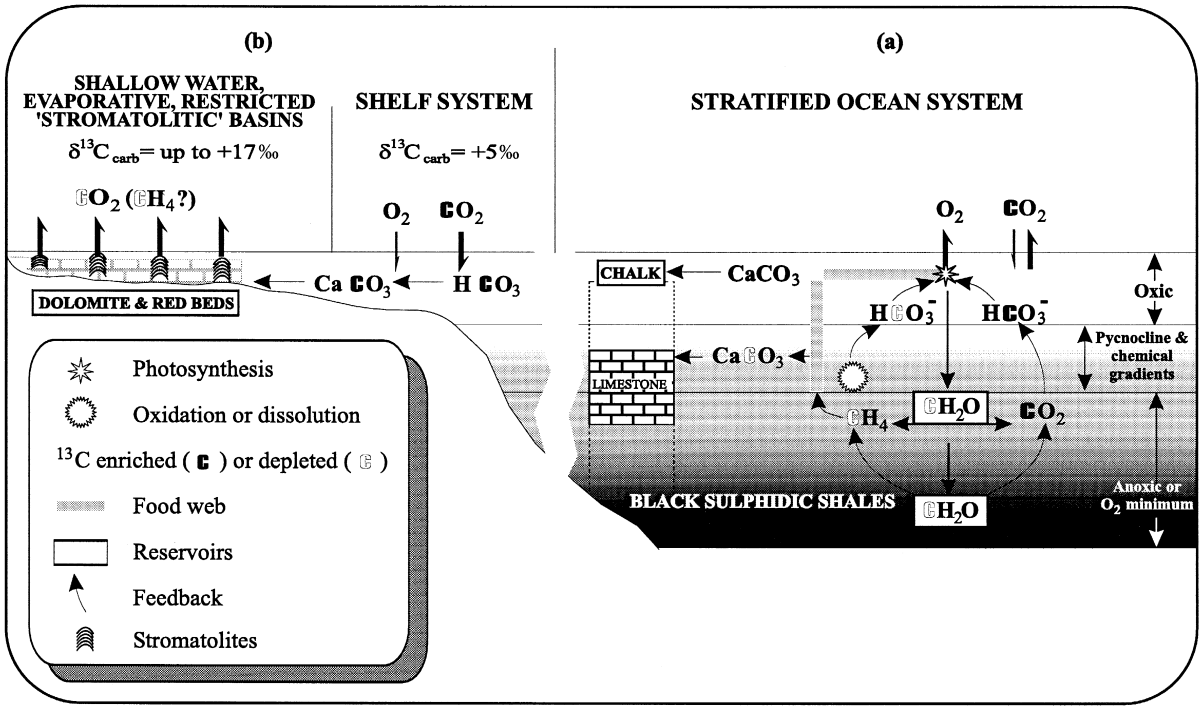

Fig. 19. Simplified model illustrating enhanced enrichment of the Tulomozerskaya carbonates in ^{13}C as compared to inferred global background value of +5‰ (modified from Melezhik and Fallick, 1997). Diagram also shows carbon transfers and reservoirs in (a) a stagnant ocean and (b) in developing marginal seas. A horizontal food-web pattern represents dominant phytoplankton components, and a vertical pattern dominant bacterial components. Carbon isotope fractionation is shown schematically by contour-face and bold-face carbon symbols.

material. According to Keith (1982), changes from a well-mixed aerated ocean to a stratified ocean provide a counterbalance between deep reduction and shallow oxidation, as well as conditions that favour optimal formation of deep-water C_{org}-rich black sulphidic shales and protopetroleum coupled with shallow-water deposits of barite, iron ore, cherty iron formation and 'red beds'. Based on the Permo-Triassic and Late Cretaceous–Early Tertiary stagnant episodes, Keith (1982) showed that stratified oceanic environments were indicated by mesopelagic limestones notably depleted in ^{13}C (Fig. 19, opposite to prior conclusions, e.g., Tappan, 1968; Jenkyns, 1980; Scholle and Arthur, 1980; Schidlowski and Junge, 1981).

One component of Keith's model definitely present in the Onega palaeobasin are widespread shallow water 'red beds' with evaporitic affinities in association with extensively developed ^{13}C-rich dolostones. However, the second component, namely a ca. 2.4–2.1 billion year-old deep-water C_{org}-rich black sulphidic shales and oceanic limestones depleted in ^{13}C deposited in a stratified oceanic environment, is missing. Therefore, the applicability of an oceanic anoxic event as the mechanism leading to development of ^{13}C-rich carbonates in Jatulian time remains an open question.

16. Conclusions

16.1. General

(1) The 2.33–2.06 Ga Palaeoproterozoic, long-lasting, single, isotopic positive excursion of $\delta^{13}C_{carb}$ is now considered as three positive shifts of $\delta^{13}C_{carb}$ separated by returns to 0‰, which all occurred between 2.40 and 2.06 Ma.

(2) The isotopic event is unique in terms of both duration (>300 Ma) and ^{13}C enrichment (up to $+18$‰). The mechanism responsible for one of the most significant carbon isotopic shifts in Earth history remains highly debatable. To date, $\delta^{13}C$ of $+10$‰ to $+15$‰ cannot be balanced by organic carbon burial (f_{org}) as there is no geological evidence for an enhanced C_{org} accumulation prior to or synchronous with the excursion.

(3) For the interval 2.4–2.06 Ga, there is a paucity in published $\delta^{13}C_{org}$ data at the time when the positive carbonate excursion developed. Consequently, neither Δ_c nor f_{org} can be established with meaningful precision. Surprisingly, the Palaeoproterozoic isotopic event is followed by formation of a vast reservoir of ^{13}C-depleted organic material (down to -42‰ at Shunga) and by one of the earliest known oil-generation episodes at 2.0 Ga. The latter time is also marked by the first appearance, and then by the worldwide development, of diagenetic carbonate concretions marked by negative $\delta^{13}C_{carb}$ values. This may be the first reliable evidence that organic material was recycled during diagenesis under oxic conditions.

(4) None of the three positive excursions of $\delta^{13}C_{carb}$ is followed by a negative isotopic shift significantly below 0‰, as has usually been observed in younger isotopic events, reflecting an overturn of major marine carbon reservoirs. This may indicate that f_{org} was constant, implying that the mechanism involved in the production of organic carbon was different. Onset of intensive methane cycling resulting in Δ_c change is another possibility.

(5) A 'cause-and-effect' relationship between the excursion and a series of related phenomena is still not fully understood, and global $\delta^{13}C_{carb}$ values are not well constrained. The majority of sampled $^{13}C_{carb}$-rich localities represent shallow-water stromatolitic dolostones, 'red beds' and evaporites formed in non-marine or in marine restricted intracratonic basins, and may not reflect global $\delta^{13}C_{carb}$ values.

16.2. Application to the Tulomoserskaya formation

(1) Closely spaced drill core samples ($n=73$) of stromatolitic dolomite and magnesite from the Palaeoproterozoic ($>1980\pm27$ Ma) Tulomozerskaya Formation in the Onega palaeobasin, Russian Karelia, have been analysed for $\delta^{13}C_{carb}$, $\delta^{18}O_{carb}$, trace and major elements in order to demonstrate that different processes were involved in the formation of sampled $^{13}C_{carb}$-rich carbonates.

(2) The 800 m-thick magnesite–stromatolite–dolomite–'red beds' succession is interpreted as having formed in a complex combination of environments: peritidal shallow marine, low energy protected bights, or barred basins; evaporative ephemeral ponds in upper tidal zones of a carbonate flat; and coastal sabkhas and playa lakes.

(3) The carbon and oxygen isotopes were measured from bulk carbonates. The carbonate rocks exhibit extreme $\delta^{13}C$ enrichment throughout with values ranging from +5.7 to +17.2‰ vs. PDB (mean + 9.9 ± 2.3‰) and $\delta^{18}O$ from 18.6 to +26.0‰ vs. SMOW (mean 22 ± 1.6‰). The $\delta^{13}C$ records show a substantial decrease from +17.2‰ to +8‰ upward in the succession while the $\delta^{18}O$ values display no apparent systematic variation.

(4) Elemental ratios suggest that oxygen isotope exchange between some of the carbonates and meteoric fluids was very likely. The least altered $\delta^{18}O$ of 26.0‰ is still not considered to be an initial value.

(5) Dolomites apparently precipitated from pore waters, which were isotopically similar to basinal water. Overall sedimentological, depositional and geochemical patterns of the Tulomozerskaya sequence are superficially similar to those of evaporites and ^{13}C-rich dolostones developed during the Permian positive excursion of carbonate $^{13}C/^{12}C$.

(6) The Tulomozerskaya isotopic excursion is characteristic of the global 2.4–2.06 Ga positive shifts of carbonate $^{13}C/^{12}C$, although it reveals the greatest enrichment in ^{13}C known from this interval.

(7) The isotopic excursion seems driven by a combination of factors. An external basin(s) is considered to have provided an enhanced C_{org} burial and global seawater enrichment in ^{13}C: the global background value for the isotopic shift at Tulomozero time (ca. 2.0 Ga) is roughly estimated at around +5‰.

(8) An explosion of stromatolite-forming microbial communities in shallow-water basins, evaporative and partly restricted environments is believed to be an extra local factor in seawater ^{13}C enrichment. These processes, which may have enhanced $\delta^{13}C$ from +5‰ up to +17‰, are locally perhaps due to evaporation, high bioproductivity, enhanced uptake of ^{12}C, and pene-contemporaneous recycling of organic material in cyanobacterial mats with the production and consequent loss of CO_2 (and CH_4?).

(9) The case described should be taken into account when interpreting carbon isotopic data and attempting to discriminate between the local enrichment in ^{13}C and background of globally enhanced $\delta^{13}C$ values. We suggest that other ca. 2 Ga high $\delta^{13}C$ values — from localities where environmental interpretations are not available or are not being adequately taken into account — the reported values may not represent global $\delta^{13}C$ values.

Acknowledgements

This research has been carried out by the Geological Survey of Norway (NGU) jointly with the Scottish Universities Research and Reactor Centre (SURRC) (Glasgow, Scotland) and Institute of Geology (IG) of the Russian Academy of Sciences (Petrozavodsk, Karelia). Access to core material of the Nevskaya and Karelian Geological Expeditions is acknowledged with thanks. B. Pokrovsky (Geological Institute of the Russian Academy of Sciences, Moscow) donated unpublished isotopic data on Shark Bay stromatolites and shells. The field work was financially supported by Norsk Hydro. The isotope analyses were performed at SURRC supported by the Consortium of Scottish Universities and the Natural Environment Research Council. XRF analyses have been performed at NGU and financed by the Kola Mineral Resource Project. Electron-probe microanalyses and electron-microscope studies were carried out at the IKU Petroleum Research in Trondheim. IG, and partly NGU and SURRC were supported by INTAS-RFBR 095-928. I.J Fairchild, A.J. Kaufman and P. Padget read an earlier version of manuscript and provided useful comments. We acknowledge constructive criticism by two official referees, P.F. Hoffman and J. Karhu. This paper has the EUROPROBE publication number 251.

References

Aharon, P., Schidlowski, M., Singh, I.B., 1987. Chronostratigraphic markers in the end-Precambrian carbon isotope record of the lesser Himalaya. Nature 327, 699–702.

Akhmedov, A.M., Krupenik, V.A., Makarikhin, V.V., Medvedev, P.V., 1993. Carbon isotope composition of carbonates in the early Proterozoic sedimentary basins. Printed report, Institute of Geology of the Karelian Scientific Centre, Petrozavodsk, 58 pp. (in Russian).

Amard, B., Bertrand-Sarfati, L., 1997. Microfossils in 2000 Ma old stromatolites of the Franceville Group, Gabon. Precambrian Res. 81, 197–221.

Amelin, Yu.V., Heaman, L.M., Semenov, V.S., 1995. U–Pb geochronology of layered mafic intrusions in the eastern Baltic Shield: implications for the timing and duration of Palaeoproterozoic continental rifting. Precambrian Res. 75, 31–46.

Asmerom, Y., Jacobsen, S., Knoll, A.H., Butterfield, N.J., Swett,

K., 1991. Strontium isotope variations of Neoproterozoic seawater: implications for crustal evolution. Geochim. Cosmochim. Acta 55, 2883–2894.

Baker, A.J., Fallick, A.E., 1989a. Evidence from Lewisian limestone for isotopically heavy carbon in two-thousand-million-year-old sea water. Nature 337, 352–354.

Baker, A.J., Fallick, A.E., 1989b. Heavy carbon in two-billion-year-old marbles from Lofoten-Vesterålen, Norway: implications for the Precambrian carbon cycle. Geochim. Cosmochim. Acta 53, 1111–1115.

Balashov, Yu.A., 1995. Geochronology of Palaeoproterozoic rocks of the Pechenga-Varzuga structure, Kola Peninsula. Petrology 4, 3–25, in Russian.

Banner, J.L., 1995. Application of the trace element and isotope geochemistry of strontium to studies of carbonate diagenesis. Sedimentology 42, 805–824.

Barbey, P., Convert, J., Moreau, B., Capdevila, R., 1984. Petrogenesis and evolution of an early Proterozoic collisional orogenic belt: the Granulite Belt of Lapland and the Belomorides (Fennoscandia). Geol. Soc. Finland Bull. 56, 161–188.

Beauchamp, B., Oldershaw, A.E., Krouse, R., 1987. Upper Carboniferous to Upper Permian ^{13}C-enriched primary carbonates in the Sverdrup Basin, Canadian Arctic: comparisons to coeveal western North American ocean margins. Chem. Geol. (Isotope Geosci. Sect.) 65, 391–413.

Becker, R.H., Clayton, R.N., 1972. Carbon isotope evidence for the origin of a banded iron-formation in Western Australia. Geochim. Cosmochim. Acta 36, 577–595.

Behrens, E.W., Land, L.S., 1972. Subtidal Holocene dolomite, Baffin Bay, Texas. J. Sediment. Petrol. 2, 155–161.

Bekasova, N.B., Dudkin, O.B., 1981. Composition and origin of Palaeoproterozoic concretionary phosphorites from Pechenga (Kola Peninsula). Lithol. Miner. Deposits 6, 107–113, in Russian.

Bekker, A., 1998. Chemostratigraphy and climatostratigraphy of the Paleoproterozoic Snowy Pass Supergroup, Wyoming and its application for correlation with other sequences in north America. Unpub. MSc Thesis, Univ. of Minnesota, 104 pp.

Bekker, A., Karhu, J.A., 1996. Study of carbon isotope ratios in carbonates of the Early Proterozoic Snowy Pass Supergroup, WY and its application for correlation with the Chocolay Group, MI and Huronian Supergroup, ON. In: Abstracts of Institute on Lake Superior Geology, Annual Meeting, 42nd, Part 1, pp. 4–5.

Berger, W.H., 1977. Carbon dioxide excursion and the deep sea record: aspects of the problem. In: Andersen, N.R., Malahoff, A. (Eds.), The Fate of Fossil Fuel CO_2 in the Oceans. Plenum, New York, pp. 505–542.

Bonatti, C., Emiliani, C., Ostlund, G., Rydel, H., 1971. Final desiccation of the Afar Rift, Ethiopia. Science 172, 468–469.

Botz, R., Müller, G., 1981. Petrographie, anorganische Geochemie und Isotopen-Geochemie der Karbonatgesteine des Zechstein, 2. Geol. Jahrb., Reihe D 47, 3–112.

Botz, R., Stoffers, P., Faber, E., Tietze, K., 1988. Isotope geochemistry of carbonate sediments from lake Kivu (East–Central Africa). Chem. Geol. 69, 299–308.

Brand, U., Veizer, J., 1980. Chemical diagenesis of multicomponent carbonate system: 1. Trace elements. J. Sediment. Petrol. 50, 1219–1250.

Brasier, M.D., Rozanov, A.Yu., Zhuravlev, A.Yu., Corfield, R.M., Derry, L.A., 1994. A carbon isotope reference scale for the Lower Cambrian succession in Siberia: report of IGCP Project 303. Geol. Mag. 131, 767–783.

Brenchley, P.J., Marshall, J.D., Cardenn, G.A.F., Robertson, D.B.R., Long, D.G.F., Meidla, T., Hints, L., Anderson, T.F., 1994. Bathymetric and isotopic evidence for a short-lived Late Ordovician glaciation in a greenhouse period. Geology 22, 295–298.

Brenchley, P.J., Marshall, J.D., Hints, L., Nõlvak, J., 1997. New data solving an old biostratigraphic problem: the age of the upper Ordovician brachiopod Holorhynchus giganteus. J. Geol. Soc. London 154, 335–342.

Broecker, W.S., 1970. A boundary condition on the evolution of atmospheric oxygen. J. Geophys. Res. 75 (18), 3553–3557.

Bros, R., Stille, P., Gauthier-Lafaye, F., Weber, F., 1992. Sm–Nd isotope dating of Proterozoic clay material: an example from the Francevillian sedimentary series, Gabon. Earth Planet. Sci. Lett. 113, 207–218.

Budd, D.A., 1997. Cenozoic dolomites of carbonate islands: their attributes and origin. Earth Sci. Rev. 42, 1–47.

Buick, I.S., Uken, R., Gibson, R.L., Wallmach, T., 1998. High-$\delta^{13}C$ Paleoproterozoic carbonates from the Transvaal Supergroup, South Africa. Geology 26, 875–878.

Burne, R. V, Morre, L.S., 1987. Microbiolites: organosedimentary deposits of benthic microbial communities. PALAIOS 2, 241–254.

Carpenter, S.J., Lohman, K.C., 1997. Carbon isotope ratios of Phanerozoic marine cements: re-evaluation the global carbon and sulphur systems. Geochim. Cosmochim. Acta 61, 4831–4846.

Carrigan, W.J., Cameron, E.M., 1991. Petrological and stable isotope studies of carbonate and sulfide minerals from the Gunflint Formation, Ontario: evidence for the origin of early Proterozoic iron-formation. Precambrian Res. 52, 347–380.

Castenhols, R.W., Bauld, J., Pierson, B.K., 1992. Photosynthetic activity in modern microbial mat-building communities. In: Schopf, J.W., Klein, C. (Eds.), The Proterozoic Biosphere. Cambridge Univ. Press, pp. 279–285.

Chevé, S.R., Schrijver, K., Tasse, N., 1985. Cryptalgalaminate dolomite of the Dunphy Formation, Labrador Trough; diagenetic and tectono-metamorphic evolution related to copper mineralization. Canadian J. Earth Sci. 22, 1835–1857.

Clark, D.N., 1980. The diagenesis of Zechstein carbonate sediments. Contrib. Sedimentol. 9, 167–203.

Compston, W., 1960. The carbon isotopic compositions of certain marine invertebrates and coals from the Australian Permian. Geochim. Cosmochim. Acta 18, 1–22.

Corsetti, F.A., Kaufman, A.J., 1994. Chemostratigraphy of Neoproterozoic–Cambrian Units, White-Inyo region, eastern California and western Nevada: implications for global correlation and faunal distribution. Palaois 9, 211–219.

Dahl-Jensen, T., Hobbs, R.W., Klemperer, S.L., Matthews, D.H., Snyder, D.B., Long, R., Matthews, T., Blundell, D.J., Lund, C.E., Palm, H., Pedersen, L.B., Roberts, R.G., Elming, S.A.,

Heikkinen, P., Korhonen, H., Luosto, U., Hjelt, S.E., Komminaho, K., Yliniemi, J., Meissner, R., Sadowiak, P., Wever, T., Dickmann, T., Flueh, E.R., Berthelsen, A., Thybo, H., Balling, N., Normark, E., 1990. Evidence for early Proterozoic plate tectonics from seismic reflection profiles in the Baltic Shield. Nature (London) 348, 34–38.

Davies, R.G., 1976. Former magnesium calcite and aragonite submarine cements in upper Paleozoic reefs of the Canadian Arctic: a summary. Geology 5, 11–15.

Davies, R.G., Krouse, H.R., 1975. Carbon and oxygen isotope composition of late Paleozoic calcite cements, Canadian Arctic Archipelago — preliminary results and interpretation. Geol. Surv. Can., Paper 75-1, Part B, 215–220.

Degens, E.T., Epstein, S., 1964. Oxygen and carbon isotope ratios in coexisting calcites and dolomites from recent and ancient sediments. Geochim. Cosmochim. Acta 28, 23–44.

Derry, L.A., Kaufman, A.J., Jacobsen, S.B., 1992. Sedimentary cycling and environmental changes in the Late Proterozoic: evidence from stable and radiogenic isotopes. Geochim. Cosmochim. Acta 56, 1317–1329.

Des Marais, D.J., 1994. Tectonic control of the crustal organic carbon reservoir during the Precambrian. Chem. Geol. 114, 303–314.

Des Marais, D.J., 1997. Isotopic evolution of the biogeochemical cycle during the Proterozoic Eon. Org. Geochem. 27, 185–193.

Des Marais, D.J., Bauld, J., Palmisano, A.C., Summons, R.E., Ward, D.M., 1992a. The biochemistry of carbon in modern microbial mats. In: Schopf, J.W., Klein, C. (Eds.), The Proterozoic Biosphere. Cambridge Univ. Press, pp. 299–308.

Des Marais, D.J., Strauss, H., Summons, R.E., Hayes, J.M., 1992b. Carbon isotope evidence for the stepwise oxidation of the Proterozoic environment. Nature (London) 359, 605–609.

Dimroth, E., 1978. Région de la Fosse du Labrador (54°30′ and 56°30′). Ministère des Richesses naturelles du Québec, RG 193, pp. 396.

Dix, G.R., Thomson, M.L., Longstaffe, F.J., McNutt, R.H., 1995. Systematic decrease of high $\delta^{13}C$ values with burial in Late Archaean (2.8 Ga) diagenetic dolomite: evidence for methanogenesis from the Crixas Greenstone Belt, Brasil. Precambrian Res. 70, 253–268.

Dorman, F.H., 1968. Some Australian oxygen isotope temperatures and a theory for a 30-million-year world-temperature cycle. J. Geol. 76, 297–313.

Eriksson, P.G., Reczko, B.F.F., 1995. The sedimentary and tectonic setting of the Transvaal Supergroup floor rocks to the Bushveld complex. J. Afr. Earth Sci. 4, 487–504.

Fairchild, I.J., 1991. Origins of carbonate in Neoproterozoic stromatolites and the identification of modern analogues. Precambrian Res. 53, 281–299.

Fairchild, I.J., Hambrey, M.J., Spiro, B., Jefferson, H.T., 1989. Late Proterozoic glacial carbonates in northeast Spitsbergen: new insights into the carbonate–tillite association. Geol. Mag. 126, 469–490.

Fairchild, I.J., Marshall, J.D., Bertrand-Sarafati, J., 1990. Stratigraphic shifts in carbon isotopes from Proterozoic stromatolitic carbonates (Mauritania): influences of primary mineralogy and diagenesis. Am. J. Sci. 290A, 46–79.

Feng, J., 1986. Sulfur and oxygen isotope geochemistry of Precambrian marine sulfate and chert. Unpub. M.S. thesis, Northern Illinois Univ.

Friedman, I., 1970. Some investigations of deposition of travertine from hot springs: I. The isotopic chemistry of a travertine-depositing spring. Geochim. Cosmochim. Acta 34, 1303–1315.

Gauthier-Lafaye, F., Weber, F., 1989. The Francevillian (Lower Proterozoic) uranium ore deposits of Gabon. Econ. Geol. 84, 2267–2285.

Golubev, A.I., Akhmedov. A.M., Galdobina, L.P., 1984. Geochemistry of the early Proterozoic 'black shale' complexes of the Karelo-Kola Region. Leningrad, Nauka, 193 pp. (in Russian).

Grotzinger, J.P., 1989. Facies and evolution of Precambrian carbonate depositional systems: emergence of the modern platform archetype. In: Crevello, P.D., Wilson, J.L., Sarg, J.F., Read, J.F. (Eds.), Controls on Carbonate Platform and Basin Development. Society of Economic Palaeotologists and Mineralogists, Tulsa, OK, pp. 79–106.

Guerrera, A., Peacock, S.M., Knauth, L.P., 1997. Large ^{18}O and ^{13}C depletion in greenschist facies carbonate rocks, western Arizona. Geology 25, 943–946.

Han, T.-M., Runnegar, B., 1992. Megascopic Eukariotic algae from 2.1-billion-year-old Negaunee Iron-Formation, Michigan. Science 257, 232–235.

Hanski, E.J., Huhma, H., Smolkin, V.F., Vaasjoki, M., 1990. The age of ferrropicritic volcanism and comagmatic Ni-bearing intrusions at Pechenga, Kola Peninsula, USSR. Geol. Soc. Finland Bull. 62, 123–133.

Hayes, J.M., 1983. Geochemical evidence bearing on the origin of aerobiosis, a speculative hypothesis. In: Schopf, J.W. (Ed.), Earth's Earliest Biosphere: Its Origin and Evolution. Princeton Univ. Press, New Jersey, pp. 291–301.

Hayes, J.M., 1994. Global methanotrophy at the Archean-Proterozoic transition. In: Bengsten, S. (Ed.), Proceedings of Nobel Symposium 84, Chapter for Early Life on Earth. Columbia Univ. Press, New York, pp. 220–236.

Hoffman, P.F., Kaufman, A.J., Halverson, G.P., 1998. A Neoproterozoic snowball Earth. Science 281, 1342–1346.

Holland, H.D., 1994. Early Proterozoic atmospheric change. In: Bengston, S. (Ed.), Early Life on Earth. Columbia Univ. Press, New York, pp. 237–244.

Hudson, J.D., 1977. Stable isotopes and limestone lithification. J. Geol. Soc. London 133, 637–660.

Irwin, H., Curtis, C., Coleman, M., 1977. Isotopic evidence for source of diagenetic carbonates formed during burial of organic-rich sediments. Nature 260, 209–213.

ISSC (International Subcommision on Stratigraphic Classification of IUGS Commission on Stratigraphy), 1976. In: Hedberg, H.D. (Ed.), International Stratigraphic Guide: A Guide to Stratigraphic Classification, Terminology and Procedure. Willey, New York, 200 pp.

Iyer, S.S., Babinski, M., Krouse, M., Chemale, F. Jr., 1995. Highly ^{13}C-enriched carbonate and organic matter in the Neoproterozoic sediments of the Bambui Group, Brazil. Precambrian Res. 73, 271–282.

Jacobson, R.L., Usdowski, H.E., 1976. Partitioning of strontium

between calcite, dolomite and liquid. Contrib. Mineral. Petrol. 59, 171–185.

Jenkyns, H.C., 1980. Cretaceous anoxic events from continents to oceans. J. Geol. Soc. London 137, 171–188.

Jørgensen, B.B., Nelson, D.C., Ward, D.M., 1992. Chemostratigraphy and decomposition in modern microbial mats. In: Schopf, J.W., Klein, C. (Eds.), The Proterozoic Biosphere. Cambridge Univ. Press, pp. 287–293.

Kakegawa, T., Kawai, H., Ohmoto, H., 1992. Origins of pyrites in the ~2.5 Ga Mt. McRae Shale, the Hamersly District. Geochim. Cosmochim. Acta 62, 3205–3220.

Karhu, J.A., 1993. Palaeoproterozoic evolution of the carbon isotope ratios of sedimentary carbonates in the Fennoscandian Shield. Geol. Surv. Finland, Bull. 371, 1–87.

Karhu, J.A., Holland, H.D., 1996. Carbon isotopes and rise of atmospheric oxygen. Geology 24, 867–879.

Karhu, J.A., Melezhik, V.A., 1992. Carbon isotope systematics of early Proterozoic sedimentary carbonates in the Kola Peninsula, Russia: correlations with Jatulian formations in Karelia. In: Balagansky, V.V., Mitrofanov F.P. (Eds.), Correlations of Precambrian Formations of the Kola–Karelia Region and Finland, Apatity. Kola Scientific Centre of the Russian Academy of Sciences, pp. 48–53.

Katz, A., Kolodny, Y., Nissenbaum, A., 1977. The geochemical evolution of the Pleistocene Lake Lisisan–Dead Sea system. Geochim. Cosmochim. Acta 41, 1609–1626.

Kaufman, A.J., Knoll, A.H., 1995. Neoproterozoic variations in the C-isotopic composition of seawater: stratigraphic and biogeochemical implications. Precambrian Res. 73, 27–49.

Kaufman, A., Hayes, J.M., Klein, C., 1990. Primary and diagenetic control of isotopic compositions of iron-formation carbonates. Geochim. Cosmochim. Acta 54, 3461–3473.

Kaufman, A.J., Hayes, J.M., Knoll, A.H., Germs, G.J.B., 1991. Isotopic compositions of carbonates and organic carbon from upper Proterozoic successions in Namibia: stratigraphic variation and the effects of diagenesis and metamorphism. Precambrian Res. 49, 301–327.

Kaufman, A.J., Knoll, A.H., Awramik, S.M., 1992. Biostratigraphic and chemostratigraphic correlation of Neoproterozoic sedimentary succession: upper Tindir Group, north-western Canada, as a test case. Geology 20, 181–185.

Kaufman, A.J., Jacobsen, S.B., Knoll, A.H., 1993. The Vendian record of Sr and C isotopic variations in seawater: implications for tectonics and paleoclimate. Earth Planet. Sci. Lett. 120, 409–430.

Kaufman, A.J., Knoll, A.H., Semikhatov, M.A., Grotzinger, J.P., Jakobsen, S.B., Adams, W., 1996. Integrated chronostratigraphy of Proterozoic–Cambrian boundary beds in the western Anabar region, northern Siberia. Geol. Mag. 133, 505–553.

Kaufman, A.J., Knoll, A.H., Narbonne, G.M., 1997. Isotopes, ice ages, and terminal Proterozoic earth history. Proc. Natl. Acad. Sci. U.S.A. 95, 6600–6605.

Keith, M.L., 1982. Violent volcanism, stagnant oceans and some inferences regarding petroleum, strata-bound ores and mass extinctions. Geochim. Cosmochim. Act. 46, 2621–2637.

Keith, M.L., Weber, J.M., 1964. Carbon and oxygen isotopic composition of selected limestones and fossils. Geochim. Cosmochim. Acta 28, 1787–1863.

Knoll, A.H., Kaufman, A.J., Semikhatov, M.A., 1995a. The carbon-isotopic composition of Proterozoic carbonates: Riphean succession from northwestern Siberia (Anabar Massif, Turukhansk Uplift). Am. J. Sci. 295, 823–850.

Knoll, A.H., Grotzinger, J.P., Kaufman, A.J., Kolosov, P., 1995b. Integrated approaches to terminal Proterozoic stratigraphy: an example from the Olenek Uplift, northeastern Siberia. Precambrian Res. 73, 252–270.

Knoll, A.H., Hayes, J.M., Kaufman, A.J., Swett, K., Lambert, I.B., 1986. Secular variation in carbon isotope ratios from Upper Proterozoic successions of Svalbard and East Greenland. Nature 321, 832–838.

Kontinen, A., 1987. An early Proterozoic ophiolite — the Jormua mafic–ultramafic complex, northern Finland. Precambrian Res. 35, 313–341.

Kretz, R., 1982. A model for distribution of trace elements between calcite and dolomite. Geochim. Cosmochim. Acta 46, 1979–1981.

Kroopnick, P.M., Margolis, S.V., Wong, C.S., 1977. $\delta^{13}C$ variations in marine carbonate sediments as indicators of the CO_2 in the ocean. In: Andersen, N.R., Malahoff, A. (Eds.), The Fate of Fossil Fuel CO_2 in the Oceans. Plenum, New York, pp. 295–321.

Krylov, I.N., Perttunen, V., 1978. Aphebian stromatolites of the Tervola region, northwestern Finland. In: Raaben, M.E. (Ed.), Lower Riphean Boundary and Aphebian Stromatolites. Proceedings of the Geological Institute of the USSR Academy of Sciences, 312, 87–105.

Land, L.S., Hoops, G.K., 1973. Sodium in carbonate sediments and rocks: a possible index to the salinity of diagenetic solutions. J. Sediment. Petrol. 43, 614–616.

Larue, D.K., 1981. The Chocolay Group, Lake Superior region, U.S.A.: sedimentological evidence for deposition in basinal and platform settings on an Paleoproterozoic craton. Geol. Soc. Am. Bull. 92, 417–435.

Lloyd, R.M., Hsü, K.J., 1971. Stable-isotope investigations of sediments from the DSDP III cruise to south Alantic. Sedimentology 19, 45–58.

Lowe, D.R., 1992. Major events in the geological development of the Precambrian Earth. In: Schopf, J.W., Klein, C. (Eds.), The Proterozoic Biosphere: A Multidisciplinary Study. Cambridge Univ. Press, New York, pp. 67–76.

Lucia, F.J., Major, R.P., 1994. Porosity evolution through hypersaline reflux dolomitization. In: Purser, B., Tucker, M., Zenger, D. (Eds.), Dolomites: A Volume in Honor of Dolomieu. Int Assoc. Sedimentol. Spec. Publ. 21, 325–341.

Magaritz, W., 1989. ^{13}C minima follow extinction events: a clue to faunal radiation. Geology 17, 337–340.

Magaritz, W., Schultze, K.H., 1980. Carbon isotope anomaly of the Permian period. Contrib. Sedimentol. 9, 269–277.

Magaritz, M., Turner, P., 1982. Carbon cycle changes of the Zechstein Sea: isotopic transition zone in the Marl Slate. Nature 297, 389–390.

Magaritz, M., Turner, P., Käding, K.-C., 1981. Carbon isotope

change at the base of Upper Permian Zechstein sequence. Geol. J. 16, 243–254.

Magaritz, M., Anderson, R.Y., Holser, W.T., Saltzman, E.S., Garber, J., 1983. Isotope shift in the Late Permian of the Delaware Basin, Texas, precisely timed by varved sediments. Earth Planet. Sci. Lett. 66, 111–124.

Magaritz, M., Holser, W.T., Kirschvink, J.L., 1986. Carbon isotope events across the Precambrian/Cambrian boundary on the Siberian Platform. Nature 320, 258–259.

Master, S., 1998. Carbon and oxygen isotopic profile through the high-$\delta^{13}C$ Palaeoproterozoic Lomagundi dolomite, Magondi Supergroup, Zimbabwe. The Ninth International Conference on Geochronology, Cosmochronology and Isotope Geology, 20–26 August, China. Chinese Science Bulletin 43, 88.

McCrea, J.M., 1950. On the isotopic chemistry of carbonates and a paleotemperature scale. J. Chem. Phys. 18, 849–857.

McKenzie, J.A., 1981. Holocene dolomitisation of calcium carbonate sediments from coastal sabkhas of Abu Dhabi, U.A.E. — a stable isotope study. J. Geol. 89, 185–198.

McNaughton, N.J., Wilson, A.F., 1983. ^{13}C-rich marbles from the Proterozoic Einasleigh Metamorphics, northern Queensland. Geol. Soc. Austral. J. 30, 175–178.

Melezhik, V.A., 1992. Palaeoproterozoic sedimentary and rock-forming basins of the Fennoscandian Shield. Nauka, Leningrad, 258 pp. (in Russian).

Melezhik, V.A., Fallick, A.E., 1996a. A widespread positive $\delta^{13}C_{carb}$ anomaly at around 2.33–2.06 Ga on the Fennoscandian Shield: a paradox? Terra Nova 8, 141–157.

Melezhik, V.A., Fallick, A.E., 1996b. Organic carbon recycling in the Early Precambrian: how much do we know about it? Sixth V.M. Goldschmidt Conference, Heidelberg 1996. J. Conference Abstracts 1, 339.

Melezhik, V.A., Fallick, A.E., 1996c. Links between Early Proterozoic palaeogeography, rise and decline of stromatolites and positive $\delta^{13}C_{carb}$ anomaly. The 22nd Nordic Geological Winter meeting, 8-11 January 1996 in Turku-Åbo, Finland. Abstracts Vol., p. 135.

Melezhik, V.A., Fallick, A.E., 1997. Paradox regained? Reply. Terra Nova 9, 148–151.

Melezhik, V.A., Predovsky, A.A., 1989. Karelian inversion of carbonate accumulation on the Baltic Shield: does it reflect a global change in the Precambrian environment? Trans. USSR Acad. Sci., Earth Sci. Section 306, 1441–1445, in Russian.

Melezhik, V.A., Fallick, A.E., Medvedev, P.V., Makarikhin, V.V., 1996. Carbonate rocks of Karelia: geochemistry and carbon-oxygen isotope systematics in the Jatulian stratotype and potential for magnesite deposits. Norges geologiske undersøkelse, Open Report 96.086, 61 pp.

Melezhik, V.A., Fallick, A.E., Clark, T., 1997a. Two billion year old isotopically heavy carbon: evidence from the Labrador Trough, Canada. Can. J. Earth Sci. 34, 271–287.

Melezhik, V.A., Fallick, A.E., Makarikhin, V.V., Lubtsov, V.V., 1997b. Links between Palaeoproterozoic palaeogeography and rise and decline of stromatolites: Fennoscandian Shield. Precambrian Res. 82, 311–348.

Melezhik, V.A., Fallick, A.E., Semikhatov, M.A., 1997c. Could stromatolite-forming cyanobacteria have influenced the global carbon cycle at 2300–2060 Ma? Norges Geol. Undersøk. Bull. 433, 30–31.

Melezhik, V.A., Grinenko, L.N., Fallick, A.E., 1998. 2000-Ma sulphide concretions from the 'Productive' Formation of the Pechenga Greenstone Belt, NW Russia: genetic history based on morphological and isotopic evidence. Chem. Geol. 148, 61–94.

Melezhik, V.A., Fallick, A.E., Filippov, M.M., Larsen, O., 1999. Karelian shungite-an indication of 2000 Ma-year-old metamorphosed oil-shale and generation of petroleum: geology, lithology and geochemistry. Earth-Sci. Rev. 47, 1–40.

Melezhik, V.A., Fallick, A.E., Medvedev, P.V., Makarikhin, V.V., 1999a. Palaeoproterozoic magnesite–stromatolite–dolomite–'red beds' association, Russian Karelia: palaeoenvironmental constraints on the 2.0 Ga positive carbon isotope shift. Norsk Geol. Tidsskrift. (submitted).

Melezhik, V.A., Fallick, A.E., Medvedev, P.V., Makarikhin, V.V., 1999b. Palaeoproterozoic magnesite: lithological and isotopic evidence for playa/sabkha environments. Sedimentology (submitted).

Mirota, M.D., Veizer, J., 1994. Geochemistry of Precambrian carbonates: VI. Aphebian Albanel Formations, Quebec, Canada. Geochim. Cosmochim. Acta 58, 1735–1745.

Murata, K.J., Friedman, I., Gulbrandsen, R.A., 1972. Geochemistry of carbonate rocks in Phosphoria and related formations of the western phosphate field. U.S. Geol. Survey Prof. Paper 800-D, D103–D110.

M'Rabet, A., 1981. Differentiation of environments of dolomite formation, Lower Cretaceous of Central Tunisia. Sedimentology 28, 331–352.

Narbonne, G.M., Kaufman, A.J., Knoll, A.H., 1994. Integrated chemostratigraphy and biostratigraphy of the Windermere Supergroup, north-western Canada: implications for Neoproterozoic correlations and the early evolution of animals. Geol. Soc. Am. Bull. 106, 1281–1292.

Ojakangas, R.M., 1985. Evidence for early Proterozoic glaciation: dropstone unit diamictite association. Geol. Surv. Finl. Bull. 331, 51–72.

Osaki, S., 1973. Carbon and oxygen isotopic compositions of Tertiary and Permian Dolomites of Japan. Geochem. J. 6, 163–177.

Pekkala, Y., 1985. Petrography, geochemistry and mineralogy of the Precambrian metasedimentary carbonate rocks in North Kuusamo, Finland. Geol. Surv. Finland. Bull., 332, 62 pp.

Perry, E.C., Tan, F.C., 1973. Significance of carbon isotope variations in carbonates from the Biwabik Iron Formation, Minnesota. Genesis of Precambrian iron and manganise deposits: UNESCO Earth Science, 9, 299–305.

Perttunen, V., 1991. Kemin, Karungin, Simon ja Runkausken kartta-alueiden kallioperä. Summary: Pre-Quaternary rocks of the kemi, Karunki, Simo and Runkaus map-sheet areas. Explanation to the maps of Pre-Quaternary rocks, sheets 2541,2542 +2524, 2543 and 2544, Geological Map of Finland 1:100 000, 80 pp.

Pierre, C., 1982. Teneurs en isotopes stables (^{18}O, ^{2}H, ^{13}C, ^{34}S) et

conditions de génèse des évaporites marines: application à quelques milieux actuels et au Messinian de la Méditerranée, D.S.N. Thesis, Université de Paris-Sud, Orsay, 226 pp.

Pokrovsky, B.G., Gertsev, D.D., 1993. Upper Precambrian carbonates with anomalously light isotopic composition of carbon (south central Siberia). Lithol. Min. Deposits 1, 64–80, in Russian.

Pokrovsky, B.G., Melezhik, V.A., 1995. Variations of oxygen and carbon isotopes in Palaeoproterozoic carbonate rocks of the Kola Peninsula. Stratigraphy and Geological Correlation 3 (5), 42–53.

Pokrovsky, B.G., Vinogradov, V.I., 1991. Isotopic composition of strontium, oxygen and carbon in the Upper Precambrian carbonates of the western slope of the Anabar Uplift (Kotuikan River). Transactions of the USSR Academy of Sciences 320, 1245–1250, in Russian.

Puchtel, I.S., Arndt, N.T., Hofmann, A.W., Haase, K.M., Kröner, A., Kulikov, V.S., Kilikova, V.V., Garbe-Schönberg, C.-D., Nemchin, A.A., 1998. Petrology of mafic lavas within the Onega plateau, central Karelia: evidence for 2.0 Ga plume-related continental crustal growth in the Baltic Shield. Contrib. Mineral. Petrol. 130, 134–153.

Pukhtel, I.S., Zhuravlev, D.Z., Ashikhmina, N.A., Kulikov, V.S., Kulikova, V.V., 1992. Sm–Nd age of the Suisarskay suite on the Baltic Shield. Transactions Russian Acad. Sci. 326, 706–711, in Russian.

Qing, H., Veizer, J., 1994. Oxygen and carbon isotopic composition of Ordovician brachiopods: implications for coeval seawater. Geochim. Cosmochim. Acta 58, 4429–4442.

Rao, C.P., Green, D.C., 1982. Oxygen and carbon isotopes of Early Permian cold-water carbonates, Tasmania, Australia. J. Sediment. Petrol. 52, 1111–1125.

Reeder, R.J., 1983. Crystal chemistry of the rhombohedral carbonates. In: Reeder, R.J. (Ed.), Carbonates: Mineralogy and Chemistry. Mineral. Soc. Am., Rev. Mineral. 44, 1–47.

Reitsema, R.H., 1980. Dolomite and nahcolite formation in organic rich sediments: isotopically heavy carbonates. Geochim. Cosmochim. Acta 44, 2045–2049.

Rosenbaum, J.M., Sheppard, S.M.F., 1986. An isotopic study of siderites, dolomites and ankerites at high temperatures. Geochem. Cosmochim. Acta 50, 1147–1159.

Saito, T., Van Donk, J., 1974. Oxygen and carbon isotope measurements of Late Cretaceous and Early Tertiary foraminifera. Micropaleontology 20, 152–177.

Salop, L.I., 1982. Geological Development of the Earth in Precambrian, Leningrad, Nedra, 343 pp. (in Russian).

Schidlowski, M., Aharon, P., 1992. Carbon cycle and carbon isotope record: geochemical impact of life over 3.8 Ga of Earth history. In: Schidlowski, M., Golubic, S., Kimberly, M.M., Trudinger, P.A. (Eds.), Early Organic Evolution: Implications for Mineral and Energy Resources. Springer, Berlin, pp. 145-175.

Schidlowski, M., Junge, C.E., 1981. Coupling among the terrestrial sulphur, carbon and oxygen cycles: numerical modelling based on revised carbon isotope record. Geochim. Cosmochim. Acta 45, 589–594.

Schidlowski, M., Eichmann, R., Junge, C.E., 1976. Carbon isotope geochemistry of the Precambrian Lomagundi carbonate province, Rhodesia. Geochim. Cosmochim. Acta 40, 449–455.

Scholle, P.E., Arthur, M.A., 1976. Carbon-isotopic fluctuations in Upper Cretaceous sediments: an indicator of paleo-oceanic circulation. Geol. Soc. Am. Abstr. Programs 8, 1089, Abstract Volume.

Scholle, P.E., Arthur, M.A., 1980. Carbon isotope fluctuations in Cretaceous pelagic limestones: potential stratigraphic and petroleum exploration tool. Am. Assoc. Pet. Geol. Bull. 64, 67–87.

Schrijver, K., Bertrand, R., Changton, A., Tassé, N., Chevé, R., 1986. Fluids in cupriferous dolostones and dolomite veins, Proterozoic Dunphy Formation, Labrador Trough. Can. J. Earth Sci. 23, 1709–1723.

Semikhatov, M.A., Raaben, M.A., 1994. Dynamics of global diversity of Proterozoic stromatolites: 1. Northern Eurasia, China and India. Stratigraphy and Geological Correlation 2 (6), 10–32.

Shackleton, N.J., 1977. Carbon-13 in Uvigerina: tropical rainforest history and the equatorial Pacific carbonate dissolution cycles. In: Andersen, N.R., Malahoff, A., (Eds.), The Fate of Fossil Fuel CO_2 in the Oceans. Plenum, New York, pp. 401–427.

Shields, G., 1997. Paradox lost? Comment. Terra Nova 9, 148–151.

Silvennoinen, A., 1972. On the stratigraphic and structural geology of the Rukatunturi area, northeastern Finland. Geol. Surv. Finland.Bull., 257, 48 pp.

Smith, L.H., Kaufman, A.J., Knoll, A.H., Linl, P.K., 1994. Chemostratigraphy of predominantly siliciclastic Neoproterozoic successions: a case study of the Pocatello Formation and Lower Brigham Group, Idaho, USA. Geol. Mag. 131, 301–314.

Sochava, A.V., 1979. Precambrian and Phanerozoic 'Red Beds'. Leningrad, Nauka, 207 pp. (in Russian).

Sokolov, V.A., 1987. The Jatulian Superhorizon. In: Sokolov, V.A., (Ed.), The Geology of Karelia. Leningrad, Nauka, pp. 51–59 (in Russian).

Sreenivas, B., Kumar, B., Srinivasan, R., Roy, A.B., 1996. Carbon and oxygen isotope composition of the carbonate rocks of the Proterozoic Aravalli Supergroup, Udaipur region, Rajasthan, India: evidence for heavy $\delta^{13}C$ excursion. In: Aggarwal, S.K., Jain, H.C. (Eds.), Seventh National Symposium on Mass Spectrometry. DRDE, Gwalior, November 26–28, 1996, pp. 428–431.

Stiller, M., Rounick, J.S., Shasha, S., 1985. Extreme carbon-isotope enrichments in evaporitic brines. Nature 316, 434–435.

Strauss, H., Moore, T.B., 1992. Abundances and isotopic compositions of carbon and sulfur species in whole rock and kerogen samples. In: Schopf, J.W., Klein, C. (Eds.), The Proterozoic Biosphere: A Multidisciplinary Study. Cambridge Univ. Press, pp. 709–798.

Sturt, B.A., Melezhik, V.A., Ramsay, D.M., 1994. Early Proterozoic regolith at Pasvik, NE Norway: palaeoenvironmental applications for the Baltic Shield. Terra Nova 6, 618–633.

Talbot, M.R., 1990. A review of the palaeohydrological interpretation of carbon and oxygen isotopic ratios in primary lacustrine carbonates. Chem. Geol. (Isot. Geosci. Sect.) 80, 261–279.

Talbot, M.R., Kelts, K. 1990. Palaeolimnological signatures from carbon and oxygen isotopic ratios in carbonates from organic carbon-rich lacustrine sediments. In: Katz, B.J. (Ed.), Lacustrine Basin Exploration: Case Studies and Modern Analogues. Tulsa, AAPG Memoir, 50, pp. 99–112.

Tappan, H., 1968. Primary production, isotopes, extinctions and the atmosphere. Paleogeogr. Paleoc. Paleoecol. 4, 187–210.

Tikhomirova, M., Makarikhin, V.V., 1993. Possible reasons for the $\delta^{13}C$ anomaly of lower Proterozoic sedimentary carbonates. Terra Nova 5, 244–248.

Timopheev, P.P., Kholodov, V.N., Zverev, V.P., 1986. Evolution of natural water mass of the Earth, and sedimentary process. Trans. USSR Acad. of Sci., Earth Sci. Section 288, 444–447, in Russian.

Treloar, P.J., 1988. Geological Evolution of the Magondi Mobile Belt, Zimbabwe. Precambrian Res. 38, 55–73.

Tucker, M.E., 1986. Carbon isotope excursions in Precambrian/Cambrian boundary beds, Morocco. Nature 319, 48–50.

Tucker, M.E., Wright, V.P., 1990. Carbonate Sedimentology. Oxford, 482 pp.

Vahrenkamp, V.C., Swart, P.K., 1990. Late Cenozoic dolomites of the Bahamas: metastable analogues for the genesis of ancient platform dolomites. In: Purser, B., Tucker, M., Zenger, D. (Eds.), Dolomites: A Volume in Honor of Dolomieu. Int Assoc. Sedimentol. Spec. Publ. 21, 133–153.

Veizer, J., 1978. Strontium: Abundance in common sediments and sedimentary rock types. In: Wedepohl, K.H. (Ed.), Handbook of Geochemistry II/5 Section 38 L. Springer, Berlin.

Veizer, J., 1983. Chemical diagenesis of carbonates: theory and application of the trace element technique. In: Arthur, M.A., Anderson, T.F., Kaplan, I.R., Veizer, J., Land, L.S. (Eds.), Stable Isotope in Sedimentary Geology. Society for Economic Petrology and Mineralogy Short Course Notes 10. Tulsa, OK, pp. 3.1–3.100.

Veizer, J., 1999. Isotopic record of Phanerozoic climate change. Journal of Conference Abstracts, Vol. 4, No. 1. Conference of European Union of Geosciences, March 28th–April 1st, Strasbourg, France, p. 224.

Veizer, J., Hoefs, J., 1976. The nature of O^{18}/O^{16} and C^{13}/C^{12} secular trends in sedimentary carbonate rocks. Geochim. Cosmochim. Acta 40, 1387–1395.

Veizer, J., Lemieux, J., Jones, B., Gibling, R.M., Savelle, J., 1978. Palaeosalinity and dolomitisation of a Lower Paleozoic carbonate sequence, Somerest and Prince of Wales Islands, Arctic Canada. Can. J. Earth Sci. 15, 1448–1461.

Veizer, J., Holser, W.T., Wilgus, C.K., 1980. Correlation of $^{13}C/^{12}C$ and $^{34}S/^{32}S$ secular variations. Geochim. Cosmochim. Acta 44, 579–587.

Veizer, J., Hoefs, J., Lowe, D.R., Thurston, P.C., 1989. Geochemistry of Precambrian carbonates: II. Archean greenstone belts and Archean seawater. Geochim. Cosmochim. Acta 53, 859–871.

Veizer, J., Clayton, R.N., Hinton, R.W., Von Brunn, V., Mason, T.R., Buck, S.G., Hoefs, J., 1990. Geochemistry of Precambrian carbonates: III. Shelf seas and non-marine environments of the Archean. Geochim. Cosmochim. Acta 54, 2717–2729.

Veizer, J., Clayton, R.N., Hinton, R.W., 1992a. Geochemistry of Precambrian carbonates: IV. Early Paleoproterozoic (2.25 ± 0.25 Ga) seawater. Geochim. Cosmochim. Acta 56, 875–885.

Veizer, J., Plumb, K.A., Clayton, R.N., Hinton, R.W., Grotzinger, J.P., 1992b. Geochemistry of Precambrian carbonates: V. Late Paleoproterozoic seawater (1.8 ± 0.25 Ga). Geochim. Cosmochim. Acta 56, 2487–2501.

Watson, R.S., Trewin, N.H., Fallick, A.E., 1995. The formation of carbonate cement in the Forth and Balmoral Fields, northern North Sea: a case for biodegradation, carbonate cementation and oil leakage during early burial. In: Harley, A.J., Prosser, D.J. (Eds.), Characterization of Deep Marine Clastic Systems. Geological Society Special Publication 94, 177–200.

Winter, B.L., Knauth, L.P., 1992. Stable isotope geochemistry of early Proterozoic carbonate concretions in the Animikie Group of the Lake Superior region: evidence for bacterial processes. Precambrian Res. 54, 131–151.

Yudovich, Ya.E., Makarikhin, V.V., Medvedev, P.V., Sukhanov, N.V., 1991. Carbon isotope anomalies in carbonates of the Karelian Complex. Geoch. Int. 28 (2), 56–62.

Zachos, J.C., Arthur, M.A., 1986. Paleoceanography of the Cretaceous/Tertiary boundary event; inferences from stable isotopic and other data. Paleoceanography 1, 5–26.

Zagnitko, V.N., Lugovaya, I.P., 1989. Isotope Geochemistry of Carbonate and Banded Iron Formations of the Ukrainian Shield. Kiev, Naukova Dumka, 315 pp. (in Russian).

Anthony E. Fallick graduated from Glasgow University with degrees in Physics (BSc) and Chemistry (PhD). He held postdoctoral positions in Geology and Geography at McMaster University (Ontario), and in Minerology and Petrology at Cambridge University, before moving in 1980 to the Scottish Universities Research and Reactor Centre. He is currently Director of SURRC and Professor of Isotope Geosciences in Glasgow University.

Victor A. Melezhik was educated at the University of Leningrad, Russia. He obtained his Ph.D. in minerology, petrology and geochemistry from the University of Voronezh and D.Sc. in sedimentology from the Geological Institute of the Russian Academy of Sciences in Moscow, Russia. He was involved in exploration work for various deposits and did research in the Urals, Siberia, Far east and north-west Russia before moving in 1990 to the Geological Survey of Norway. In 1996 he was awarded a professor competence by the Norwegian National Committee. Since 1973 his main research interests have been Precambrian basinal environments as revealed by the sedimentary, biological, geochemical and isotopic records.

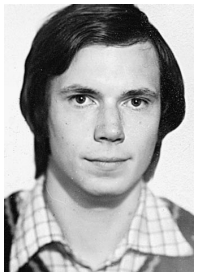

Pavel V. Medvedev was born in Petrozavodsk, Russia in 1961. He obtained a Ph.D. in geology from the Leningrad Mining Institute in 1991. Since 1983 he has been working at the Institute of Geology in Petrozavodsk, Russia where he is currently a Senior Scientist in the Laboratory of Stratigraphy and Lithology. His research interest is a Precambrain palaeontology.

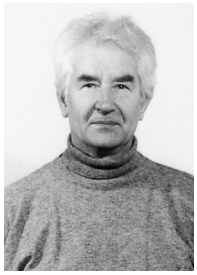

Vladimir V. Makarikhin obtained his Ph.D. from the Leningrad Mining Institute in Russia in 1979. In 1959–1971 he was involved in research and geological mapping of Timan, Polar Urals and Paj-Hoj, north Russia. Since 1979 his main research interest has been Precambrian fossils. He is currently a Senior Scientist at the Laboratory of Stratigraphy and Lithology in the Institute of Geology in Petrozavodsk, Russia.